The role of the ventromedial frontal lobe in assigning value to objects and spatial locations

Gabriel Pelletier

Integrated Program in Neuroscience

McGill University, Montreal

A thesis submitted to McGill University in partial fulfillment of the requirements of the degree of Doctor of Philosophy.

© 2020 Gabriel Pelletier

Table of Contents

Abstract

Moment-to-moment decisions vary widely in their nature and complexity, from simple choices such as which snack to buy from a vending machine or which neighbourhood park to visit when walking the dog, to potentially life-changing choices between job offers. Options under deliberation are often composed of multiple attributes which must somehow be integrated in the choice process. Inspired by economics theories, decision neuroscience research has shown that neural signals in the ventromedial frontal lobes (VMF) scale with subjective value for a wide range of decision types. VMF has been proposed as a key neural substrate for value integration and the comparison of option values on an abstract preference scale, allowing rational decisions between complex, otherwise incommensurable options. However, lesion students have found that VMF damage does not impair all value-based decisions, instead suggesting that this region might be critical only for certain aspects of value-assignment. The specific contributions of the VMF to information integration during value-based decisions remain unclear.

This doctoral work took a novel perspective inspired by the well-known distinctions between object and spatial processing pathways in the brain. The work presented here explored the role of the human VMF in assigning value to complex objects, or to spatial locations. I present converging evidence from patients with VMF damage and from functional MRI in healthy participants arguing that the VMF has a specific role in assigning value to complex objects when value is predicted by the configural relationship between attributes, and not when individual attribute values can be arithmetically combined. A third study provided evidence that lesions to the VMF also impaired decisions when value was solely predicted by

spatial location, providing evidence that this region has a causal role in decisions based on 'where' in addition to 'what'. These findings argue that the VMF might be specifically involved in decisions requiring binding to infer value from the association between attributes of objects, and the spatial relationship between objects and the environment. This work engages with well-established work on the neuroscience of visuospatial and object processing to refine our understanding of the neural basis of subjective evaluation of complex, multi-attribute alternatives. This contributes to a novel, more comprehensive framework for understanding the role of VMF in motivated behaviour.

Résumé

Les décisions que nous prenons couvrent un large éventail quant à leur nature et leur complexité, variant de choix simples comme quel aliment sélectionner dans un machine distributrice, ou dans quelle direction aller promener le chien, jusqu'aux décisions pouvant changer le cours de notre vie comme quelle offre d'emplois accepter. Ces options sont généralement composées de plusieurs attributs qui sont considérés et intégrés dans le processus décisionnel afin de maximiser les conséquences positives d'une décision. Jusqu'ici principalement basée sur des données corrélationnelles de neuroimagerie, la recherche en neuroscience de la prise de décision propose que le cortex préfrontal ventromédian (VMF) est responsable de l'intégration des attributs d'une décision en un signal abstrait représentant une valeur subjective pour chaque option, indépendant de ce qui est évalué, ce qui permet de prendre des décisions parmi des options qui n'ont autrement rien de comparable. Par contre, des études chez des patients qui ont une lésion du VMF suggèrent que cette région n'est pas nécessaire pour la prise de décision dans toutes conditions, mais est plutôt requise pour intégrer seulement certains types d'information au processus décisionnel. Le rôle précis du VMF dans l'intégration d'information durant la prise de décision demeure irrésolu.

Ces travaux de doctorat examinent les rôles du VMF dans la prise de décision basée sur la valeur associée à différents types d'information traités par des processus perceptuels et relationnels distincts. Cette thèse inclue trois études utilisant des méthodes complémentaires, chez des patients avec lésion au VMF et utilisant l'imagerie par résonance magnétique fonctionnelle chez des participants en santé. Il est démontré que le VMF est nécessaire afin de prendre des décisions parmi des objets complexes lorsque plusieurs attributs doivent être

considérés en combinaison pour révéler la valeur d'une option. Cette condition requière aussi l'implication de régions du lobe temporal médial impliquées dans la reconnaissance d'objets complexes. En revanche, le VMF n'es pas impliqué lors de décisions qui nécessitent l'intégration de plusieurs attributs ayant chacun une valeur. De plus, il est démontré que les lésions au VMF détériorent le processus décisionnel lorsque la valeur des objets est associée à leur position dans l'environnement, suggérant que le VMF est nécessaire pour décider sur la base d'où les options se trouvent, en plus de ce de quoi ils sont faits. Ces résultats proposent que le VMF est spécifiquement impliqué dans la prise de décisions qui requiert des processus associatifs supportés par le lobe temporal médial, pour intégrer la valeur liée aux relations entre les attributs d'objets, et aux relations spatiales entre les objets et leur environnement. En utilisant les connaissances établies des mécanismes neuronaux responsables de la reconnaissance d'objets et de la cognition spatiale, cette thèse offre une nouvelle perspective sur l'étude de la prise de décision, et raffine notre compréhension des rôles du VMF dans la prise de décision basée sur la valeur d'options complexes.

Acknowledgements

I would first and foremost like to thank my supervisor, Dr. Lesley Fellows for her invaluable support throughout my doctoral degree. Her generosity, high degree of commitment at every step of the way and her curiosity have played a major role in making this work possible. I have grown on many levels under her mentorship, and I am grateful to have been her student. I would also like to thank my advisory committee members, Dr. Alain Dagher and Dr. Signy Sheldon for their thoughtful comments, questions and practical advices along the way.

I am grateful to have had the chance to share the lab with many great people. Avi, thank you for helping me getting started in doing research with lesion patients. Ana Lucia, Jamie and Matt S., thank you for welcoming me with open arms when I started in the lab. Gloria, Maral, Yvonne and Michael, thank you for your support, for providing technical advice, helping me with manuscript revisions and, importantly, thank you for the hours of friendly discussions about anything and nothing which were much needed in the last stretch of my PhD. I would also like to thank the undergraduate honours students with whom I worked in close collaboration: Matt P, Elsie and Juliette each brought fresh waves of curiosity and energy to the lab. Thank you Christine for your generous help in recruiting patients for my research projects.

I would like to thank Dr. Tom Schonberg for welcoming me in his lab, and for being a wonderful temporary co-supervisor during two extended research stays in Tel Aviv, Israel. Tom has taught me all about open science and infused me with his contagious energy and open mind. I cannot thank the Tel-Aviv lab members enough for their generous support. I especially want to thank Nadav, Tom Salomon, Shiran, Merav, Rani and Anastasia for their kindness in

teaching me neuroimaging, for facilitating my research work, and for introducing me to the Israeli culture. Thank you all for making your lab a home away from home.

I would like to express my gratitude for the financial support that made this work possible. I have been supported by the Mouvement Desjardins, McGill's faculty of medicine, the Integrated Program in Neuroscience and the Montreal Neurological Institute. The research collaboration with Tel Aviv University was supported by the Zavalkoff Family Foundation, The Brain@McGill and the Israeli Ministry for Higher Education.

I am eternally grateful to my close friends within the Constellation and Malebranche, who were always there to provide me with well-needed, sometimes forced but always appreciated, distractions throughout my PhD. Finally, I would like to give very special thanks to my grandparents, my brother Guillaume and my parents Roger and Line, who have inspired me and who provided continuous, kind and unconditional support throughout my life.

Contributions of authors

Study 1 (Chapter 2)

Pelletier, G., & Fellows, L. K. (2019). A Critical Role for Human Ventromedial Frontal Lobe in Value Comparison of Complex Objects Based on Attribute Configuration. *The Journal of Neuroscience*, 39(21), 4124–4132. https://doi.org/10.1523/JNEUROSCI.2969-18.2019.

Study 2 (Chapter 3)

Pelletier, G., Aridan, N., Fellows, L. K., & Schonberg, T. The value of the whole is not merely the value of the sum of the parts — A neuroimaging investigation of multi-attribute object evaluation. *To be submitted for publication.*

Study 3 (Chapter 4)

Pelletier, G., & Fellows, L. K. (2020). Value Neglect: A Critical Role for Ventromedial Frontal Lobe in Learning the Value of Spatial Locations. *Cerebral Cortex*, 30(6), 3632–3643. https://doi.org/10.1093/cercor/bhz331.

In Study 1 and Study 3, Gabriel Pelletier planned the experiment and designed the experimental tasks, recruited participants, collected and analyzed the data and drafted the manuscripts. Lesley K Fellows was involved in the conceptualization of the studies, provided input on data analysis, critical revisions and final approval of the manuscripts.

In Study 2, Gabriel Pelletier planned the experiment and designed the experimental tasks, recruited participants, collected and analyzed the data and drafted the manuscript.

Nadav Aridan helped in recruiting participants and data collection, participated in data analysis and provided revisions on the manuscript. Lesley K Fellows was involved in the conceptualization of the study, provided critical revisions and final approval of the manuscript. Tom Schonberg was involved in the conceptualization of the study, provided input on data analysis, critical revisions and final approval the manuscript.

Other contributions

Aridan, N., Pelletier, G., Fellows, L. K., & Schonberg, T. (2019). Is ventromedial prefrontal cortex critical for behavior change without external reinforcement? *Neuropsychologia*, 124, 208–215. https://doi.org/10.1016/j.neuropsychologia.2018.12.008.

Chapter 1. Introduction

General introduction and thesis overview

The decisions we make shape the courses of our lives. In turn, our experiences influence how we perceive the world and changes our decisions. Humans demonstrate a remarkable flexibility in solving complex decision problems, integrating many sources of information, imagining the outcomes of alternatives never encountered, and trading-off various costs and benefits. From an evolutionary perspective, the development of the prefrontal cortex (PFC) and the increased complexity of the connections both within the PFC and with the rest of the brain are thought to have occurred as mammals evolved to live in more complex environments, requiring a wider behavioural repertoire and more refined decision-making (Teffer and Semendeferi, 2012). Early evidence that the PFC supports motivated decision-making came from patients suffering brain injuries, such as the classic case of Phineas Gage. After a head injury that likely caused extensive damage to the ventromedial frontal lobes (VMF), this patient had striking changes in personality and decision-making behaviour with serious consequences on his life (Damasio et al., 1994; Harlow, 1868). Since then, studies of the functions of VMF have repeatedly implicated this region in flexibly updating expectations of rewards and punishments as well as processing emotional content more generally, and in deploying this information to support decision-making (Murray et al., 2007a).

Recently, a new field of research has emerged at the interface of neuroscience and economics. Neuroeconomics focuses on the neural correlates of value-based decision-making, or, in other words, choices based on personal (subjective) preferences (Glimcher and Rustichini,

2004). The fields of economics and consumer research provide neuroscientists with a formal and quantifiable measure of subjective value, or 'utility'. Neuroeconomics research has sought evidence that this intrinsically personal variable is encoded in the brain. A large body of work has addressed the neural underpinnings of economic utility, providing converging support that a few regions, including the VMF, carry information that reflects subjective value (Bartra et al., 2013; Levy and Glimcher, 2012; Peters and Büchel, 2010).

Models inspired by economics have proven useful in laying the foundation of modern decision neuroscience. However, the focus on isolating subjective value as an abstract 'quantity' to find its neural signature means that decision neuroscience research has largely remained agnostic about how other domains of cognition typically viewed as lower-level such as perceptual processes, relate to this putative valuation system. In consequence, our understanding of the neurobiology of subjective value remains incomplete. It might even be that the economic utility view at the center of neuroeconomics since its inception is not the most appropriate way to understand the brain mechanisms involved in value-based choice. This thesis offers an alternative perspective on the study of subjective value. I will build on the known mechanisms through which the brain organizes visual information to better understand how value is constructed and how everyday decisions are made about real objects situated in actual spatial locations. I propose that the brain evolved to address such concrete choices, rather than the more abstract notions of risk and monetary amounts that are more often the focus of neuroeconomics. Bridging distant streams of neuroscience research, this thesis aims to refine our understanding of subjective value and adds to the current understanding of VMF functions.

In this chapter, I will first describe the anatomy of the VMF and its major connections, before providing a critical review of current neuroeconomics perspectives on the role of this region in reward-guided behaviour. I will then review key concepts regarding the brain basis of relevant higher-order visual-perceptual processes, notably object recognition and spatial cognition, and consider how subjective value processes might intersect with these systems. I will end with a brief overview of the research methods used in this thesis. The subsequent chapters present three studies providing evidence of the roles of the VMF in value-based decisions using experimental paradigms that were inspired by, or adapted from, the fields of object recognition and spatial cognition. I first tested the effects of VMF damage on value-based choices between complex objects in conditions relying on distinct object-processing mechanisms (Chapter 2). The second study presents converging and complementary evidence from functional neuroimaging on the involvement of the VMF and regions important for object recognition in choices between complex objects (Chapter 3). The last experiment examines the effect of VMF damage on choices based on the value of spatial locations, and tests whether decisions based on object- and spatial location-value associations are dissociable functions within VMF (Chapter 4). The thesis will conclude with a general discussion (Chapter 5) about the links across these studies and consideration of future directions in this effort to understand how perception and value are inter-related in the brain.

Anatomy of the ventromedial frontal lobe (VMF)

General anatomy of the VMF

The VMF is a large and heterogeneous region comprising several cytoarchitectonic areas. There is variability in the field of decision neuroscience in the anatomical nomenclature,

with different conventions employed according to the species and methods, and even across researchers using the same methods (Pearson et al., 2014). Thus, it is important to begin with a clear anatomical definition of the region of interest under scrutiny in this thesis.

Following the human lesion literature, we define the VMF as the region comprising the medial aspect of the orbitofrontal cortex (OFC), the gyrus rectus, and the ventral aspect of the anterior cingulate cortex and frontal pole (Fellows, 2011; Vaidya and Fellows, 2017). This broad region can be further described on the basis of microarchitecture using the cytoarchitectonic areas described by Brodmann (Brodmann, 1909, 2006). More recently these maps have been refined to identify homology across the macaque and human to facilitate cross-species comparisons (Petrides and Pandya, 1994; Petrides et al., 2012). **Figure 1.1A** shows the borders used to define the VMF region of interest, with a schematic depiction of the Petrides and Pandya (1994) cytoarchitectonic areas comprised in the VMF. On its medial aspect, the VMF includes area 25 and the ventral portion of areas 24, 32 and 10, bordered dorsally (for our purposes) by an arbitrary boundary at the genu of the corpus callosum. Area 14 spans the VMF's most ventral portion on the medial wall and the most medial portion of the orbital surface. The orbitofrontal surface of VMF also comprises areas 11 and 13 and is bordered laterally by the lateral orbital sulcus and area 47/12.

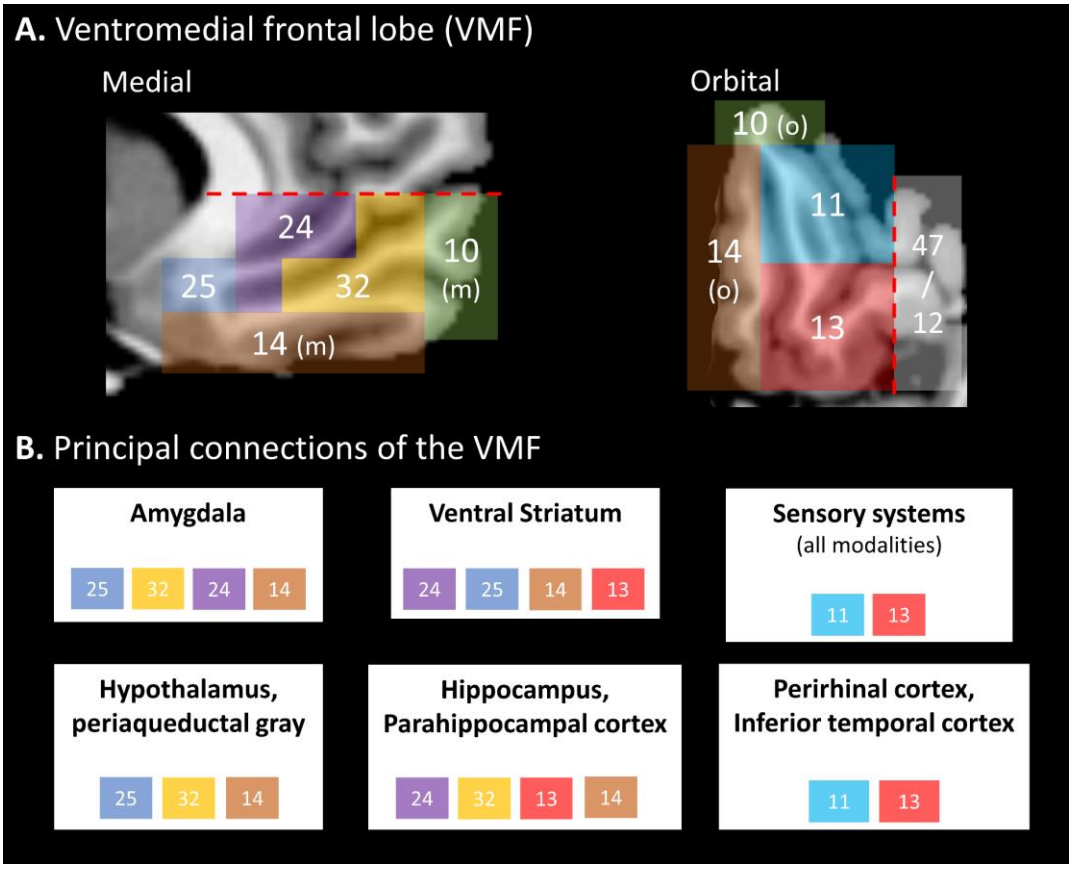

Figure 1.1. (**A**) The ventromedial frontal (VMF) region of interest used in this thesis and schematic depiction of the Petrides and Pandya (1994) cytoarchitectonic areas, superimposed on the MNI standard brain. Red dashed lines represent boundaries of the VMF regions of interest. (**B**) Non-exhaustive summary of the main connections between sub-regions of the VMF (colored squares), and other brain regions as described in this section. This graphical presentation does not address directionality of connections, although most are reciprocal, either through direct bi-directional connections, or with synaptic relays via other brain regions.

This definition of the VMF is common in studies examining the effect of prefrontal damage on reward-guided behaviour in humans. Studies of naturally occurring brain lesions typically have low spatial resolution due to the relatively large volume of damaged tissue and the variability in lesion volume and location across patients. Moreover, the medial OFC and the ventral aspect of the medial wall of the prefrontal cortex are commonly injured together. Further, lesions typically affect underlying white matter to varying degree. Thus, conclusions about the specific contributions of sub-regions within the VMF cannot typically be drawn with this method.

Studies using functional magnetic resonance imaging (fMRI) often report subjective value-related activations in the ventromedial prefrontal cortex (vmPFC). The term vmPFC is used in varying ways and is not clearly defined based on anatomical landmarks or architectonic areas. It most often is used to refer to the ventral portion of the medial wall of the PFC, although some researchers also include the medial orbitofrontal gyrus and the ventral-anterior ACC as part of the vmPFC. Mirroring this variability in activation loci, an influential meta-analysis that surveyed fMRI studies of the correlates of subjective value identified activity in a large vmPFC region, more or less the VMF as we define it here (Bartra et al., 2013). In this thesis, the region of interest is referred to as VMF except for the fMRI experiment reported in Chapter 3, in which the term vmPFC is used in keeping with the fMRI literature.

In contrast with neuroimaging work in humans, research in non-human primates commonly reports neural correlates of reward in medial orbitofrontal cortex (area 11 and 13) (Kennerley et al., 2008; Padoa-Schioppa and Assad, 2006; Rudebeck et al., 2013a) and rarely in the ventral portion of the medial wall (although see (Kaping et al., 2011)). It is unclear whether

this reflects cross-species differences in the neural correlates of decision variables or is due to the different methodologies. Functional MRI in humans has a notoriously poor signal detection sensitivity on the orbital surface (Deichmann et al., 2003), and the medial PFC is not readily accessible for single neuron recordings in macaques (Kaskan et al., 2017). Nevertheless, there is general agreement on similarities across macaques and humans in the position, cytoarchitectonic properties and connections of the areas of the VMF, indicating that this region of the PFC is comparable across species (Mackey and Petrides, 2010).

Connectivity and networks

The VMF receives and sends projections to large portions of the brain, and sub-regions within the VMF are densely interconnected with each other. **Figure 1.1B** presents a general summary of the main extrinsic connections of sub-regions of the VMF. Two major networks of the VMF were described based on axonal tracing studies in the macaque (Carmichael and Price, 1996; Price, 2007). The orbital network comprises areas 11 and 13, and receives inputs from most sensory systems, including auditory, somatosensory, olfactive regions, and, importantly for the research presented in this thesis, higher level associative visual areas including the perirhinal cortex and the inferior temporal cortex. The medial network on the other hand comprises the medial part of area 11 and area 14 on the orbital surface, and areas 10, 24, 25 and 32 on the medial wall. In contrast with the orbital network, the medial network does not have important connections with sensory regions. Instead, it is strongly interconnected with limbic structures such as the amygdala and has outputs to midbrain structures associated with the monitoring of visceral states in the hypothalamus and periaqueductal gray. Especially pertinent for the work presented here, the medial network also receives projections from the

hippocampus and parahippocampal cortex, as do areas of the orbital network but to a much lesser extent (Barbas, 2000).

The VMF further has extensive connections with temporal lobe regions through the uncinate fasciculus. The uncinate is a major white matter tract linking the perirhinal cortex, the entorhinal cortex and the temporal pole with the OFC (areas 11, 13) (Petrides and Pandya, 2007; Thiebaut de Schotten et al., 2012). Given these connections, the uncinate fasciculus might be important in supporting the mutual influence of associative-mnemonic processes and knowledge about reward and punishment history to guide motived behaviour (Heide et al., 2013).

In addition to connections with other areas of the cerebral cortex, VMF is tightly interconnected with the basal ganglia, especially with the striatum, a subcortical structure implicated in reward processing and value updating (Schultz et al., 1997). The ventral striatum receives afferent inputs from the medial OFC, as well as from medial PFC, and the ventral ACC (Haber, 2011). The striatum communicates back to the same VMF regions through cortico-striatal loops, relaying through the ventral pallidum and the thalamus (Ray and Price, 1993).

These connections provide VMF with unique access to rich sources of information about the external environment, internal states and memory systems (Rolls, 2006), making this region a plausible neural substrate for associating reward with various aspects of the environment, supporting the integration of information relevant to motivated behaviour.

Subjective value and the VMF

Evidence for a general role of VMF in value-based choice

Moment-to-moment decisions can be dramatically different; for example, one might need to choose between two job offers just after choosing a meal at a restaurant, then decide between doing the laundry or going for a walk. Choice alternatives may have no elements in common besides being considered in the same decision problem, and the values of the alternatives can be situated on very different scales from one decision to another. How are we capable of such flexibility in comparing alternatives and ultimately choosing what we expect will maximize positive outcomes across decisions varying from the trivial to the momentous? Economists have theorized that all types of expected rewards are converted to a common 'utility' scale used for comparison and choice (von Neumann et al., 1944; Samuelson, 1937, 1947). The notion of subjective value as a quantifiable, abstract variable allowed this inherently personal and internal phenomenon of preference to be viewed as a mathematically tractable construct. This, in turn, provided a framework to study the neurobiological mechanisms underlying decision making (Delgado et al., 2016; Glimcher and Rustichini, 2004).

A substantial effort has been made to identify the neural correlates of subjective value as defined by economic theory. Typically, subjective value estimates are obtained for several stimuli (e.g. food items, trinkets, and so on) for each participant through preference ratings, willingness to pay procedures, or inferred from a series of binary decisions, before searching for brain regions or neurons where activity tracks value. In a meta-analytic review of over 200 fMRI studies, Bartra and colleagues identified areas in which neural activity reflected subjective value (Bartra et al., 2013). They were interested in brain regions where blood oxygenation level

dependent response (BOLD) in these areas was positively correlated with subjective value, and dissociable from saliency or arousal signals, such that responses to very low value stimuli (negative valence) are the weakest and responses to very high value stimuli are the strongest. They sought regions that encoded value in a domain-general way, i.e. where BOLD signal varied parametrically with the value for multiple categories of stimuli and for different reward types. This analysis found that the VMF was the principal area which consistently met these criteria across published experiments using fMRI to study subjective value in humans. Value-related signal is also commonly observed in macaque VMF, using neurophysiological recordings. For example, firing rates of OFC neurons track the value of images predicting simple juice offers varying in taste and quantity (Hunt et al., 2018; Kennerley et al., 2011; Padoa-Schioppa and Assad, 2006; Wallis and Miller, 2003). Based on this body of work, the prevailing view is that the discrete "utility" quantity theorized from economic models has a neurobiological foundation, and that the VMF supports a neural "common currency" for value, independent of the perceptual cues that predict the reward and of the response required to obtain it (Bartra et al., 2013; Chib et al., 2009; Levy and Glimcher, 2012; Rangel et al., 2008).

Multi-attribute value construction

Despite this extensive body of work, how the brain instantiates an abstract value quantity supporting every decision is still unclear. There is some evidence that the VMF may act as a hub to integrate reward-related information from distributed regions. Most real-life choices involve alternatives made up of multiple value-related attributes. For instance, choosing between job offers, one might have to take into account the work environment, salary, proximity to home and so on in order to make the best decision. Behavioural economics

and psychology research suggests that such decisions arise from a constructive process: when faced with a decision problem, value is computed "on the fly" by assigning values to the individual attributes and then comparing between attributes across options or integrating the value of attributes within-options to make a choice (Bettman et al., 1998). This idea was partly motivated by the robust and replicable finding that manipulating the attributes of one option can affect the value of other unchanged options (Heath and Chatterjee, 1995; Huber et al., 1982; Simonson and Tversky, 1992). This evidence suggests that value is not merely revealed, but flexibly constructed within the course of a decision. This claim is further supported by studies using process tracing measures such as eye-tracking or mouse tracking, which demonstrate that the order in which attributes are sampled during the course of a decision depends, among other factors, on information provided by previously surveyed attributes, independent of the whole option's value (Hunt et al., 2018; Payne, 1976; Payne et al., 1988; Russo and Dosher, 1983).

Multi-attribute value assignment has not yet been studied extensively from a neuroscience perspective. Work to date suggests that the values associated with component attributes are separately represented in the brain, and that signal in the VMF reflects the combined value of attributes (i.e. whole option value) (Basten et al., 2010; Berker et al., 2019; Kahnt et al., 2011; Kurtz-David et al., 2019; Lim et al., 2013; Park et al., 2011; Philiastides et al., 2010; Suzuki et al., 2017). Further, when the goals of the decision-maker are manipulated to change the weight of specific attributes, as revealed by choice behaviour, changes in how those attributes are weighted are reflected in VMF value signal (Hare et al., 2009, 2011a; Rudorf and

Hare, 2014). These studies are consistent with the proposal that the VMF integrates information relating to component attributes to build whole option value representations.

Inconsistencies in the current models of value-based choice

If, in fact, VMF is integrating multiple attribute values into a common currency signal, which is then drawn on for option comparison and choice, then VMF damage should disrupt decisions in general, independent of *what* is being decided upon, and decisions requiring the integration of multiple attributes should be more impaired than decisions between simpler options. However, causal evidence supporting these predictions is still lacking: Indeed, existing lesion work yields mixed support for this neuroeconomic view of VMF as a general value-integration or value-tracking region.

Studies found that damage to the VMF disrupts value-based behaviour, leading to inconsistent preference judgements and sub-optimal decisions based on reward history in humans (Bechara et al., 1997; Camille et al., 2011a; Fellows and Farah, 2007; Henri-Bhargava et al., 2012) as well as in non-human primates (Rudebeck and Murray, 2011; Rudebeck et al., 2013a). While this evidence is consistent with the view that VMF codes for a general economic value quantity, closer examination of the effects of VMF damage on multi-attribute decisions suggests a more nuanced picture. In a political choice task, VMF patients showed normal and consistent ratings of distinct attributes (i.e. attractiveness and perceived competence) of hypothetical political candidates, but analysis of subsequent binary choices between the same candidates showed that VMF damage affected how these attributes were used to guide choice (Xia et al., 2015). Healthy and frontal-damaged controls made choices as though they

considered both attributes, whereas choices of the VMF group were only predicted by attractiveness ratings. This suggested that either VMF is critical for constructing value from more than one attribute, or is specifically required to interpret the value of certain classes of attributes.

In another experiment, participants made decisions between hypothetical life partners (spouses) and between hypothetical houses in a task where options were characterized by multiple (explicitly defined) attributes, and where the number of attributes per option varied across trials (Bowren et al., 2018). Following the choice task, participants rated the value and degree of importance of each attribute individually. Choice consistency was then calculated, defined as the number of trials where the chosen option had the greatest value as defined by summing the value rating for each attribute, modulated by the importance rating (weight) for that attribute. Bowren and colleagues found that VMF damage led to worse choice consistency in the spouse condition, but spared decisions between houses, again arguing against a generic role for the VMF in value-based choice. Furthermore, in both conditions, VMF damage did not lead to more inconsistent decisions involving more attributes per options compared to simpler decisions, suggesting that this region is not required to integrate information across attributes in a general sense.

Another study found that VMF patients can make internally consistent value ratings for complex visual stimuli (works of art), but how they weighted different attributes to arrive at that value judgment systematically differed from controls (Vaidya et al., 2018). Simpler, directly visually accessible attributes such as color balance were relied upon just as much in VMF participants and control groups, but more complex attributes such as the emotionality of the

artworks were underweighted after VMF damage. Again, this finding is not consistent with a general value integration deficit, pointing perhaps to a more specific role for VMF in using complex, not directly observable information to determine value.

This idea is supported by lesion work in animal models. In non-human primates, OFC lesions led to a deficit in updating the value of an object predictive of food reward after the animals were sated with that food, a manipulation which, in intact subjects, leads the object to be selected less often than an object paired with a non-sated food (Izquierdo et al., 2004; Rudebeck and Murray, 2011). However, OFC-lesioned monkeys performed indistinguishably from controls when deciding between the sated and non-sated foods directly, indicating that OFC damage does not disrupt updating the value of food options themselves, but only of the associated objects. Studies in rats similarly found that OFC lesions impair decisions when value has to be inferred through stimulus-stimulus association, but not when value was directly paired with a stimulus (Gallagher et al., 1999; Jones et al., 2012). This body of work suggests that the OFC has a critical role in deciding based on value information only accessible through representations of the associative structure linking elements of experiences, and not in integrating the values directly paired with sensory cues to the choice process.

To sum up, existing lesion evidence suggests that VMF is not critical for all value-based decisions and is not necessary for value integration under all conditions. Instead, this region might only be needed to integrate certain types of information. This calls for a more nuanced view of VMF's role in value assessment and underlines the needs to define the conditions under which VMF is necessary for value-based decision-making. Why VMF would be required for the integration of some sources of information and not others for decision-making is an open

question. I suggest this requires reconsideration of the view that the brain represents subjective value as a common currency. One approach, pursued here, is to examine the involvement of the VMF in value-based decisions requiring different sensory pathways and associative structures between sensory cues and value.

Associative learning research has shown that learning about outcomes predicted by cues or attributes of objects individually (elemental learning) and learning about specific configuration of cues (configural learning) are dissociable processes supported by different brain regions (Duncan et al., 2018; Melchers et al., 2008; Rudy and Sutherland, 1995). So far, decision neuroscience has examined choices between multi-attribute options from an elemental perspective, i.e. attributes are assumed to be individually evaluated and to independently contribute to overall valuation. However, many real-life decisions likely involve evaluating attribute configurations. For instance, when deciding between which meal to order from a restaurant menu, we typically do not consider each listed ingredient in isolation to estimate the overall value of a dish. We instead grasp the configuration of ingredients to estimate how delicious it could be. It is unclear whether decisions based on elemental and configural value associations rely on separate neural substrates, but one possibility from the lesion evidence reviewed above is that VMF is required to integrate higher-level information for value estimations, in the sense that those values must be inferred from the configural association among lower-level attributes.

A second gap in the common currency hypothesis is the lack of causal evidence supporting domain-general value representations in the VMF. Lesion work in humans and macaque has found double dissociation between action- and stimulus-value learning, the latter

being impaired after VMF damage, and the former being impaired after dorsal-medial PFC damage (Camille et al., 2011b; Rudebeck et al., 2008). This is evidence of distinct neural pathways for object- and action-value associations and suggests that the role of the VMF is material-specific to some degree. From a perceptual perspective, dissociable dorsal and ventral anatomical pathways are involved in the processing of visual information relating to spatial locations and action generation, and information relating to object recognition respectively (Ungerleider and Mishkin, 1982) (reviewed below). Previous work implicating VMF in value-related processes has largely focused on choices between "goods", typically food items, complex real-world objects, or artificial objects stimuli (shapes and colors) associated with rewards. The literature is largely silent on choices driven by the value of *where* objects are located, rather than *what* they are. Such choices are of relevance in the context of foraging for instance, where animals can learn that the upper part of a tree usually contains the sweetest fruits and so climb higher to get them (Trapanese et al., 2018). For the moment, it is unclear whether the role of VMF in value-based decisions between objects extends to decisions based on the value of spatial locations.

We still have a very incomplete understanding of the neurobiological basis of value-based decisions. Isolating value as an abstract quantity has provided the field of decision neuroscience with elegant means to track its neural representation, notably in VMF, but does not account for several findings in VMF-lesioned patients. This thesis proposes a shift to away from the economic utility framework and towards a view grounded in what is known about perception, relating value to the information that it is associated with and leveraging the known brain mechanisms involved in the processing of that information. This thesis focuses on visually

presented decision options; thus, I will next describe some of the major organising principles of visual perception, and review evidence that value might be intricately tied with these processing streams.

Real-life decisions do not exclusively draw on vision, and often involve information processed through all senses which together contribute to a holistic appreciation. Although neuroimaging studies have found that VMF signal also correlates with the subjective value of odors (Howard et al., 2015), sounds (Salimpoor et al., 2015), and tastes (Grabenhorst et al., 2010), how the brain integrates multimodal value-relevant information to guide choice is still unclear. This interesting issue, while not the focus of the experiments in this thesis, will be returned to in Chapter 5.

Object recognition and value processing in the ventral visual stream

The ventral visual stream for object recognition

There is substantial evidence that the visual system is organized in two major pathways: a dorsal stream for the processing of spatial locations and actions, coursing from the occipital lobe dorsally through the parietal cortex, and the ventral visual stream (VVS) important for object recognition, coursing from the occipital pole through the ventral temporal cortex (Goodale and Milner, 1992; Macko et al., 1982; Mishkin et al., 1983; Ungerleider and Mishkin, 1982). The VVS is a hierarchically organized processing stream believed to transform inputs from the retina into holistic object representations robust to changes in low-level visual features such as lighting, location, orientation and size. As visual processing travels anteriorly from occipital lobe regions (v1, v2) to the ventral temporal cortex, each stage integrates inputs

from lower stages, leading to neural representations that are increasingly complex and detached from low-level visual properties.

Strong evidence for this hierarchical framework was provided by axonal tracing and electrophysiological recordings in monkeys demonstrating rich direct connections among VVS regions, paired with a posterior-anterior increasing gradient in response latency and increasing size of the neuronal receptive field (Kravitz et al., 2011; Rousselet et al., 2004). In addition to the properties of single neurons, evidence for hierarchical object processing at a larger, macro-scale is supported by lesion and neuroimaging work in humans and non-human primates. Several studies found that damage to the perirhinal cortex (PRC), a structure located anteriorly in the medial temporal lobe, impairs discrimination between complex objects in configural conditions, requiring the recognition of specific combinations of attributes (i.e. in conditions where several objects share multiple attributes), but spares object discrimination in elemental conditions, when it can be achieved on the basis individual attributes (Barense et al., 2007; Bussey et al., 2002, 2003; Rudy and Sutherland, 1995). Functional MRI and positron emission tomography studies in healthy participants in a task requiring object recognition in different viewing conditions found that PRC activity was more sensitive to whole objects and less sensitive to changes in viewpoint compared to the lateral occipital complex (LOC), situated earlier in the VVS hierarchy (Devlin and Price, 2007; Erez et al., 2016). The LOC, on the other hand, was found to be more sensitive to the specific attributes of an object and less to the configuration of attributes compared to the PRC (Erez et al., 2016). This body of work led to the proposal that posterior regions of the hierarchy achieve attribute-level recognition, feeding converging inputs to successive stages to ultimately achieve configural object recognition at the

apex of the VVS, in the PRC (Bussey and Saksida, 2002; Cowell et al., 2006; Saksida and Bussey, 2010). Importantly, this model states that attribute-level representations at lower levels and whole object representations at the highest level of the hierarchy can be independently associated with outcomes, which is consistent with the finding that disruption of the PRC does not impair behaviour in task relying on single-attribute discrimination.

Value representations in the visual cortex

Most studies of VVS function have focussed on its role in transforming external inputs from the retina into meaningful object representations, which are typically thought to be passed on to memory and executive centers to support higher-order functions such as decision-making and categorization. A handful of fMRI studies directly asked whether visual regions might also be involved in processing the values of well-learned objects. In humans, BOLD signal in early visual cortex (V1 and V2) was modulated by the value associated with the color of a shape (Serences, 2008), and was stronger when observing reward-predicting shapes compared to neutral ones in macaques (Nelissen et al., 2012). Another study in non-human primates found value modulation in BOLD response to objects in a more anterior VVS region; the object-selective inferotemporal cortex (IT) (Kaskan et al., 2017), likely a homolog of the human LOC (Grill-Spector et al., 2001). While this evidence suggests that value might be processed in the VVS, these studies cannot clearly disentangle the effects of subjective value and saliency (Maunsell, 2004). As a result, BOLD responses interpreted as value representations might instead reflect increased top-down attention to value-associated stimuli. Selective attention is known to enhance activity in the visual cortex (Maunsell and Cook, 2002; Moran and Desimone, 1985).

In an effort to mitigate these limitations, Persichetti and colleagues used an adaptation fMRI design in humans to examine the similarity of responses to objects associated with a range of positive and negative values, while attention was diverted away from the stimuli. They showed that BOLD signal in the VVS, from V1 to the LOC, was sensitive to the value of objects (maximally different signal between high gains and high losses), over and above effects of behavioural saliency (i.e. reflected in similar signal between high gains and high losses) (Persichetti et al., 2015). In addition, another fMRI study in macaques found that the receipt of a reward learned to be predicted by an object, but delivered in the absence of any visual stimulation, enhanced BOLD signal in the same VVS voxels involved in the visual processing of the value-predicting object, spanning from V1 to area IT (Arsenault et al., 2013). This work argues that subjective value *per se*, in addition to attention or saliency, is represented in the VVS.

Additional support for this idea was provided by a study in macaques using single-unit recordings that allow insights into the timing of VVS value-related signals (Mogami and Tanaka, 2006). Activity was recorded at a high temporal resolution in two successive regions of the VVS sharing direct connections; area IT and the PRC. Consistent with the view that the PRC is situated higher in the visual processing hierarchy than IT, firing patterns of IT neurons exhibited object selectivity slightly sooner after stimulus onset than PRC neurons. Firing rates in both regions were also modulated by object value. This effect was more reliable in PRC than in IT, and value selectivity again emerged faster after stimulus onset in IT than in the PRC. These data are not consistent with value modulation reflecting attention or feedback from putative value

regions that serially back-propagate down the VVS. Instead, they suggest that object-value might be processed in part within the ventral-visual stream circuitry during object recognition.

In this section, I provided an overview of the hierarchical model of object processing along the VVS, wired to incrementally integrate visual information from early visual cortex, to the representations of object attributes in the LOC and ultimately form configural object representations in the PRC. I then presented emerging evidence suggesting that regions across the VVS, including LOC and PRC, might have a role in processing the subjective value of objects in addition to their physical properties.

If value is processed at different stages of the VVS, could it be that that value construction for multi-attribute options might be at least partially occurring in the VVS? This question remains largely unanswered, partially because of the sparse crosstalk between decision neuroscience and object processing research. Echoing hierarchical organization in the VVS, a study of multi-attribute decisions found that choice behaviour and neural data were best explained by a computational model leveraging both attribute values and whole option values (integrated across attributes) (Hunt et al., 2014), suggesting that value construction might occur as object recognition unfolds, from elemental attribute recognition and value computation at earlier VVS stages, up to configural object recognition and the processing of the holistic associated value at later stages. The second and third chapters of this thesis directly address the gap between object processing and multi-attribute value-based choice research by examining value-based decisions for complex objects in conditions known to rely on distinct stages of the object processing hierarchy.

Spatial cognition and reward

Research on rewarded-guided decisions to date has focused on choices based on value associated with the identity of stimuli (e.g. I prefer red over green apples). Little is known about the mechanisms of value-based choice based on *where* options are, rather than *what* they are, despite the importance of spatial location for many decisions. In rodents, approach or avoidance responses can be triggered by the spatial location of a visual stimulus on the retina, as a fast approaching shadow in the upper part of the visual field likely signals a predator whereas something detected in the lower visual field is likely to be a prey or a feeding source (Comoli et al., 2012). Rodents and primates can also use more complex spatial information stored in memory to navigate to previously rewarded locations in the environment (Trapanese et al., 2018). This exemplifies two distinct classes of reference frames for spatial cognition. Egocentric reference systems (i.e. retinotopic, body-centered) are involved in the perception of the immediate surroundings. Allocentric reference frames are anchored in the environment, making them invariant to the location and orientation of the observer, critical for goal-directed navigation. I will next provide an overview of these two systems of spatial cognition and describe how value might intersect with spatial information to drive decision-making.

The dorsal visual stream and egocentric reference frame

The dorsal visual stream courses from the occipital cortex dorsally to the posterior parietal lobule and is specialized in the processing of visual inputs that relate to object location, size, orientation and motion. This stream is thought to process aspects of stimuli appearing in the contralateral visual field for the purposes of generating motor actions to act upon the stimuli (Goodale and Milner, 1992; Mishkin et al., 1983). Retinotopic representations early in

the dorsal visual stream give rise to a variety of egocentric spatial representations mapping out the immediate environment in relation to the observer's body, head, eyes and limbs (Kravitz et al., 2011).

Egocentric spatial representations are thought to be the canvas for the deployment of spatial attention at the intersection of the dorsal visual stream and the frontoparietal attention network (Corbetta and Shulman, 2011). It has been proposed that the behavioural relevance of all locations of the visual field is represented in an attentional priority map which integrates low-level visual saliency with top-down signals relating to goals and prior knowledge (Fecteau and Munoz, 2006; Gottlieb, 2007; Klink et al., 2014; Ptak, 2012). According to this model, the location with the highest priority has a competitive advantage for attentional orienting, facilitating the detection of behaviourally relevant targets in cluttered scenes. Studies have shown that objects associated with higher rewards can 'capture' attention. They are more likely to be fixated first, are detected faster and are more likely to be chosen (Anderson, 2015; Anderson et al., 2011; Chelazzi et al., 2013), consistent with the idea that locations in the visual field at which high-value stimuli appear gain attentional priority. Another study manipulated the values of spatial locations themselves, and found that associating reward to targets appearing in a given spatial location, regardless of the target's identity, confers an attentional advantage to this location in a subsequent unrelated task in the same spatial environment (Chelazzi et al., 2014). This work provides evidence that spatial locations can gain incentive value through reward feedback, and that learned values modulate egocentric spatial representations.

As opposed to value learned from multiple experiences, the relative location of stimuli in relation to the observer is not a stable property; whereas the location of a known feeding site in relation to an animal's position changes whether it is coming from the north or the east, the expected value of this location based on acquired knowledge about its abundance should remain unchanged. Thus, it is unlikely that the egocentric spatial reference frame supports value-based decisions based on the value of spatial locations alone. Research in patients with unilateral neglect provides support for this claim: Such patients suffer from deficits in orienting attention in egocentric space typically after lesions in the right hemisphere to the inferior parietal lobule, inferior frontal gyrus and/or superior temporal gyrus, which disrupt processing in the frontoparietal network (Corbetta and Shulman, 2011; Karnath et al., 2011; Mesulam, 1999). Lucas and colleagues found that in a search task, when the reward associated with the selection of a target was evenly distributed across the screen, neglect patients mainly chose targets appearing in their ipsilesional hemifield and neglected targets on the contralesional side, as expected (Lucas et al., 2013). However, when a reward bias was introduced such that targets appearing in the neglected hemifield were more rewarded, patients exhibited a selection bias towards those targets. Moreover, the extent of the reward-induced spatial bias was similar in patients and healthy controls. Although this perhaps surprising finding has not yet been replicated or extended, it suggests that the value associated with spatial information can weigh in decisions even when the attentional priority maps of egocentric space are disrupted by damage to the frontoparietal network, arguing that other brain mechanisms might support the biasing of decisions to rewarded locations. VMF is a candidate region for providing

the value signal required for such biasing, but whether it is involved in this process has not been tested.

Spatial navigation and the allocentric reference frame

In parallel to fronto-parietal egocentric spatial representations to support detection of and reaching to behaviorally relevant targets, the brain also encodes spatial information in a separate allocentric reference frame supported by the medial temporal lobe (Burgess, 2006; Zaehle et al., 2007). Cells in which activity is modulated as a function of the location of an animal in a coordinate system anchored in the outside world, independently of the orientation of the observer (i.e. allocentric) have been found in the hippocampus of rats (O'Keefe and Nadel, 1978), monkeys (Rolls and O'Mara, 1995) and humans (Ekstrom et al., 2003). Place-selective cells in the hippocampus converge on grid cells in the entorhinal cortex to form a neural 'map' which animals rely upon to navigate in the environment (McNaughton et al., 2006).

An extensive body of research using conditioned place preference paradigms in rodents demonstrates that spatial locations encoded in an allocentric reference frame can gain incentive value. Studies have shown that the hippocampus has a causal role in the acquisition and retrieval of spatial location-value associations using food and drug reinforcers (Tzschentke, 2007). Optogenetic manipulations in rats have shown that the activation of hippocampal place cells at the time of reward delivery is critical to inducing a preference for this location (Trouche et al., 2016). Another study using neuronal recordings found that pairing a location with reward selectively enhances activity in the hippocampal place cells which encode the rewarded

location, and strengthens functional coupling between these cells and dopaminergic neurons in the striatum (Sjulson et al., 2018). These data argue that allocentric hippocampal maps store information regarding rewards available in the environment, suggesting that this system is not merely a neutral, objective map but additionally contains information regarding the motivational relevance of spatial locations.

In contrast to this rodent literature, there has been little research on the neural basis of decision-making based on the value associated with allocentric spatial locations in humans. Only indirect evidence is available from studies in which participants navigate a virtual environment aiming to reach an instructed goal location to receive a generic reward, with no value-based decision-making required. A study using intracranial recordings in humans during spatial navigation revealed that activity in hippocampus place selective cells is sensitive to the proximity of a rewarded location (Ekstrom et al., 2003). A neuroimaging study similarly found that BOLD signal in the hippocampus and in the VMF was positively correlated with the distance from a goal (i.e. the closer the reward, the greater the BOLD signal) (Viard et al., 2011). It was also found that VMF damage in humans disrupts spatial navigation to a rewarded goal (Dahmani et al., 2018). Theses studies suggest that in addition to the hippocampus, the VMF might be involved in spatial navigation tasks where performance is rewarded. However, these data do not directly address whether VMF is required for assigning value to spatial locations to influence decision-making. To sum up, evidence from animal models suggests that hippocampus allocentric spatial representations might store the value of 'where', but it remains unclear whether the VMF is involved in leveraging allocentric spatial location-value associations to drive choice.

The allocentric and egocentric spatial reference systems are not mutually exclusive; they are deployed in parallel and interact with each other depending on task demands (Burgess, 2006). It has been proposed that the frontoparietal network might integrate location-value associations from the hippocampus, among many other inputs involved in the formation of attentional priority maps of egocentric space (Klink et al., 2014). Studies have found that the VMF has a role in guiding attention to reward-predictive attributes of objects (Vaidya and Fellows, 2015a), suggesting that this region is important in tagging choice-relevant dimensions to modulate attentional priority maps, leading to a biasing of attention and in turn a biasing of choice towards objects with higher-value attributes. It remains unclear whether this role of the VMF in directing attention to rewarded object features generalizes to rewarded spatial locations.

The fourth chapter of this thesis provides a first step in answering these unresolved questions by testing whether VMF has a causal role in decisions based on spatial location-value associations. We further explored whether decision-making based on the value of locations and objects are dissociable processes within the VMF or are systematically disrupted together.

Overview of the methods used in this thesis

To study complex cognitive processes such as decision-making in humans, multiple methods are important to gather converging evidence, drawing on the strengths and offsetting the limitations of different techniques. Triangulation, whereby a research question is tackled with different methodological approaches, improves the replicability of findings and helps to mitigate the systematic biases inherent to any one research technique, which might lead to

incorrect conclusions, regardless of how often results using that single method were replicated (Lawlor et al., 2016; Munafò and Smith, 2018). This thesis contains original research using human lesion methodology and functional MRI, which I will briefly describe with an emphasis on a few key points relevant to the work presented here.

Human lesion methodology

The study of behavioural change caused by focal brain damage is at the foundation of cognitive neuroscience, and despite the advent of non-invasive *in vivo* neuroimaging methods, is still of relevance due to the power of this methodology to draw causal links between a brain region and a cognitive function (Vaidya et al., 2019). Whereas the first major contributions in cognitive neuroscience came from single case reports (e.g. (Harlow, 1868; Scoville and Milner, 1957)), modern lesion studies typically compare groups of patients with well-matched control groups, which helps in mitigating effects due to inter-individual differences in premorbid cognitive functions.

Lesion studies can be broadly classified as either behaviour-based, where patients with similar behavioural symptoms are grouped together before examining whether the deficit is systematically associated with damage to a common structure, or lesion-based. This thesis provides a lesion-based approach, whereby patients are grouped according to the anatomical area affected by the lesion, before comparing behavioural performance between groups in carefully designed experimental tasks. This approach is hypothesis-driven and is well suited to test the contribution of an *a priori* defined region of interest (ROI) to a given function.

Experimental paradigms designed to study decision-making always involve additional cognitive functions that are not the focus of scrutiny. Thorough neuropsychological characterisation of patients with tests that tap those additional cognitive functions is important to control for potential confounding deficits. In addition, the inclusion of control tasks tailored to the experimental paradigm of interest further helps in narrowing down the interpretation of the observed deficits. The extent of neuropsychological screening and inclusion of additional tasks are often limited by practical considerations, primarily the time and effort which patients can offer (Fellows et al., 2008).

Brain damage in human participants are obviously not under experimental control. As a result, there is variability in lesion extent and location within patient groups, with damage often extending beyond the boundaries of the ROI. The inclusion of a lesioned control group, composed of subjects with brain damage elsewhere, sparing the ROI, allows more confidence as to the anatomical specificity of the observed deficit. In addition, other factors common to brain lesion patients that are not shared by healthy controls (e.g. psychoactive medications, comorbidities) can be mitigated by the addition of a lesioned control group.

A major contribution of lesion studies to contemporary neuroscience is the possibility of isolating component processes of complex behaviours, by showing that one or more brain areas is necessary for the process, and by demonstrating dissociations, i.e. that one component process is spared while another is impaired if brain area X is damaged. Demonstrating a dissociation is not trivial, as one criterion ('spared') relies on the statistical null finding of no significant difference between groups. To meet criteria for a dissociation, a case must be significantly impaired in task A but not in task B and, additionally, the difference between the

case's performance in task A and task B must be significantly abnormal compared with the difference observed in the normative sample (Crawford and Garthwaite, 2006; Crawford et al., 2010).

Lesion studies are inferentially powerful but have limitations. Brain lesions in humans are not random in their anatomical distribution, following patterns that relate to the underlying etiology. For example, strokes follow vascular territories. In consequence, some brain regions are commonly injured together, which can hinder the interpretation of structure-function relationships (Rorden et al., 2007). Damage is not necessarily restricted to neurons in the gray matter of the injured territory, but might affect underlying white matter tracts, including fibres of passage, potentially disrupting brain function distant from the lesion site (Rudebeck and Murray, 2011; Rudebeck et al., 2013b). Finally, whereas it is possible to interrogate multiple regions of interest within the same study given a large enough patient sample with distributed lesions (e.g. (Vaidya and Fellows, 2015b, 2016)), it is not feasible with human lesion methodology to examine whether and how brain regions interact to support behaviour, or to ask questions regarding the temporal dynamics of the involvement of several brain regions during an experimental task.

Functional MRI

Functional MRI is used to study the healthy brain non-invasively. This method has better spatial resolution than lesion methodology and allows activity across the whole brain to be observed simultaneously. FMRI measures changes in oxygenated compared to deoxygenated blood flow (blood oxygen level-dependent or BOLD signal), which provides an indirect measure

of the level of activation of neuronal ensembles. In consequence, fMRI is a correlative method, providing evidence about which voxels (volumetric unit for MRI signal) are more or less active during a condition relatively to another condition or baseline. No conclusions can be drawn about whether the observed signal is causally involved in the behaviour (Logothetis, 2008).

The advent of fMRI revolutionized the study of human brain function, but while this technique has become widely popular in cognitive neuroscience, it comes with serious limitations which are of increasing concern to the scientific community. Signal recorded with fMRI only indirectly relates to neuronal activation and is very sensitive to external non-neuronal factors, leading to a very low signal-to-noise ratio. This, along with typically small sample sizes due to high operating costs, means that fMRI research has suffered from low power to detect effects of interest (Button et al., 2013). In addition, extensive pre-processing and numerous analysis steps are required before raw fMRI data can be interpreted, each of which can be carried out in several possible ways at the discretion of the researcher. The countless researcher degrees of freedom in fMRI analysis paired with the low power issue is associated with very low replicability and high false positive rates in neuroimaging research (Botvinik-Nezer et al., 2020a; Button et al., 2013; Carp, 2012).

One way to mitigate these issues is through pre-registration. Publicly registering the hypotheses, detailed analysis plan and sample size before collecting data limits the opportunistic use of the researcher's degrees of freedom oriented towards obtaining statistically significant results in desired or expected regions (a.k.a. p-hacking) (Wicherts et al., 2016). Pre-registration is commonplace and even mandatory in other fields such as clinical trials, and there are calls to increase its use in neuroscience in order to improve replicability and

strengthen the community's confidence in conclusions drawn from fMRI studies (Nosek et al., 2018; Poldrack et al., 2017).

Power in fMRI research can be improved by using region-of-interest approaches (Poldrack, 2007). Mass univariate analysis of neuroimaging data necessitates stringent statistical correction for multiple comparisons because of the large number of units (brain voxels) independently tested for an effect. Restricting analyses to pre-specified ROIs greatly reduces the number of comparisons to correct for, increasing the potential to detect task effects. However, ROIs must be defined prior to data analysis to avoid statistical fallacies due to circularity in data analysis (i.e. double dipping) (Kriegeskorte et al., 2009). Thus, such designs are heavily hypothesis driven and, paired with pre-registration, provide stronger conclusions than exploratory whole-brain analyses which are likely to be underpowered.

This thesis takes a triangulation approach with an fMRI experiment (Chapter 3) using a similar paradigm and based on the findings of a lesion study (Chapter 2). We adopted a region of interest approach to fMRI analysis, based on our own prior work in lesion patients and the existing fMRI literature. The detailed hypotheses, analysis plan, regions of interests, and sample size for the fMRI study were publicly pre-registered.

Specific aims of the thesis

In this chapter, I reviewed how subjective value is currently conceptualized in decision neuroscience and pointed to inconsistencies in current models of VMF contributions to value-guided behaviour. I further highlighted the gaps in knowledge between the neural processes

underlying our ability to recognize objects and navigate our environment, and those underlying subjective value which support decisions about the goals we will pursue in that environment.

The overarching aim of this thesis is to refine our understanding of VMF contributions to value-based decisions. Novel experimental paradigms were designed to manipulate the value of visual stimuli and examine the neural substrates of this value assignment. First, I tested the effects of VMF damage on value-based choices between complex objects in two conditions known to rely on distinct object-processing regions, by experimentally associating value with individual (elemental) attributes or whole (configural) objects (Chapter 2). The second study used functional neuroimaging to complement the findings of the first study by simultaneously probing activity in the VMF and in the VVS during value estimation of complex objects (Chapter 3). Last, I tested the effect of VMF damage on decisions in which value was a function of spatial location (Chapter 4).

Decision-making based on expected rewards is a major determinant of human behaviour. Yet, we have an incomplete understanding of how the brain represents subjective value and how such representations relate to the neural mechanisms supporting other aspects of cognition. This thesis offers a fresh perspective on the study of value-driven behaviour. This work provides evidence that subjective value is better understood in relation to how the brain perceives the world rather than as an abstract quantity.

Chapter 2. A critical role for human ventromedial frontal lobe in value comparison of complex objects based on attribute configuration

Preface

Neuroimaging studies of multi-attribute decision-making have implicated the VMF in elemental value integration, whereby attributes are separately valued, and integrated in whole option-value representations (Basten et al., 2010; Lim et al., 2013). Studies in patients with VMF damage instead suggest that the VMF might be more narrowly involved in inferring value from configural associations between attributes (Vaidya and Fellows, 2020). Object processing research has established that the recognition of elemental attributes of objects and the recognition of whole objects from attribute configurations rely on dissociable neural substrates within the VVS. However, no work has directly tested whether brain regions that carry value signals are sensitive to whether value is predicted by elemental or configural characteristics of decision options.

In this study, published in The Journal of Neuroscience, we leveraged object processing research to design experimental conditions in which value was associated either with elemental attributes or attribute configurations through reward learning. We tested whether VMF damage disrupted decisions based on the integration of elemental attribute-values, on the configural association between attributes, or both.

A Critical Role for Human Ventromedial Frontal Lobe in Value Comparison of Complex Objects Based on Attribute [*]

Gabriel Pelletier and Lesley K. Fellows

Department of Neurology & Neurosurgery, Montreal Neurological Institute, Faculty of Medicine, McGill University

[*] Original source: Pelletier, G., & Fellows, L. K. (2019). A Critical Role for Human Ventromedial Frontal Lobe in Value Comparison of Complex Objects Based on Attribute Configuration. The Journal of Neuroscience, 39(21), 4124–4132. https://doi.org/10.1523/JNEUROSCI.2969-18.2019

Abstract

In making decisions, we often choose from among options with multiple value-relevant attributes. Neuroeconomic models propose that the value associated with each attribute is integrated in a global value for each option. However, some evidence from patients with ventromedial frontal lobe (VMF) damage argues against a very general role for this region in value integration, suggesting instead that it contributes critically to a specific value inference or comparison process. Here, we tested value-based decision-making involving artificial multi-attribute objects in humans with focal damage to the VMF (N = 12) compared with a healthy group matched for age and education (N = 24) and with a group with frontal lobe damage sparing the VMF (N = 12). In a "configural" condition, overall object value was predicted by the conjunction of two attributes, while in an "elemental" condition, object value could be assessed by combining the independent values of individual attributes. Patients with VMF damage were impaired in making choices when value was uniquely predicted by the configuration of attributes, but intact when choosing based on elemental attribute values. This is evidence that the VMF is critical for inferring the value of whole objects in a multi-attribute choice. These findings have implications for models of value-based choice and add to emerging views of how this region may interact with medial temporal lobe systems involved in configural object processing and relational memory.

Significance statement

Neuroeconomic models propose that the ventromedial frontal lobe (VMF) supports multi-attribute decisions by integrating the values of attributes. However, researchers have been uncertain about the underlying mechanisms for this process. Patients with VMF damage made multi-attribute choices under two conditions: in one, attribute values could be summed to guide choice; in the other, value was predicted by the conjunction of attributes. VMF damage impaired only the latter. This argues that the VMF is critical for inferring value from configural information to guide multi-attribute object choice. This region may be key for judging the emergent "value of the forest," rather than for integrating the individual "value of each tree."

Introduction

In making decisions, we often choose among options with multiple attributes. For instance, snacks can be characterized on taste, price, and healthiness. Individual attributes might directly predict subjective value: if one craves sweets, chocolate will be valued over peanuts. However, value can also emerge from the interaction of attributes. For example, for those who enjoy sucré-salé flavors, the combination of peanuts and chocolate in the same snack would yield a value greater than the sum of the value of each attribute.

Neuroeconomic models propose that subjective value is encoded in a common currency within the ventral prefrontal cortex (Bartra et al., 2013). The overall value of objects composed of multiple value-predictive attributes (e.g., colors and shapes associated with monetary rewards) can be decoded from spatially distributed patterns of BOLD activity in the human ventromedial prefrontal cortex (vmPFC; (Kahnt et al., 2011)). Researchers have likewise found within the vmPFC or adjacent medial orbitofrontal cortex (OFC) signals reflecting value derived from the nutrient components of food items (Suzuki et al., 2017), monetary costs and benefits (Basten et al., 2010), and esthetic and semantic aspects of T-shirt graphics (Lim et al., 2013). In nonhuman primates, activity in the OFC correlates with the subjective value of juice options varying in taste and quantity (Padoa-Schioppa and Assad, 2006). These findings have been taken as evidence that multiple-attribute values are integrated into an overall option value representation within the vmPFC/OFC, subsequently influencing choice (Levy and Glimcher, 2012).

However, direct evidence that this region is necessary for value integration is lacking. Damage to the vmPFC and adjacent OFC [together termed "ventromedial frontal lobe" (VMF)] has been shown to change how multi-attribute information (presented as text) is acquired during decision-making (Fellows, 2006), and to affect which attributes (inferred from faces) influence choice (Xia et al., 2015). Compared with healthy and other frontal-damaged individuals, people with VMF damage differed in how they weighted specific attributes when evaluating visual art (Vaidya et al., 2018). These observations could be consistent with a deficit in attribute-value integration, as predicted by value-integration models. Puzzlingly, however, these VMF-damaged patients seemed to systematically neglect specific attributes, rather than showing a generic reduction in the attributes that were considered. Other recent work found that VMF damage impaired value-based decisions about spouses, but not houses, and that the number of attributes per option did not affect choice consistency in either condition (Bowren et al., 2018). Together, this argues against a general role for the VMF in combining attributes to assess value, calling instead for a more specific account. One possibility is that this region is required for inferring value from the configural relationship among multiple lower-level attributes. In our opening example, the VMF would thus be required to predict the unique value of peanuts and chocolate together, and perhaps not for summing the individual values of each of those attributes alone.

This hypothesis was inspired by object-processing research showing that encoding of individual attributes and the conjunctions of attributes is supported by partly dissociable neural substrates. Configural processes rely on the medial temporal lobe (MTL): damage to the hippocampus impairs working memory for object-location configurations (Olson et al., 2006)

and object–outcome associative learning predicted by attribute configurations (Rudy and Sutherland, 1995). The perirhinal cortex represents complex objects distinct from the combined representations of their parts (Erez et al., 2016), and damage to this region impairs object discrimination based on configurations (Bussey et al., 2005). In contrast, attribute–outcome associations and object discrimination based on individual object parts do not rely on an intact MTL. There are both strong anatomical connections (Heide et al., 2013) and evidence of functional connectivity (Andrews-Hanna et al., 2014; Eichenbaum, 2017) between the MTL and VMF. These regions may interact during decision-making (Gluth et al., 2015; McCormick et al., 2018). Thus, how attributes of complex objects are represented in the MTL may be relevant to understanding the role of the VMF in assigning value to such objects.

Here, we tested the hypothesis that the VMF plays a specific role in inferring value from multi-attribute configurations. We asked whether VMF damage impairs decisions for choosing objects when values were predicted by attribute configurations, by the integration of individual attribute values, or both.

Materials and methods

Participants

Twenty-four patients with focal frontal lobe damage were recruited through the cognitive neuroscience research database at McGill University. All patients with a fixed lesion primarily affecting the frontal lobes were eligible. Lesions were characterized with magnetic resonance or computed tomography imaging, and registered manually, using MRIcro software, to the Montreal Neurological Institute standard brain by a neurologist blind to task

performance ((Rorden and Brett, 2000); www.mccauslandcenter.sc.edu/crnl/mricro). Patients were assigned a priori to a group with damage involving the VMF, the region of interest in this study (VMF, N = 12) or a frontal comparison group with damage sparing the VMF (FC, N = 12). **Figure 2.1** depicts lesion extent and overlap for the VMF and FC groups. In the VMF group, damage was unilateral in 11 of 12 cases (eight right, three left) and bilateral in one case. By design, VMF lesions affected the medial OFC in all cases to some degree. VMF damage extended to adjacent ventral regions in most cases, most commonly the vmPFC (in eight) and lateral OFC (in four). In six of 12 VMF patients, damage extended into the medial frontal lobe superior to the genu of the corpus callosum. Such dorsomedial damage was also present in four of 12 FC patients. Twenty-four healthy comparison (HC) participants matched for age and education were also recruited from a companion database that drew participants from the Montreal area via community advertisement. Healthy controls scored >26 on the Montreal Cognitive Assessment and denied any current psychiatric or neurologic diagnosis or the use of psychoactive medications.

Damage to the VMF was caused by aneurysm in two cases, hemorrhagic stroke in one case, and tumor resection in nine cases. Damage in the FC group was caused by ischemic stroke in six cases, hemorrhagic stroke in two cases, and tumor resection in four cases. Nine patients (seven VMF, two FC) were taking one or more psychoactive drugs, most commonly an antidepressant or anticonvulsant. All patients had fixed, circumscribed lesions of ≥6 months duration (mean, 8.3 years; SD, 4.9 years; **Table 2.1**).

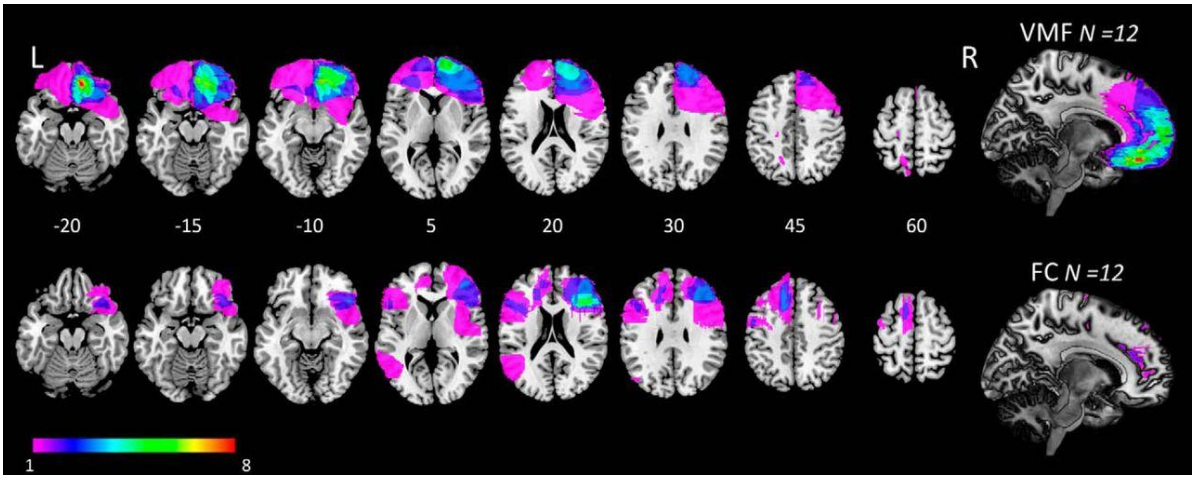

Figure 2.1. Lesion overlap in the VMF (top row) and FC (bottom row) groups. Colors indicate extent of lesion overlap, as shown in the legend. Numbers indicate axial slices by z-coordinate in Montreal Neurological Institute space. L, Left; R, Right.

Table 2.1. Demographic characteristics

Group	*N*	Age (years)	Sex (M/F)	Handedness (right/left/ ambidextrous)	Education (years)	HADS		estimated IQ[a]	Lesion laterality (right/left/ bilateral)	Lesion volume (cc)
						Anxiety scale	Depression scale			
HC	24	61 (11.6)	7/17	23/1/0	16 (3.0)	3.8 (3.0)	2.2 (2.1)	126 (4)	–	–
VMF	12	57 (10.7)	5/7	10/0/2	14.5 (3.0)	5.6 (1.7)	3.9 (3.7)	120 (8)	8/3/1	20 (8–192)
FC	12	60 (10.7)	5/7	10/2/0	15.1 (2.9)	5.8 (4.0)	5.1 (3.6)*	120 (10)	6/6/0	24 (5–37)

All values mean (SD), except sex (count) and lesion volume [median (range)]. *$p < 0.05$, Mann–Whitney *U* test compared to healthy controls. [a]Not all subjects completed the estimated IQ test (HC, *N* = 11; VMF, *N* = 7; FC, *N* = 6).

Neuropsychological characterization

Participants with frontal lobe damage completed tests of working memory (backwards digit span; (Lezak et al., 2012)), verbal fluency (Animal, Fluency-F; (Benton et al., 1989)), language comprehension (similar to the Token test; (De Renzi and Vignolo, 1962)), and incidental memory for faces (Bower and Karlin, 1974).

Apparatus

All HC participants and 20 patients were tested in the laboratory on a desktop computer equipped with a 19-inch monitor. Four participants with frontal damage (three VMF, one FC) were tested at home using a 15-inch laptop computer (Fujitsu). Subjects responded using a standard mouse or keyboard, depending on the task. Experiments were programmed in Matlab (version 2014b, Mathworks), using the Psychtoolbox extension (PTB-3; (Brainard, 1997)).

Experimental tasks

Participants made value-based decisions between multi-attribute objects in two conditions, elemental and configural. In the configural condition, participants learned the value of unique configurations of two attributes of an object, whereas in the elemental condition, participants learned the values of individual attributes, which then had to be combined for optimal multi-attribute decisions. Participants also completed two control tasks to assess object discrimination and memory for single attribute-value associations over a delay.

We used novel multi-attribute stimuli developed to study object processing. These pseudo-objects, called “fribbles,” are composed of a main body and four appendages, each taking one of three possible forms, referred to here as “attributes.” They were designed to

mimic perceptual characteristics of real-world objects (Barry et al., 2014; Williams and Simons, 2000). To familiarize participants with these novel stimuli and establish that VMF damage did not affect the ability to discriminate fribbles, the session began with a discrimination task adapted from a previous study on complex object perception in patients with MTL damage (Barense et al., 2007). The task was divided into two parts. In the first 12 trials, three fribbles were displayed side by side: two were identical; one was different. All fribbles had the same main body and three of four attributes in common, such that the "odd fribble out" was distinguished by a single attribute. The participants were asked to select the fribble that was different. Once the response was registered (by a mouse click), feedback was given by surrounding the selected fribble with a green (correct) or red (error) border for 1.5 s before proceeding to the next trial. The second 12 trials followed the same procedure but five fribbles were presented: two pairs of identical fribbles and one fribble that could not be paired with any other. Again, participants were instructed to click on the odd fribble out. Importantly, the odd fribble out shared all its attributes with at least two other fribbles in the set, such that it could only be identified based on the specific configuration (i.e., conjunction) of two attributes.

The main task had a learning phase followed by a decision phase for each of two conditions: elemental and configural. Participants learned a total of six fribble–value associations in two sets of three by observing the outcomes of mock auctions as fribbles were "sold," one at a time. Participants were instructed to carefully study the different fribbles and the price for which each was sold. A learning trial started with the presentation of a fribble. After a 2 s delay, the amount for which the item had been sold was presented (**Fig. 2.2**). The fribble and its selling price were displayed until the participant pressed a key to go to the next

trial. One learning block included three different fribbles, presented nine times each in random order for a total of 27 trials. The selling value associated with a fribble on a given trial was randomly drawn from a normal distribution with an SD of $5; median values are shown in **Figure 2.2**. The fribble associated with each value was randomized, counterbalanced across participants.

After each learning block, learning was assessed with a binary choice probe. On each trial, two fribbles were presented on the screen to the left and right of a central fixation cross (**Fig. 2.2**). Participants were asked to select with the corresponding arrow key which of the two fribbles they thought was worth the most. The response was coded as an error if the less valuable option was chosen, but no feedback was given to the participant. A learning probe block had a maximum of 36 trials (12 repetitions of the three pairs), but was stopped sooner if the learning criterion was violated. Learning blocks and probes were repeated until a criterion of 92% (11 of 12) correct for each of the three pairs was reached. When the criterion was reached with the first set of fribbles, participants were trained on a second set of three following the same procedure.

After learning, participants completed a decision phase that drew upon all six learned associations. On each trial, two fribbles were presented on the screen and participants were instructed to choose which fribble they wanted to have in their inventory (**Fig. 2.2C**). Participants were told that each fribble they chose would be placed in their inventory, and that this inventory would be sold at the end of the experiment with the proceeds converted into real money (maximum $7) and added to their base compensation for participation.

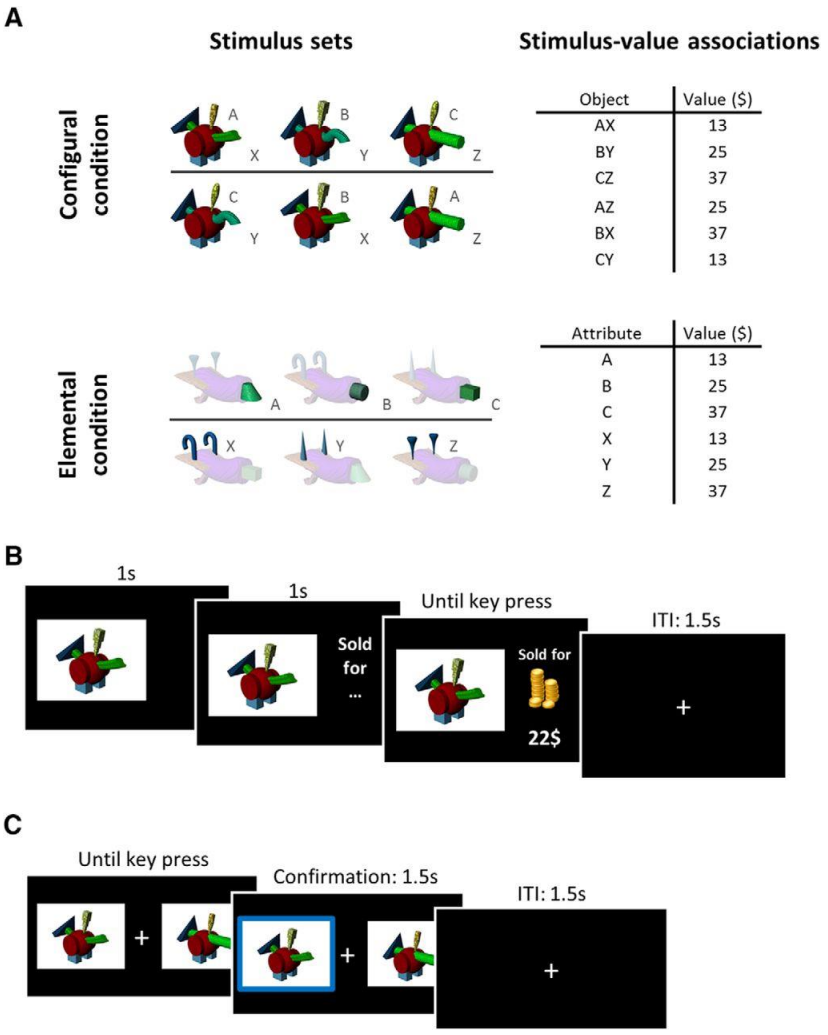

Figure 2.2. Stimulus sets and experimental paradigm. **A**, Example of stimulus sets and value associations. Stimulus sets were counterbalanced across participants and stimulus–value associations were randomly selected from six predefined lists. **B**, Structure of a learning trial. A fribble was displayed for 2 s. Then its selling price was presented until a key was pressed to move to the next trial, following a 1.5 s intertrial interval. **C**, Binary choice trial (for learning probes and final decision phases). These were self-paced: two fribbles were presented on either side of a fixation cross and participants pressed the left or right arrow key to choose which item they wanted in their inventory. Choice was confirmed with a bold border surrounding the chosen object for 1.5 s, followed by a 1.5 s intertrial interval.

In the configural condition, participants learned the value of six fribbles having the same body and two (irrelevant) attributes in common (**Fig. 2.2**). Only the configuration of the two varying attributes was value-predictive. During the decision phase, all 15 possible pairs were presented six times in random order for a total of 90 trials. In the elemental condition, values were associated with individual attributes. During the learning phase, the fribble body and irrelevant attributes were masked with a 50% transparent white mask, making the individual value-predictive attribute more salient (**Fig. 2.2**). Participants were explicitly told that the auction value was associated only with the unmasked attribute during the learning blocks, and only that attribute was relevant for the options' value during the learning probes. During the decision phase, stimuli were presented without masks, so all attributes were equally salient, and participants were instructed to take into account everything they had learned about the different parts. The stimulus set included nine different fribbles (3 × 3 attributes). Thirty-six possible pairs were presented five times each, in random order, for a total of 180 trials. Half the trials involved choices between fribbles distinguished by one attribute only (the other attribute being common to the two options), referred to as “single-attribute trials.” Half the trials involved choices between fribbles for which both value-predicting attributes were varied, referred to as “two-attribute trials.” In principle, the more valuable fribble in these trials could be selected by combining (e.g., adding) individual attribute values, as each attribute was associated with a specific value, regardless of which other attributes were present. To eliminate the possibility of an attribute-value “task set” interfering with learning the values of attribute configurations, all participants completed the configural condition first. Stimulus sets were counterbalanced across conditions and participants.

In both the elemental and configural conditions, stimulus–value associations were learned in two different sets before the decision phase. Thus, half the associations called upon in the decision phase were learned more recently. A control task was therefore included to determine whether there were groupwise differences in retaining stimulus–value associations across this delay. This task used a new set of fribbles and was completed after the decision tasks. Three attribute–value associations were trained to criterion, as in the learning phase of the elemental condition. This was followed by an unrelated task (Posner cueing task) lasting ~10 min, after which memory for the learned associations was probed with a series of binary decisions, identical to the learning probe blocks described earlier.

Statistical analysis

Task performance was assessed through accuracy and reaction times. Correct responses were defined as choices of the higher-value fribble in each pair. In the configural condition, each option's value was the mean value associated with the specific configuration of attributes during training. For the elemental condition, we defined each option's compound value by summing the mean value of each attribute (learned during training), although any method of combining the two learned values with equal weights would lead to the same stimulus-value ranking. A choice of the option with the lower objectively determined value was coded as an error. Accuracy (percentage correct) data were arcsine transformed for statistical analysis, although using the raw data yielded the same pattern of results.

Unless otherwise specified, statistical analyses were run using IBM SPSS Statistics for Windows (version 22). Performance was compared across groups using ANOVA followed by

Bonferroni-corrected pairwise comparisons where significant main effects were found. Generalized estimating equations (GEEs) were used to analyze the trial-by-trial influence of value on choice behavior using SAS (version 9.4, SAS Institute). This analysis is similar to binary logistic regression, but is better suited to modeling repeated measures where outcomes might be correlated within participants, such as in this case. The left-minus-right option value difference was used as a predictor to model the choice of the left option as a binary outcome. Demographic variables and neuropsychological test scores were compared between patient and HC groups using t tests or, when assumptions for parametric analysis were not met, Mann–Whitney U tests, without correction for multiple comparisons.

Results

Participant characteristics

Demographic and clinical information is reported in **Table 2.1**. There was no significant difference in age or years of education between groups. There was no significant group difference in premorbid IQ, estimated using the American National Reading Test (Grober and Sliwinski, 1991) at the time of enrolment in the registry (postlesion), although this measure was only available in a subset of participants. Patient groups did not differ in lesion volume. The Hospital Anxiety and Depression Scale (HADS) was used to characterize levels of anxiety and depression (Zigmond and Snaith, 1983). Scores on the depression scale (HADS-D) were higher in the FC group relative to the HC group ($p = 0.03$), but there was no significant difference between the VMF and HC groups ($p = 0.29$), nor between frontal groups ($p = 0.26$). There were no group differences in anxiety scores (HADS-A). No participant had an active clinically diagnosed mood disorder, by self-report or chart review. Neuropsychological test results are

shown in **Table 2.2**. There were no significant differences between patient groups in tests of incidental memory for faces, verbal fluency, or language comprehension. Patient groups differed in lesion etiology ($\chi^2_{(3)} = 13.04$, $p = 0.004$), but we did not find effects of etiology on any variable of interest. There was no significant difference between the patients tested at home and those tested in the laboratory on any variable of interest.

Table 2.2. Neuropsychological screening test performance for patient groups

Group	Fluency		Backwards digit span	Incidental memory (accuracy)	Sentence comprehension (accuracy)
	Animals, 60 s	Fluency-F, 60 s			
VMF	10.3 (5.1)	18.2 (2.9)	2.6 (0.8)	0.88 (0.1)	0.99 (0.02)
FC	10.5 (5.4)	17.7 (6.7)	2.9 (1.3)	0.79 (0.1)	0.96 (0.07)

Mean (SD). One VMF and one FC participant did not complete the screening tests.

Control tasks

Performance of the control tasks assessing the ability to discriminate fribbles and the ability to retain attribute–value associations across a 10 min delay is presented in **Table 2.3**. All subjects could discriminate fribbles distinguished by a single attribute or by the conjunction of two attributes. There was no main effect of group on accuracy in the three-fribble (one-way ANOVA, $F_{(2,45)} = 0.79$, $p = 0.46$, $\eta_p^2 = 0.03$) or five-fribble trials ($F_{(2,45)} = 1.47$, $p = 0.24$, $\eta_p^2 = 0.06$). There was a main effect of group on reaction times in the three-fribble trials ($F_{(2,45)} = 4.82$, $p = 0.01$, $\eta_p^2 = 0.18$). Post hoc comparisons revealed that the FC group was slower than the VMF group ($p = 0.01$), but neither patient group was different from the HC group (HC–VMF, $p = 0.26$;

HC–FC, $p = 0.22$). There was no significant group effect on reaction times in the five-fribble trials ($F_{(2,45)} = 0.61$, $p = 0.55$, $\eta_p^2 = 0.03$).

Attribute–value associations were retained very well over a 10 min delay, and there was no effect of group on accuracy (one-way ANOVA, $F_{(2,45)} = 0.49$, $p = 0.61$, $\eta_p^2 = 0.02$; **Table 2.3**).

Table 2.3. Control task performance for HC and patient groups [mean (SD)]

Group	Discrimination				Decision probe after delay	
	Three fribbles		Five fribbles			
	Accuracy (% correct)	Reaction time (ms)	Accuracy (% correct)	Reaction time (ms)	Accuracy (% correct)	Reaction time (ms)
HC	99.0 (2.8)	4940 (1317)	96.2 (8.1)	13,248 (6976)	97.6 (5.6)	1387 (412)
VMF damage	99.3 (2.4)	4165 (667)	91.0 (13.5)	11,043 (3378)	99.3 (2.4)	1288 (220)
FC	100 (0)	5755 (1539)	95.8 (5.6)	13,913 (8766)	97.9 (5.2)	1206 (299)

Table 2.4. Attribute-value task-learning phase performance [mean (SD)]

Group	Condition			
	Configural		Elemental	
	Number of learning blocks	Reaction time (ms)	Number of learning blocks	Reaction time (ms)
HC	1.4 (0.5)	3431 (1654)	1.2 (0.4)	2557 (2032)
VMF	1.7 (0.9)	2504 (664)	1.0 (0.1)	1895 (615)
FC	1.7 (0.9)	3123 (1255)	1.1 (0.3)	1647 (702)

Attribute-value learning

All subjects learned the stimulus–value associations to criterion (>92% accuracy) within four learning blocks in both conditions. Across groups, more learning blocks were needed to reach criterion in the configural compared with the elemental condition (mixed-measure ANOVA, $F_{(1,45)} = 17.04$, $p < 0.001$, $\eta_p^2 = 0.28$), but there was no significant group-by-condition interaction ($F_{(2,45)} = 1.67$, $p = 0.199$, $\eta_p^2 = 0.07$; **Table 2.4**). One HC participant was an outlier with respect to reaction times during learning probes (mean: configural condition, 8947 ms; elemental condition, 10,765 ms). After removing this participant from the analysis, we found no main effect of group on reaction times (configural, $F_{(2,44)} = 1.82$, $p = 0.18$, $\eta_p^2 = 0.08$; elemental, $F_{(2,44)} = 1.29$, $p = 0.28$, $\eta_p^2 = 0.05$). The participant with very slow responses nonetheless learned all fribble–value associations to criterion and was included in further analysis.

Multi-attribute value-based choices

Having established that patients with frontal damage could discriminate fribbles, learn elemental and configural value associations, and retain this information across a 10 min delay as well as HC participants, we next assessed multi-attribute value-based binary decisions in elemental and configural conditions. The elemental condition involved choices between all possible pairs of fribbles. In principle, half of these trials could be solved by considering the values of single attributes, rather than integrating the values of two attributes, as both options have a value-predicting attribute in common. Trials in which the options differed on both value-predictive attributes (two-attribute trials) require somehow combining the values of two attributes, and were analyzed separately from the single-attribute trials. For the purposes of analysis, we summed the trained attribute values, but the identical relative value orderings

would emerge from averaging these values, or from trading off the values of each individual attribute.

The values learned during training systematically influenced choice in both conditions (**Fig. 2.3**). GEEs were used to quantify the extent to which choices were predicted by the difference in option values, trial by trial, and to test whether this differed by frontal lesion group. Across groups, choices were significantly predicted by the option value difference in both the configural [odds ratio (OR), 2.98; 95% CI, 2.50–3.56; $p < 0.0001$] and elemental conditions (single-attribute OR, 31.35; 95% CI, 14.52–67.70; $p < 0.0001$; two-attribute OR, 5.47; 95% CI, 4.54–6.60; $p < 0.0001$).

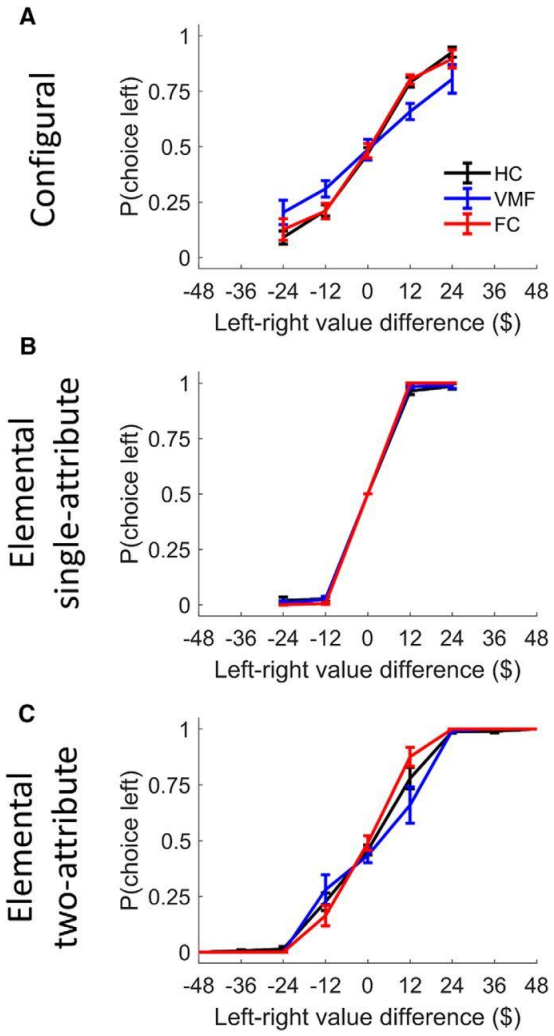

Figure 2.3. Probability of choosing the left option as a function of the relative value of the left and right options in the configural (***A***) and elemental condition divided in single-attribute (***B***) and two-attribute trials (***C***). Error bars indicate SEM.

The group-by-value interaction was then added to the model, with HC as the reference group. Compared with the HC group, the VMF group's choices in the configural condition were more weakly predicted by option value difference (interaction OR, 0.58; 95% CI, 0.39–0.84; p = 0.004). In contrast, the choices of the FC group were influenced by option value difference to a similar degree as the HC group (no significant interaction between group and value; OR, 0.94; 95% CI, 0.61–1.43; p = 0.77).

In the elemental condition, the VMF group's choices were influenced by option value difference to a similar extent as the HC group in both the single-attribute (interaction OR, 1.57; 95% CI, 0.34–7.06; p = 0.56) and two-attribute trials (interaction OR, 0.93; 95% CI, 0.64–1.37; p = 0.73). Value difference was a significantly stronger predictor of choice in the FC group compared with the HC group in the single-attribute (interaction OR, 17.20; 95% CI, 3.52–84.07; p < 0.001) and the two-attribute trials (interaction OR, 1.64; 95% CI, 1.03–2.59; p = 0.04).

As can be seen in **Figure 2.3**, the range of value differences was greater in the two-attribute trials of the elemental condition compared with that of the single-attribute trials, and of the configural condition. Because greater value differences are generally associated with easier decisions, and all groups performed at ceiling at the extreme value differences (**Fig. 2.3C**), we restricted the analysis to the two-attribute trials within the same value-difference range as the other conditions. We again found no significant difference between the HC and the VMF groups (interaction OR, 0.87; 95% CI, 0.57–1.34; p = 0.53), and value difference tended to be a marginally better predictor of choice in the FC group compared with the HC group (interaction OR, 1.61; 95% CI, 0.99–2.64; p = 0.06).

We next asked whether group differences in the influence of value on choice were reflected in significant differences in choice accuracy, defined as the percentage of trials in which the highest value option was chosen. As depicted in **Figure 2.4A**, there was a significant main effect of group on accuracy in the configural condition (one-way ANOVA, $F_{(2,45)} = 4.95$, $p = 0.01$, $\eta_p^2 = 0.18$). Post hoc tests with Bonferroni correction for multiple comparisons revealed that the VMF group was less accurate than both the HC ($p = 0.01$) and FC groups ($p = 0.04$), whereas the FC and HC groups were not significantly different ($p = 1.0$). There was no significant effect of group on reaction time (one-way ANOVA, $F_{(2,45)} = 1.37$, $p = 0.26$, $\eta_p^2 = 0.06$; **Fig. 2.3C**) in the configural condition. In contrast, there was no significant effect of group on accuracy (one-way ANOVA, $F_{(2,45)} = 2.47$, $p = 0.10$, $\eta_p^2 = 0.10$) or reaction time ($F_{(2,45)} = 0.29$, $p = 0.75$, $\eta_p^2 = 0.01$) in the elemental condition.

Separating the elemental condition by trial types, we found that, across groups, participants were less accurate in two-attribute trials compared with single-attribute trials (mixed-measures ANOVA, $F_{(1,45)} = 57.1$, $p < 0.0001$, $\eta_p^2 = 0.56$; **Fig. 2.4B**). There was a trending but nonsignificant effect of group ($F_{(2,45)} = 3.18$, $p = 0.06$, $\eta_p^2 = 0.12$) on accuracy, and no significant interaction between trial type and group ($F_{(2,45)} = 2.24$, $p = 0.12$, $\eta_p^2 = 0.09$).

Reaction times were longer in the two-attribute trials ($F_{(1,45)} = 46.03$, $p < 0.0001$, $\eta_p^2 = 0.50$; **Fig. 2.4D**). Again, there was no significant effect of group ($F_{(2,45)} = 0.29$, $p = 0.75$, $\eta_p^2 = 0.01$) and no interaction between group status and trial type ($F_{(2,45)} = 1.37$, $p = 0.26$, $\eta_p^2 = 0.06$). In summary, VMF damage had no effect on decision accuracy between objects based on elemental values, whether for objects distinguished by a single attribute value or by two attribute values.

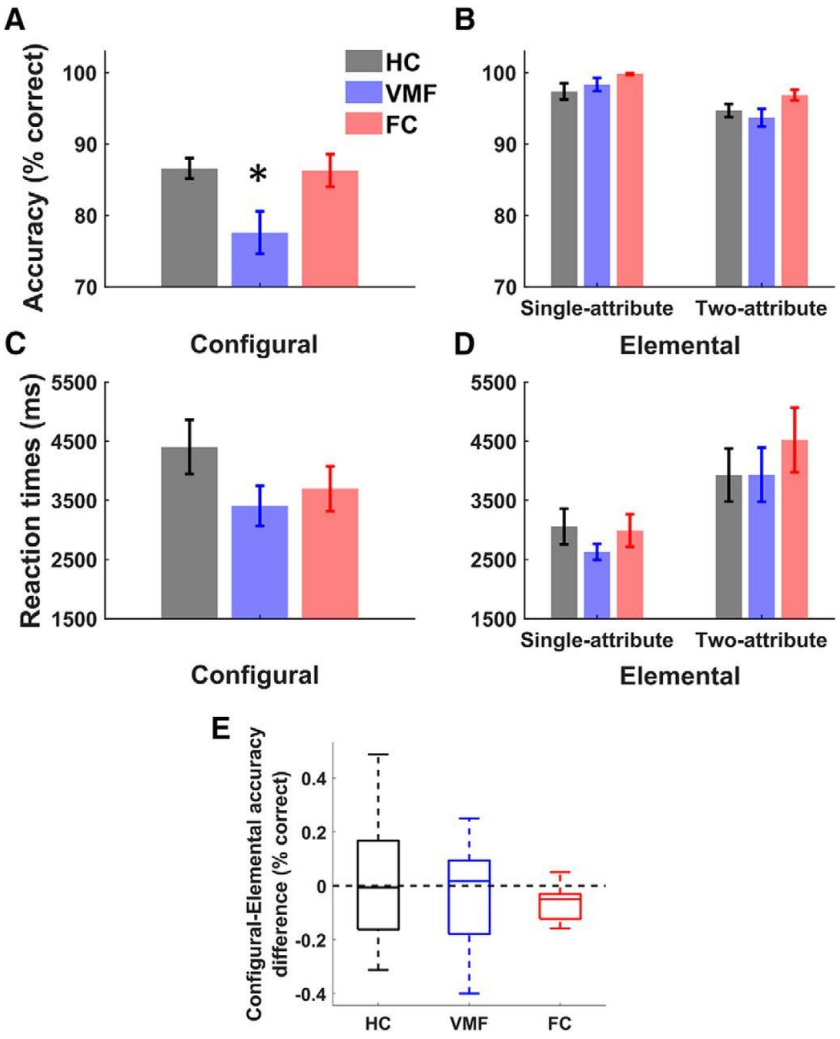

Figure 2.4. Multi-attribute decision task performance. ***A***, ***B***, Choice accuracy for the (***A***) configural and (***B***) elemental condition. ***C***, ***D***, Reaction times for the (***C***) configural and (***D***) elemental condition. Error bars indicate SEM, *$p < 0.05$. ***E***, Difference in accuracy between configural and elemental difficulty-matched trials. Distributions shown with median and quartiles.

While there was a group effect in the configural but not in the elemental condition, when the two conditions were included in the same statistical model, there was no significant group-by-condition interaction (mixed-measures ANOVA, $F_{(2,45)} = 2.37$, $p = 0.11$, $\eta_p^2 = 0.10$). However, many trials in the elemental condition did not require two attributes to be considered. We therefore undertook an additional, exploratory analysis focusing on the trials that were most similar in attribute-processing requirements across the two conditions, i.e., the 25 elemental condition trials where both attributes had to be considered to correctly assess value, and the 48 configural trials matched with these elemental trials on value difference between options. The difference in accuracy in these trials, for each subject, was then calculated (**Fig. 4E**), and this relative performance index was compared across groups. We found that the configural–elemental accuracy difference did not differ significantly from zero in the VMF (Wilcoxon signed rank test, $Z = -0.13$ $p = 0.90$), HC ($Z = 0.21$, $p = 0.84$) or FC groups ($Z = -1.47$, $p = 0.14$), indicating that accuracy was similar across conditions. There was no effect of group on accuracy difference (Kruskal–Wallis H test, $\chi^2_{(2)} = 0.88$, $p = 0.64$). As is evident in **Figure 2.4E**, the variance in this subset of trials is high, particularly in the HC and VMF groups, limiting power to detect differences with this exploratory analysis, if present.

Discussion

We provide evidence that VMF damage impairs value-based decisions between novel multi-attribute objects when overall value is predicted by the configuration of two attributes. This finding was specific to VMF damage: damage to other frontal regions did not impair value-based choices when overall value was predicted by attribute configuration. We did not find evidence that VMF damage impairs decisions between options when individual attributes are

independently predictive of value, either when value is assessed based on a single attribute, or when two attribute values are combined to make an optimal choice.

These findings argue that the VMF is involved in assessing the holistic value of multi-attribute objects. This is the first direct evidence that the VMF plays a critical role in decisions based on value information provided by the conjunction of individual attributes, each of which is uninformative on its own. The results complement previous work from our laboratory showing that VMF damage leads to the neglect of some value-predictive information in complex real-world objects (faces, art; Xia et al., 2015; Vaidya et al., 2018). The present observations raise the possibility that such information may be neglected because it relies more heavily on configural processing. This might also explain the recent observation that VMF damage impairs value-based multi-attribute decisions between social "objects" (spouses), but not between nonsocial objects (houses; Bowren et al., 2018), given the evidence that processing of social stimuli, such as faces, is fundamentally configural (Farah, 1996).

This framework may be more generally useful for guiding the growing neuroeconomics literature on multi-attribute decision-making. The neural circuits involved may depend on whether options are presented in ways that encourage holistic or attribute-level processing. Furthermore, it is possible that attributes extrinsic to an object (such as quantity) may influence value through different mechanisms than intraoption attributes (such as taste or beauty; (Berker et al., 2019)). We suggest that efforts to link research about object-processing and multi-attribute decision processes (Bettman et al., 1998) may be helpful in advancing our understanding of how the brain makes value-based choices among real-world objects.

Although the present study was not designed to study value-based learning, it is notable that the learning measures we collected suggest that the VMF is not required to learn configural whole-object values through feedback. Configural learning has been shown to rely on the hippocampus (Rudy and Sutherland, 1995), and configural reinforcement learning has been related to the functional coupling between the hippocampus and striatum (Duncan et al., 2018). Learning to choose objects based on configuration in nonhuman primates is spared after transection of the uncinate fasciculus, disrupting the direct connections between the prefrontal cortex and the temporal lobe (Gutnikov et al., 1997), which is consistent with our finding here that VMF damage does not substantially disrupt such learning in humans. As discussed above, the VMF becomes critical when configural object values must be compared with guide choice.

Decisions in the elemental condition could in principle be achieved by option-based or attribute-based strategies, either by integrating attribute values within options and then comparing the compound values, or by comparing individual attribute values. Extensive research has shown that further strategies may be engaged within these broad approaches to such decisions (e.g., trade-offs, elimination-by-attribute; Bettman et al., 1998). We cannot address which strategies might have been used here, but prior work on explicitly multi-attribute (elemental) choices where attribute information is presented in tabular format has demonstrated that VMF damage affects these processes, biasing toward simpler, within-option valuation rather than cross-option comparison strategies (Fellows, 2006).

The present work clearly shows that VMF damage does not impair learning or choices based on single value-predictive attributes, when those attribute values are explicitly trained. Could the VMF also play a role in multi-attribute decisions involving the integration of

independent attribute values? Previous fMRI research has shown that activity in the VMF tracks the value of items composed of multiple independently value-predictive attributes (Kahnt et al., 2011; Lim et al., 2013). Our findings suggest that an intact VMF is not required for choice in such conditions. However, the analysis directly comparing performance on the subset of trials with the most similar attribute processing and value-difference requirements across conditions did not demonstrate a group-by-condition interaction, and had limited statistical power. Thus, we cannot exclude the possibility that the VMF is required when independent attribute values must be traded off to make an optimal choice, at least under some conditions. Further work is needed on this question.

Participants with VMF damage could readily discriminate between complex objects in a control task that relied on configural object representations, ruling out the possibility that the observed impairment in decisions based on configural value was due to perceptual deficits. Configural object perception has been shown to rely on the perirhinal cortex, an MTL region closely related to the hippocampus. Damage to the perirhinal cortex selectively impairs object discrimination when it relies on attribute configurations (Barense et al., 2007; Bartko et al., 2007). In addition, patterns of BOLD activity in this area relate to complex objects held in working memory, but not their separate parts, and are relatively insensitive to viewpoint (Erez et al., 2016), arguing that the perirhinal cortex represents the identity of objects independent of changes in physical characteristics. Our findings suggest that the role of the VMF can be understood in similar terms: i.e., the VMF is crucial in developing predictive value representations when attributes on their own are ambiguous or separately uninformative. We

speculate that perirhinal cortex interactions with the VMF may be important for predicting object values based on attribute configurations.

This proposal aligns with other recent efforts to understand how the prefrontal cortex and the MTL interact more generally. Synthesizing the effects of human hippocampus and VMF damage in a variety of cognitive domains, McCormick and colleagues argued that the VMF plays a supervisory role over the hippocampus in initiating and organizing episodic memory retrieval (McCormick et al., 2018). This interpretation mainly stems from studies addressing autobiographical memories and mental scene construction, with so far little causal evidence available with respect to memory for complex objects of the kind commonly featured in neuroeconomics research and everyday decisions. There is some evidence for hippocampus–VMF interactions during value-based decision. One fMRI study found that when imagining the consumption of novel foods composed of two familiar ingredients, both the VMF and hippocampus tracked the construction of the compound value (Barron et al., 2013). Interestingly, the results held after controlling for the value of each element, indicating that the compound value was distinct from the linear combination of the elements (i.e., configural). Given the role of the MTL in configural processing and our findings here, the putative supervisory role of the VMF over the MTL in episodic memory retrieval may extend to subjective value construction for multi-attribute objects, particularly when individual attribute–value relationships are insufficiently informative.

An alternative account suggests that the VMF (OFC, specifically) encodes the latent (not directly observable) variables of a task to determine the current goals, i.e., representing a cognitive map of task states (Schuck et al., 2016). Task-state representations in the OFC, as they

have been studied so far, are also compatible with a role of the VMF in configural decisions. The term "configural" implies that each observable element is not informative alone. Value is instead inferred from the association between elements, with each element being part of multiple associations. Similarly, in Schuck and colleagues (2016), task states were defined by the configuration of task variables, with each unique variable being part of many states. Further work is needed to establish whether these two accounts of the role of the VMF—one emerging from computational views of goal states, the other from complex object processing—reflect the same underlying processes.

This study has limitations. While all patients included in this study had well characterized focal lesions, disruption of underlying white matter tracts (fibers of passage) can affect regions distant from the lesion site (Rudebeck et al., 2013b). Converging evidence, especially from nonhuman primates where more selective lesions are possible, would be helpful in establishing whether effects are caused by white matter disruption, cortical damage, or both. We have too few patients with left-hemisphere VMF damage to establish whether the observed effects are lateralized to the right hemisphere. The task also had limited power to assess elemental multi-attribute choices requiring trade-offs, limiting conclusions about whether the VMF is also involved under those conditions. Interestingly, we found preliminary evidence that patients with damage affecting other frontal regions had difficulty with such trials, perhaps reflecting the role of the lateral and dorsomedial prefrontal cortices in attentional set-shifting (Dias et al., 1996; Vaidya and Fellows, 2016). Further work on the prefrontal mechanisms of individual attribute-value trade-offs in multi-attribute choice is needed. Finally, task order was fixed, because we were most interested in configural processing and wanted to avoid introducing

competition between elemental and configural strategies or task sets through the training procedures. For the same reason, we minimized attentional demands in the elemental training condition. All these design choices may be relevant to the pattern of observed effects.

In conclusion, these findings do not support the view that the VMF is generically necessary for tracking or comparing value information in a common currency. Under many real-world conditions, the value of complex objects might be better understood as a property that emerges from interactions between perception and memory processes, and that critically relies on the VMF when the value is ambiguous and embedded in the relational content among the parts that compose the whole.

Footnotes

The authors declare no competing financial interests. This work was supported by the Canadian Institutes of Health Research (Grant MOP 249071) and the Natural Sciences and Engineering Research Council of Canada (RGPIN 2016-06066). We thank Christine Déry for her help with participant recruitment. We also thank the patients and healthy volunteers for their participation. Correspondence should be addressed to Gabriel Pelletier at gabriel.pelletier@mail.mcgill.ca.

Chapter 3. The value of the whole or the sum of the parts: The role of ventromedial prefrontal cortex in multi-attribute object evaluation

Preface

In the last chapter, I showed that VMF damage impairs decisions between multi-attribute objects based on the value inferred from attribute configurations, while sparing decisions based on elemental attribute values. This finding warranted further examination. First, it appears at odds with fMRI studies reporting value-related VMF activations in conditions akin to the elemental condition used in Chapter 2. Secondly, a specific role for VMF in decisions where configural object recognition is necessary for valuation suggests the existence of condition-dependent interactions between VMF and the VVS. This hypothesis could not be tested in the lesion study.

In this next study, to be submitted for publication, we sought to provide complementary evidence using fMRI and eye-tracking in healthy participants with a similar experimental task, using the same stimuli and conditions. We asked whether VMF tracks the value of objects differently in configural and elemental conditions, and whether regions within the VVS are differently involved in decision-making under those conditions.

The value of the whole or the sum of the parts: The role of ventromedial prefrontal cortex in multi-attribute object evaluation[*]

Gabriel Pelletier[1], Nadav Aridan[2], Lesley K. Fellows[1] & Tom Schonberg[2]

[1]Department of Neurology & Neurosurgery, Montreal Neurological Institute, Faculty of Medicine, McGill University; [2]Department of Neurobiology, The George S. Wise Faculty of Life Sciences, Sagol School of Neuroscience, Tel Aviv University

[*] Original source: Pelletier, G., Aridan, N., Fellows, L. K., & Schonberg, T. (2020). The value of the whole or the sum of the parts: The role of ventromedial prefrontal cortex in multi-attribute object evaluation. BioRxiv, 2020.09.29.319293. https://doi.org/10.1101/2020.09.29.319293

Abstract

Everyday decision-making commonly involves assigning values to complex objects with multiple value-relevant attributes. Drawing on what is known about complex object recognition, we hypothesized two routes to multi-attribute evaluation: assessing the value of the whole object based on attribute configuration, or summing individual attribute-values. In two samples of healthy human participants undergoing eye-tracking and fMRI while evaluating novel pseudo-objects, we found evidence for distinct forms of multi-attribute evaluation. Fixations to, and transitions between attributes differed systematically when value was associated with individual attributes or attribute configurations. Further, ventromedial prefrontal cortex (vmPFC) and the perirhinal cortex were engaged during evaluation specifically when configural processing was required. These results converge with our recent findings that damage to vmPFC disrupts decisions when evaluation requires configural processing, and not in evaluating “the sum of the parts”. This suggests that multi-attribute decisions may engage distinct evaluation mechanisms relying on partially dissociable neural substrates.

Introduction

Choosing which snack to buy from a vending machine requires assessing the value of options based on multiple attributes (e.g. color, taste, health). Value can be related to individual attributes (Suzuki et al., 2017): for example if someone likes chocolate, all snacks containing this ingredient will probably be valued above those that do not. Value can also emerge from the combination of attributes, such as for chocolate-peanut snacks, where the sweet and salty ingredients within the same snack yield a value greater than the sum of the parts.

Inspired by the object processing literature, which has shown distinct neural pathways representing individual elements of complex objects and for holistic, configural representations (Bussey and Saksida, 2002), we hypothesized that there also might be distinct brain mechanisms for multi-attribute object evaluation. We found that lesions to the ventromedial prefrontal cortex (vmPFC) impaired decisions between objects when value was associated with the unique combination of attributes, but spared decisions when value was associated with attributes individually, referred to as *configural* and *elemental* valuation respectively (Pelletier and Fellows, 2019). Here, we employ a triangulation approach (Munafò and Smith, 2018) to test this idea using fMRI and eye-tracking to examine the neural and behavioural correlates of multi-attribute valuation.

Studies of object recognition have shown that attribute-level and whole object-level processing rely on dissociable brain regions along the hierarchically organized ventral visual stream (VVS). Posterior regions are involved in processing simple attributes whereas more

anterior regions contribute to holistic (configural) object representations (Riesenhuber and Poggio, 1999). Lesions to the perirhinal cortex (PRC), a medial temporal lobe structure situated at the anterior end of the VVS (Murray et al., 2007b), impair object discrimination based on attribute configuration but spare discrimination based on individual attributes (Bartko et al., 2007; Bussey et al., 2005). Several fMRI studies found that BOLD activity in the human PRC is more sensitive to attribute configuration than to the component attributes, whereas the lateral occipital cortex demonstrates higher sensitivity to single-attributes compared to anterior regions of the VVS (Devlin and Price, 2007; Erez et al., 2016). These data suggest that configural object recognition is supported by the PRC, and that individual attribute representations at earlier stages of object processing can support behaviour when holistic recognition is not essential.

Leading neuroeconomic models suggest that the vmPFC encodes subjective value across stimuli as a "common currency" (Levy and Glimcher, 2012), which might support flexible decision-making (Delgado et al., 2016). While many of these studies have presented complex objects (e.g. foods, trinkets), they have only rarely considered how multiple attribute-values are combined. A handful of functional MRI studies have examined the neural correlates of options explicitly composed of multiple attributes. These have found that signal within the vmPFC reflects the integrated value of the component attributes when each independently contributes to value, i.e. when value is associated with individual elements of the option (Basten et al., 2010; Hunt et al., 2014; Kahnt et al., 2011; Kurtz-David et al., 2019; Lim et al., 2013; Park et al., 2011; Philiastides et al., 2010; Suzuki et al., 2017). However, this work does not address

whether there are distinctions in the neural processes underlying value construction based on component attributes and value emerging from the holistic configuration of attributes.

Eye-tracking studies provide evidence that is consistent with the claim that configural and elemental evaluation are partly dissociable. In a reinforcement learning paradigm, the amount of time spent fixating an outcome-predicting cue varied with the extent to which participants used cue-configurations or separate cues for learning (Duncan et al., 2018). It has also been found that when recognizing faces, people make more gaze transitions between attributes (e.g., eyes, nose) when configural processing is primed, and fixations are longer when elemental processing is primed (Bombari et al., 2009). It is still an open question whether eye-movements on complex objects differ between configural and elemental evaluation.

Here, we relied on the framework provided by object processing research to better understand how the brain recognizes the value of multi-attribute objects. We hypothesized that estimating value in the configural condition would engage the vmPFC and high-level object recognition regions (i.e. PRC) to a greater extent than elemental valuation. We further hypothesized that fixations to, and fixation transitions between, value-predictive attributes would differ between configural and elemental value conditions. We report data from two independent samples: one behavioural and eye-tracking study, and the other that added fMRI. The fMRI sample was based on a pilot study to determine the minimal sample size. All hypotheses and analysis steps were pre-registered (osf.io/4d2yr).

Materials and methods

Data were collected from three independent samples using the same experimental paradigm. This paradigm involved first learning and then reporting the monetary value of novel, multi-attribute pseudo-objects under elemental or configural conditions. We collected an initial behavioural sample to characterize learning, decision-making and eye gaze patterns. We then undertook a pilot fMRI study to estimate the minimal sample size needed to detect effects of interest. Informed by the pilot study, a third sample underwent fMRI and eye-tracking. Data from the behavioural sample informed the pre-registration of eye-tracking hypotheses to be replicated in the fMRI sample.

Participants

Participants were recruited from the Tel Aviv University community via online advertising and through the Strauss Imaging Center's participant database. Participants were healthy volunteers, with normal or corrected-to-normal vision, without any history of psychiatric, neurological, or metabolic diagnoses, and not currently taking psychoactive medication. The study was approved by the ethics committee at Tel Aviv University and the institutional review board of the Sheba Tel-Hashomer Medical Center.

Behavioural study

Forty-two participants were recruited to take part in the behavioural experiment. Nine participants were excluded due to poor task performance according to the exclusion criteria detailed below. The final behavioural sample included 33 participants (15 women, mean age 22

y, range 18-32). Eye tracking data was not collected in three participants due to poor calibration of the eye-tracker.

fMRI pilot study

Imaging data were collected in a pilot sample of 8 participants (four women, mean age 25 y, range 21-31) to calculate the sample size needed to detect a significantly stronger modulation of value in the configural compared to the elemental trials in the vmPFC at an alpha level of 0.05 with 95% power. Power calculations were carried out with the fmripower software (http://fmripower.org/)(Mumford and Nichols, 2008), averaging beta weights for the contrast of interest across all voxels of a pre-defined brain region. Based on these calculations, we pre-registered that 42 participants would be required. This sample size was also sufficient to detect a significant effect for the parametric modulation of value in the configural condition alone, in the vmPFC (38 participants needed for 95% power). The vmPFC region of interest and the model used to analyse the pilot data are described below. Imaging data used for power and sample-size calculations are available on OpenNeuro (https://openneuro.org/datasets/ds002079/versions/1.0.0), and the code used to create the power curves and the vmPFC ROI mask are available with the pre-registration document (osf.io/4d2yr). Pilot participants were not included in the final sample.

fMRI study

Fifty-five participants were recruited to take part in the full fMRI experiment. Nine participants were excluded due to poor task performance in the scanner, according to the pre-registered exclusion criterion (detailed below). Three participants were excluded because of MR artefacts, and one participant was excluded due to excessive motion inside the scanner

based on fMRIprep outputs (Esteban et al., 2019). The final fMRI sample thus included 42 participants (21 women, mean age 27 y, range 18-39). Eye-tracking data could not be collected in 9 participants due to reflections caused by MR-compatible vision correction glasses.

Experimental paradigm

The experimental paradigm was adapted from a recently published study (Pelletier and Fellows, 2019). Participants learned the monetary values of novel multi-attribute pseudo-objects (fribbles) in two conditions (configural and elemental), after which they were scanned while bidding monetary amounts for the objects. Fribbles were developed to study object recognition, and are designed to mimic real-world objects (Williams, 1998). They are composed of a main body and four appendages which we refer to as attributes, each available in three variations. Two fribble sets were used, one for each condition (randomly assigned for each participant); each set had the same body but different appendages.

In the configural condition, value was associated with the unique configuration (conjunction) of two attributes. In the elemental condition, value was associated with each of two individual attributes, which then could be combined to obtain the value of the whole object. Four different object sets were used across participants and the object set-condition assignment was counterbalanced. Learning order was counterbalanced across participants (configural followed by elemental and vice versa) and the order of object presentation was randomized in all experiment phases. An example of the stimuli as well as the value associations are shown on **Figure 3.1**. All four sets used across participants can be found in the Supplementary Material (**Fig. S3.1**).

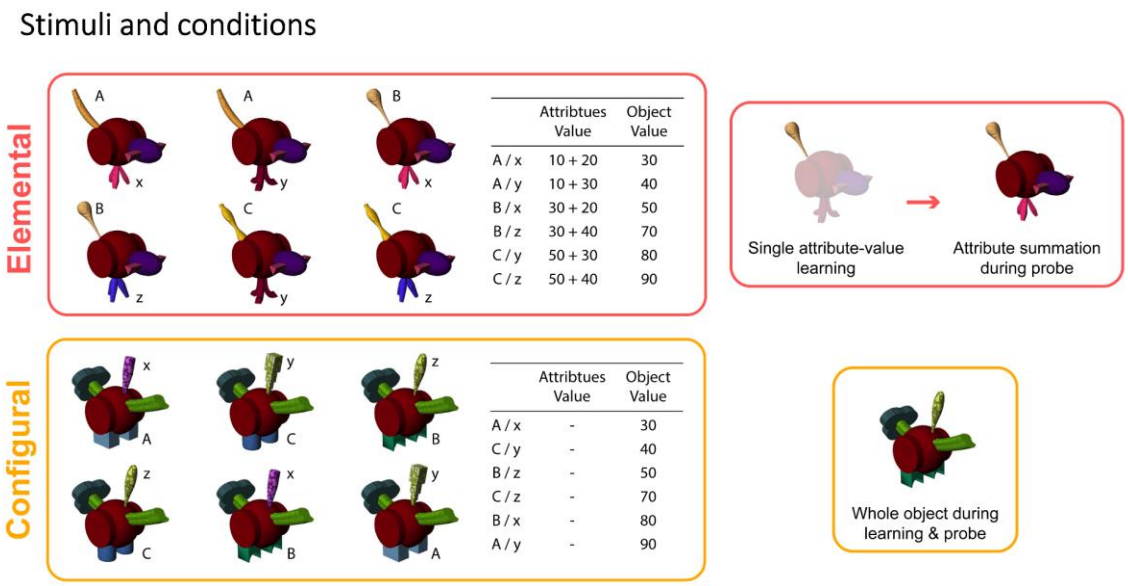

Figure 3.1. Stimuli and conditions. Example of fribble sets and object-value associations. In the elemental condition, each fribble presented in the bidding phase had two individually value-predictive attributes which had to be summed to estimate the value of the whole object. Objects were masked during the learning blocks so that value was associated with a single salient attribute, two of which had to be summed in the learning probe and bidding phase (top right). In the configural condition, each fribble had two attributes which reliably predicted value only when appearing together, i.e. in configuration. Objects were displayed without masking during the learning blocks, learning probe and bidding phase.

Learning phase

Participants were instructed before the experiment that they were acting as business owners, buying and selling novel objects. Before acquiring objects in their own inventory, they began by observing objects being sold at auction to learn their market price.

The learning phase included five learning blocks and one learning probe per condition. A block began with a study slide displaying all 6 objects to be learned in that condition, along with the average value of each object, giving the participant the opportunity to study the set for 60 s before the learning trials (**Fig. 3.2A**). The learning trials began with the presentation of an object in the center of the screen above a rating scale, asking "How much is this item worth?". Participants had 5 s to provide a value estimate for the object, using the 'left' and 'right' arrow keys to move a continuous slider and the 'down' arrow key to confirm their response. Feedback was then provided indicating the actual selling price of the object, with a bright yellow bar and the corresponding numerical value overlaid on the same rating scale. The object, rating slider and feedback were displayed for 2 s, followed by 2 s fixation cross. Each learning block presented all 6 objects 6 times each in random order for a total of 36 trials. After five learning blocks, learning was assessed with a probe consisting of 24 trials of the 6 learned objects presented four times each, in random order. Probe trials were identical to the learning trials, but no feedback was given after the value rating.

In the elemental condition, values were associated with individual attributes. During the learning blocks, the object's body and irrelevant attributes were occluded with a 50% transparent white mask, making the specific value-predictive attribute more salient (**Fig. 3.1**). Participants were explicitly told that value was associated only with the unmasked attribute.

During the learning probe, objects were presented without masks, so all attributes were equally salient, and participants were instructed to sum the values of the two attributes they had learned.

In the configural condition, objects were displayed without masks during the entire learning phase, and the value of the object was associated with the unique configuration of two attributes. In this condition, participants could not learn object-values by associating value with any single attribute, because each attribute was included in both a relatively high-value and a relatively low-value object, as depicted in the object-value table (**Fig. 3.1**).

After learning, each of the 6 objects of the elemental condition had the same overall-value (sum of the two attribute-values) as one of the 6 configural objects. The object set in each condition contained 6 value-relevant attributes, each of which was part of two different objects in each set.

Bidding task

After learning, participants placed monetary bids on the learned objects to acquire them for their inventory while eye movements were tracked and, in the fMRI studies, fMRI was acquired. The task comprised four runs (scans) each containing the 12 objects (6 per condition) repeated twice in random order for a total of 24 trials. The structure of a bidding trial is depicted in **Fig. 3.2B**. Before the bidding task, participants performed one practice run to familiarize themselves with task timings.

To make the task incentive-compatible, participants were instructed beforehand that all auctions would be resolved at the end of the session. If they bid sufficiently close to, or higher,

than the true (instructed) object's value, this object would be acquired and placed in their inventory. After the task, we would buy all the items in their inventory with a profit margin for the participant (similar to the situation where stores sell their products for a higher price than they paid from the manufacturer). The additional bonus compensation was calculated by summing the total amount paid by the experimenter to buy the participant's inventory, minus the total of the bids placed by the participant to acquire these items. The margins were set so that the maximum bonus could not exceed 10 ILS (~$3 USD equivalent). Participants were told that they could not lose money in the experiment; if the total of their bids was substantially higher than the total retail value of their inventory, the bonus compensation was 0.

Anatomical scans and functional localizer task

After the bidding task, FLAIR and T1 anatomical scans and B0 field maps were acquired for the fMRI samples, with the parameters detailed bellow.

After structural scans, participants performed a functional localizer task adapted from (Watson et al., 2012) to define participant-specific visual regions of interest for analysis of the bidding task. Images from four categories (faces, scenes, objects and scrambled objects) were presented in blocks of 15 s, each containing 20 images displayed for 300 ms with a 450 ms inter-stimulus interval. Participants were instructed to press a button using the index finger of the right hand when an image was repeated twice in a row (1-back). The task was comprised of 4 runs of 12 blocks each. A 15 s fixation block ended each run. One run contained three blocks of each image category in a counterbalanced order.

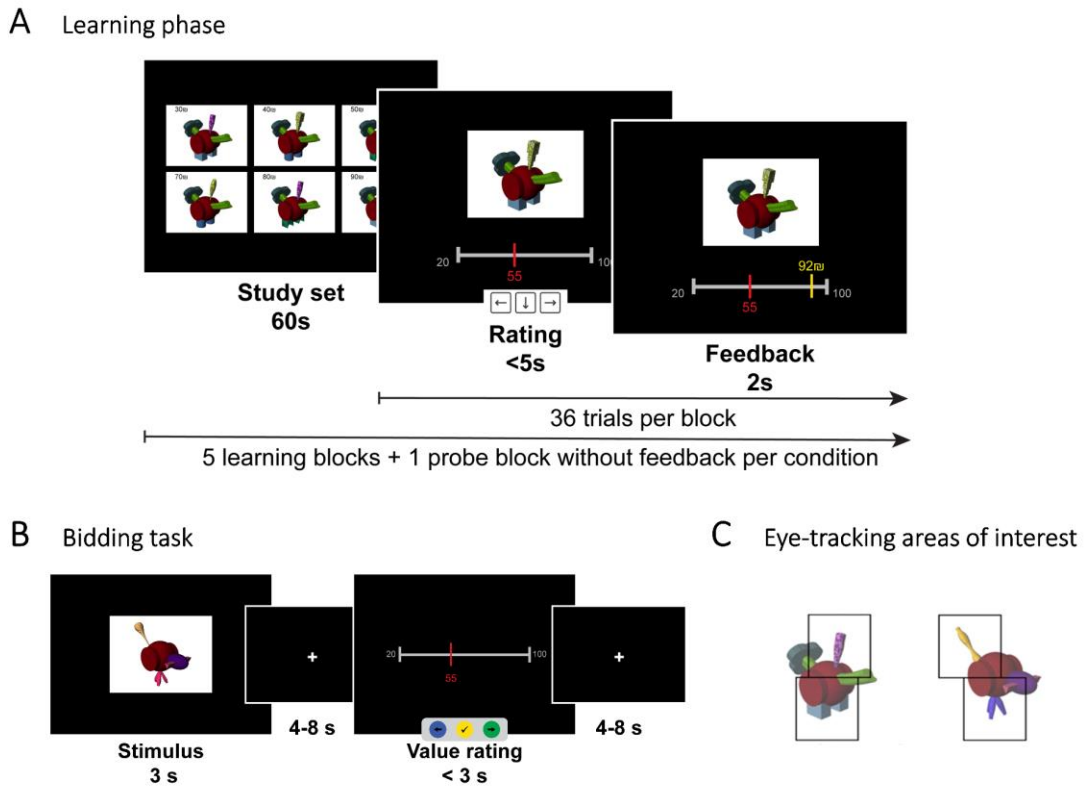

Figure 3.2. Experimental paradigm. **A)** Structure of a learning block. **B)** Trial structure of the bidding task (fMRI) task. **C)** Areas of interest (AOIs) used to assign eye fixations to the value-relevant attribute for eye-tracking analysis, depicted as black rectangle overlaid on an example object for each set.

Data acquisition

Behavioural data

All phases of the experiment were programmed in Matlab (R2017b, The Mathworks, Inc.), using the Psychtoolbox extension (PTB-3) (Brainard, 1997). During the learning phase, and during the bidding task for the behavioural sample, stimuli were displayed on a 21.5-inch monitor and responses were made using a standard keyboard. We recorded ratings and reaction time for each learning trial. During the bidding task in the fMRI, stimuli were presented on a NordicNeuroLab 32'' LCD display (1,920 x 1,080 pixels resolution, 120 Hz image refresh rate) that participants viewed through a mirror placed on the head coil. Participants responded using an MR-compatible response box. Value ratings, reaction time, and the entire path of the rating slider were recorded for each trial.

Eye tracking data

We recorded eye gaze data during the bidding task using the Eyelink 1000 Plus (SR research Ltd., Kanata, Ontario, Canada), sampled at 500 Hz. Nine-point calibration and validation were carried out before each run of the task.

fMRI data

Imaging data were acquired using a 3T Siemens Prisma MRI scanner and a 64-channel head coil. High-resolution T1-weighted structural images were acquired for anatomical localization using a magnetization prepared rapid gradient echo (MPRAGE) pulse sequence (Repetition time (TR) = 2,530 ms, echo time (TE) = 2.99 ms, flip angle (FA) = 7°, field of view (FOV) = 224 × 224 × 176 mm, resolution = 1 × 1 × 1 mm).

Functional imaging data were acquired with a T2* weighted multiband echo planar imaging protocol (TR = 1,200 ms, TE = 30 ms, FA = 70 degrees, multiband acceleration factor of 4 and parallel imaging factor iPAT of 2, scanned in an interleaved fashion). Image resolution was 2 × 2 × 2 mm voxels (no gap between axial slices), FOV = 97 × 115 × 78 mm (112 × 112 × 76 acquisition matrix). All images were acquired at a 30° angle off the anterior–posterior commissures (AC–PC) line, to reduce signal dropout in the ventral frontal cortex (Deichmann et al., 2003). We also calculated field maps (b0) using the phase encoding polarity (PEPOLAR) technique, acquiring three images in two opposite phase encoding directions (anterior-posterior and posterior-anterior), to correct for susceptibility induced distortions.

Data and code sharing

Unthresholded whole-brain statistical maps are available at NeuroVault.org (https://neurovault.org/collections/MXWQPPCW/). Neuroimaging data necessary to recreate all analyses are available in brain imaging data structure format (BIDS) on OpenNeuro (https://openneuro.org/datasets/ds002994/versions/1.0.1). Behavioural and eye-tracking data, codes for behaviour, eye-tracking and fMRI analysis, and all experiment codes are available on GitHub (https://github.com/GabrielPelletier/fribblesFMRI_object-value-construction).

Data exclusion

Participants who performed poorly in the bidding fMRI task were excluded from analysis based on pre-registered exclusion criteria. Specifically, participants with average rating error ≥ 15 ILS in both conditions, or an average rating error ≥ 15 ILS for any single object were excluded. These criteria ensured that no participant using heuristics to estimate value (i.e.

rough guessing based on a reduced number of attributes) was included in the final sample. Eye-tracking data were discarded for a trial if < 70% of samples could be labeled as fixations.

Statistical analysis

Behavioural data analysis

Value learning outside the scanner was assessed by the change in average rating error across learning blocks. Learning error was defined as the absolute difference between the rating provided by the subject and the true value of the object or attribute. A repeated-measure ANOVA with learning block (5 levels) and condition (2 levels) as within-subject factors was used to analyze rating error as learning unfolded. Group-level rating error in the learning probes was compared between conditions using a paired-sample t-test.

Accuracy in the bidding task inside the scanner was analyzed by calculating the average error (absolute difference between bid and instructed value) across the six repetitions for each of the 12 objects, as well as the average error by condition. Group-level bidding error was compared between conditions using a paired-sample t-test. Rating reaction times were similarly compared between conditions.

Eye-tracking data analysis

Eye-tracking data files in EyeLink (.edf) format were converted using the Edf2Mat Matlab Toolbox (https://github.com/uzh/edf-converter). Periods of eye blinks were removed from the data, after which the x and y coordinates and the duration of each fixation during the 3 s of object presentation were extracted. We identified each fixation according to whether it fell on one or the other of the learned attributes, or neither. The attribute AOIs were defined by

drawing the two largest equal-sized rectangles centered on the attributes of interest that did not overlap with each other. The same two AOIs were used for the 6 objects within each set. All AOIs covered an equal area of the visual field, although the positions varied between object sets. An example of the pre-registered AOIs is presented on **Fig. 3.2C**. AOIs for all object sets along with their exact coordinates in screen pixels are shown in Supplementary material (**Fig. S3.1**).

For each subject and each condition, we calculated the average number of fixations per trial, and the number of fixations in each of the AOIs. We also calculated the average duration of individual fixations within each AOI and the total time spent fixating on each AOI. Finally, we calculated the average number of transitions from one attribute-AOI to the other. We counted as a transition every instance of a fixation falling on an AOI immediately preceded by a fixation falling on the other AOI. These variables were compared between conditions at the group-level using paired-sample t-tests.

fMRI data preprocessing

Raw imaging data in DICOM format were converted to NIfTI format and organized to fit the Brain Imaging Data Structure (BIDS) (Gorgolewski et al., 2016). Facial features were removed from the anatomical T1w images using pydeface (https://github.com/poldracklab/pydeface). Preprocessing was performed using fMRIPprep 1.3.0.post2 ((Esteban et al., 2019), RRID:SCR_016216), based on Nipype 1.1.8 ((Gorgolewski et al., 2011), RRID:SCR_002502).

Anatomical data preprocessing: The T1-weighted (T1w) image was corrected for intensity non-uniformity (INU) with N4BiasFieldCorrection (Tustison et al., 2010), distributed with ANTs 2.2.0 (Avants et al., 2008)(RRID:SCR_004757) and used as T1w-reference throughout the workflow. The T1w-reference was then skull-stripped using antsBrainExtraction.sh (ANTs 2.2.0), using OASIS30ANTs as target template. Brain surfaces were reconstructed using recon-all (FreeSurfer 6.0.1, RRID:SCR_001847, (Dale et al., 1999)), and the brain mask estimated previously was refined with a custom variation of the method to reconcile ANTs-derived and FreeSurfer-derived segmentations of the cortical gray-matter of Mindboggle (RRID:SCR_002438, (Klein et al., 2017)). Spatial normalization to the ICBM 152 Nonlinear Asymmetrical template version 2009c ((Fonov et al., 2009) RRID:SCR_008796) was performed through nonlinear registration with antsRegistration (ANTs 2.2.0), using brain-extracted versions of both T1w volume and template. Brain tissue segmentation of cerebrospinal fluid (CSF), white-matter (WM) and gray-matter (GM) was performed on the brain-extracted T1w using fast (FSL 5.0.9, RRID:SCR_002823, (Zhang et al., 2001)).

Functional data preprocessing: For each of the 8 BOLD runs per subject (across all tasks and sessions), the following preprocessing was performed. First, a reference volume and its skull-stripped version were generated using a custom methodology of fMRIPrep. A deformation field to correct for susceptibility distortions was estimated based on two echo-planar imaging (EPI) references with opposing phase-encoding directions, using 3dQwarp (Cox and Hyde, 1997) (AFNI 20160207). Based on the estimated susceptibility distortion, an unwarped BOLD reference was calculated for a more accurate co-registration with the anatomical reference. The BOLD reference was then co-registered to the T1w reference using bbregister (FreeSurfer)

which implements boundary-based registration (Greve and Fischl, 2009). Co-registration was configured with nine degrees of freedom to account for distortions remaining in the BOLD reference. Head-motion parameters with respect to the BOLD reference (transformation matrices, and six corresponding rotation and translation parameters) were estimated before any spatiotemporal filtering using mcflirt (FSL 5.0.9, (Jenkinson et al., 2002)). The BOLD time-series (including slice-timing correction when applied) were resampled onto their original, native space by applying a single composite transform to correct for head-motion and susceptibility distortions. These resampled BOLD time-series will be referred to as preprocessed BOLD in original space, or just preprocessed BOLD. The BOLD time-series were resampled to MNI152NLin2009cAsym standard space, generating a preprocessed BOLD run in MNI152NLin2009cAsym space. First, a reference volume and its skull-stripped version were generated using a custom methodology of fMRIPrep. Several confounding time-series were calculated based on the preprocessed BOLD: framewise displacement (FD), DVARS and three region-wise global signals. FD and DVARS were calculated for each functional run, both using their implementations in Nipype (following the definitions by (Power et al., 2014)). The three global signals were extracted within the CSF, the WM, and the whole-brain masks. Additionally, a set of physiological regressors were extracted to allow for component-based noise correction (CompCor, (Behzadi et al., 2007)). Principal components were estimated after high-pass filtering the preprocessed BOLD time-series (using a discrete cosine filter with 128s cut-off) for the two CompCor variants: temporal (tCompCor) and anatomical (aCompCor). Six tCompCor components are then calculated from the top 5% variable voxels within a mask covering the subcortical regions. This subcortical mask is obtained by heavily eroding the brain mask, which

ensures it does not include cortical GM regions. For aCompCor, six components are calculated within the intersection of the aforementioned mask and the union of CSF and WM masks calculated in T1w space, after their projection to the native space of each functional run (using the inverse BOLD-to-T1w transformation). The head-motion estimates calculated in the correction step were also placed within the corresponding confounds file. All resamplings can be performed with a single interpolation step by composing all the pertinent transformations (i.e. head-motion transform matrices, susceptibility distortion correction when available, and co-registrations to anatomical and template spaces). Gridded (volumetric) resamplings were performed using antsApplyTransforms (ANTs), configured with Lanczos interpolation to minimize the smoothing effects of other kernels (Lanczos, 1964). Non-gridded (surface) resamplings were performed using mri_vol2surf (FreeSurfer).

Confound files were created for each scan (each run of each task of each participant, in .tsv format), with the following columns: standard deviation of the root mean squared (RMS) intensity difference from one volume to the next (DVARS), six anatomical component based noise correction method (aCompCor), frame-wise displacement, and six motion parameters (translation and rotation each in 3 directions) as well as their squared and temporal derivatives (Friston 24-parameter model (Friston et al., 1996)). A single time point regressor (a single additional column) was added for each volume with FD value larger than 0.9, in order to model out volumes with excessive motion. Scans with more than 15% scrubbed volumes were excluded from analysis.

fMRI data analysis

fMRI data were analyzed using FSL FEAT (fMRI Expert Analysis Tool) of FSL (Smith et al., 2004). A general linear model (GLM) was estimated to extract contrasts of parameter estimate at each voxel for each subject for each of the four fMRI runs (first level analysis). Contrasts of parameter estimate from the four runs were then averaged within participants using a fixed effect model (second level analysis). Group-level effects were estimated using a mixed effect model (FSL's FLAME-1).

General linear model: The GLM included one regressor modelling the 3-s object presentation time for configural trials, and one regressor modelling object presentation for elemental trials. The model also included one regressor modelling object presentation for the configural trials modulated by the value rating of the object provided on each trial (mean centered), and the equivalent regressor for elemental trials. We included four regressors modelling the rating epoch of the trial, with two unmodulated regressors modelling the rating scale for configural trials and elemental trials separately, and two regressors modelling the rating scale epoch modulated by value ratings (mean-centered) for configural trials and elemental trials separately. The duration of the rating event in these four regressors was set to the average rating reaction time across all participants and runs. Rating reaction times were accounted for in the model using a separate regressor modelling the rating epoch for all trials, modulated by the trial-wise reaction time (mean-centered). The duration was set to the maximum response time of 3 s in cases where the time limit was reached. To account for accuracy, two additional confound regressors were added to the model; one regressor modelling object presentation for all trials modulated by the absolute difference between the

participant's rating and the instructed object value, and one regressor modelling the rating events with the same modulator. All regressors included in this GLM were convolved with a canonical double-gamma hemodynamic response function. Their temporal derivatives were also included in the model, with the motion and physiological confounds estimated by fMRIPrep as described above.

Regions of interest (ROI)

A vmPFC ROI was defined using the combination of the Harvard-Oxford regions frontal pole, frontal medial cortex, paracingulate gyrus and subcallosal cortex, falling between MNI x = -14 and 14 and z < 0, as in (Schonberg et al., 2014). This ROI was used for small volume correction where specified.

In addition, we defined four ROIs along the ventral visual stream of the brain; the perirhinal cortex (PRC), parahippocampal place area (PPA), fusiform face area (FFA) and the lateral occipital complex (LOC) using functional localizer data, as in (Erez et al., 2016). The PRC was defined based on a probabilistic map (Devlin and Price, 2007) created by superimposing the PRC masks of 12 subjects, segmented based on anatomical guidelines in MNI-152 standard space. We thresholded the probabilistic map to keep voxels having more than 30% chance of belonging to the PRC, as in previous work (Erez et al., 2016). The lateral occipital complex (LOC) was defined as the region located along the lateral extent of the occipital pole that responded more strongly to objects than scrambled objects ($p < 0.001$, uncorrected). The fusiform face area (FFA) was defined as the region that responded more strongly to faces than objects. The PPA was defined as the region that responded more strongly to scenes than to objects. For each of these contrasts, a 10 mm radius sphere was drawn around the peak voxel in each

hemisphere using FSL (fslmaths). To analyze brain activity in these regions during the bidding task, contrasts of parameter estimate maps from the second-level analysis (average of the four runs for each participant) were converted to percent signal change (as described in (Mumford, 2007)), before averaging across all voxels within each ventral visual stream ROI. Group-level activations were compared against 0 using one-sample t-tests.

Functional connectivity analysis

Functional connectivity was assessed using generalized psychophysiological interaction analysis (gPPI), to reveal brain regions where BOLD time-series correlate significantly with the time-series of a target seed region in one condition more than another (McLaren et al., 2012). The seed region was defined based on the significant activation cluster found in the group-level analysis for the configural trials value-modulation contrast, small-volume corrected for the vmPFC ROI (**Fig. 3.6A**). The seeds' neural response to configural and elemental trials were estimated by deconvolving the mean BOLD signal of all voxels inside the seed region (Gitelman et al., 2003).

The gPPI-GLM included the same regressors as the main GLM described above, plus two psychophysiological interaction (PPI) regressors of interest: one regressor modelling the seed region's response to configural trials, and one regressor modelling the seed region's response to elemental trials. These regressors were obtained by multiplying the seed region time-series with an indicator function for object presentation of the corresponding condition, and then re-convolving the result with the double-gamma hemodynamic function. The model additionally included one regressor modelling the BOLD time-series of the seed region.

Inference criteria

For behavioural and eye-tracking analysis, we used the standard threshold of $p < 0.05$ for statistical significance, and we report exact *p*-values and effect sizes for all analyses. Neuroimaging data are reported at the group level with statistical maps thresholded at $Z > 3.1$ and cluster-based Gaussian Random Field corrected for multiple comparisons with a (whole brain corrected) cluster significance threshold of $p < 0.05$. We report analyses restricted to the vmPFC ROI using the same inference criteria, with increased sensitivity to detect effects in this region defined *a priori* due to fewer comparisons (small volume correction). Ventral visual stream ROI results are reported using the statistical threshold of $p < 0.05$, Bonferroni-corrected for four comparisons as the number of ROIs ($p < 0.0125$).

Deviations from preregistration

The most substantial deviation from the pre-registered analysis concerns the main GLM defined for fMRI analysis. The pre-registered model did not include accuracy confound regressors (one for value modulation during object presentation and one for value-modulation during value rating), which we added after behavioural data analysis revealed a trend difference in accuracy between conditions. We also controlled for reaction times differently than what was stated in the pre-registration, this was done due to a mistake in the pre-registered analysis plan that was different from the usual process of accounting for RT (Botvinik-Nezer et al., 2020b; Salomon et al., 2020; Schonberg et al., 2014). These changes to the GLM make the model more stringent and allow for a clearer interpretation of the value-related activations reported here, ruling out the possibility that they might reflect reaction-time or difficulty/accuracy.

Results

Behaviour

We first present the behavioural results from the behavioural and fMRI studies, to establish the replicability of the behavioural effect.

Learning phase

Participants learned the value of novel multi-attribute objects under two conditions, elemental and configural. Learning behaviour differed between conditions in both the behavioural and the MRI sample (this phase of the task was performed outside the scanner in both studies), with configural associations being generally harder to learn than elemental ones, as detailed below.

Rating error decreased across learning trials and was generally higher in the configural condition as depicted in **Figure 3.3A**. This was formalized by a repeated measures ANOVA with block and condition as within-subject factors, which revealed a main effect of block (behavioural sample $F_{(4, 128)} = 58.21$, $p < 0.001$, $\eta_p^2 = 0.45$; fMRI sample $F_{(4, 164)} = 60.73$, $p < 0.001$, $\eta_p^2 = 0.40$) and a main effect of condition (behavioural sample $F_{(1, 32)} = 372.14$, $p < 0.001$, $\eta_p^2 = 0.56$; fMRI sample $F_{(1, 41)} = 470.84$, $p < 0.001$, $\eta_p^2 = 0.56$) on rating error. We also found a significant block by condition interaction (behavioural sample $F_{(4, 128)} = 37.98$, $p < 0.001$, $\eta_p^2 = 0.35$; fMRI sample $F_{(4, 164)} = 30.20$, $p < 0.001$, $\eta_p^2 = 0.25$). This interaction reflects that accuracy becomes more similar across conditions as learning wore on, although rating error remained significantly greater in the configural compared to the elemental condition on the last (fifth)

learning block (paired-sample T-test, behavioural sample $t_{(32)} = 4.69$, $p < 0.001$, Cohen's $d = 0.817$; fMRI sample $t_{(41)} = 6.46$, $p < 0.001$, Cohen's $d = 0.90$).

Along with the increase in accuracy, reaction times decreased across learning blocks (main effect of block, behavioural sample $F_{(4, 128)} = 7.17$ $p < 0.001$, $\eta_p^2 = 0.09$; fMRI sample $F_{(4, 164)} = 26.38$, $p < 0.001$, $\eta_p^2 = 0.22$). Reaction times were significantly faster in the elemental compared to the configural condition (main effect of condition, behavioural sample $F_{(1, 128)} = 467.58$, $p < 0.001$, $\eta_p^2 = 0.62$; fMRI sample $F_{(1, 164)} = 391.35$, $p < 0.001$, $\eta_p^2 = 0.51$). We found no significant block by condition interaction in the behavioural sample ($F_{(4, 128)} = 0.387$, $p = 0.818$, $\eta_p^2 = 0.005$), but we did find a significant interaction in the fMRI sample ($F_{(4, 164)} = 4.35$, $p = 0.002$, $\eta_p^2 = 0.05$).

Learning probe

After five learning blocks, participants completed a learning probe without feedback, to assess the ability to assign value to the objects (**Fig. 3.3B**). The learning probe was the first phase in which participants had to sum two attribute-values in the elemental condition. This phase was also performed outside the scanner.

In the learning probe, accuracy was lower in the elemental condition compared to the configural condition in the behavioural sample (paired-sample T-test; $t_{(32)} = 2.13$, $p = 0.041$, Cohen's $d = 0.372$) but was not significantly different between conditions in the fMRI sample ($t_{(41)} = 1.30$, $p = 0.201$, Cohen's $d = 0.201$). Participants were slower in the elemental compared to the configural condition in both samples (behavioural sample $t_{(32)} = 5.47$, $p < 0.001$, Cohen's $d = 0.953$; fMRI sample $t_{(41)} = 9.56$, $p < 0.001$, Cohen's $d = 1.48$).

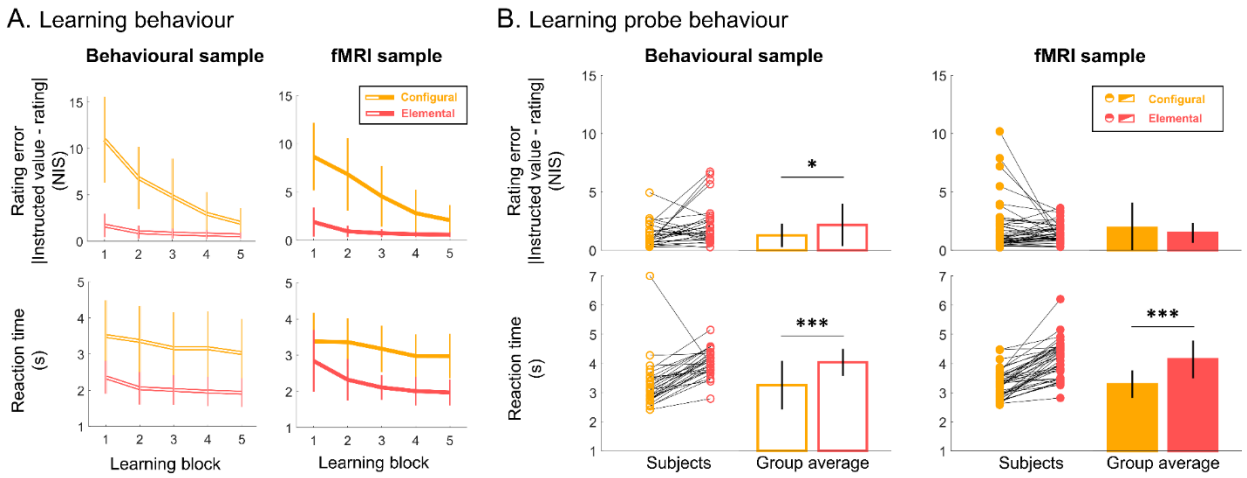

Figure 3.3. Accuracy and reaction time during the learning phase. **A)** Accuracy (top) and reaction time (bottom) across learning blocks in configural and elemental conditions. **B)** Accuracy (top) and reaction time (bottom) during the learning probe following the 5 learning blocks, by condition. Accuracy is measured in terms of rating error, corresponding to the absolute difference between value rating and the instructed value of the fribble, averaged across all trials within a learning block or within the learning probe, by condition. Instructed value corresponds to the value of the single salient attribute in the learning blocks in the elemental condition, and to the sum of the two attributes in the learning probe. In the learning blocks and probes in the configural condition, instructed value corresponds to the value associated with the configuration of two attributes. Error bars represent one standard deviation. *indicates a significant difference between conditions at $p < 0.05$, *** $p < 0.001$.

Bidding task

After learning, participants were shown objects from the configural and elemental sets and were asked to bid. Participants in the fMRI study performed the learning and probe phases outside the scanner and then performed the bidding stage while scanned with fMRI.

Bidding accuracy was high and not significantly different between the configural (mean rating error = 2.26NIS, SD = 1.66) and elemental (M = 2.04NIS, SD = 1.66) conditions for the behavioural sample ($t_{(32)} = 1.08$, $p = 0.289$, Cohen's $d = 0.188$) (**Fig. 3.4**). In the fMRI sample, bids tended to be closer to the instructed value (smaller error) in the elemental (M = 2.18NIS, SD = 1.02) compared to the configural condition (M = 2.55NIS, SD = 1.63), although the difference did not reach significance and the effect was marginal ($t_{(41)} = 1.90$, $p = 0.065$, Cohen's $d = 0.293$). Nevertheless, we included a trial-by-trial accuracy measure in the fMRI GLM analysis to control for this potential confound. Rating reaction times were not significantly different between conditions (behavioural sample $t_{(32)} = 1.80$, $p = 0.081$, Cohen's $d = 0.314$; fMRI sample $t_{(41)} = 0.251$, $p = 0.803$, Cohen's $d = 0.038$).

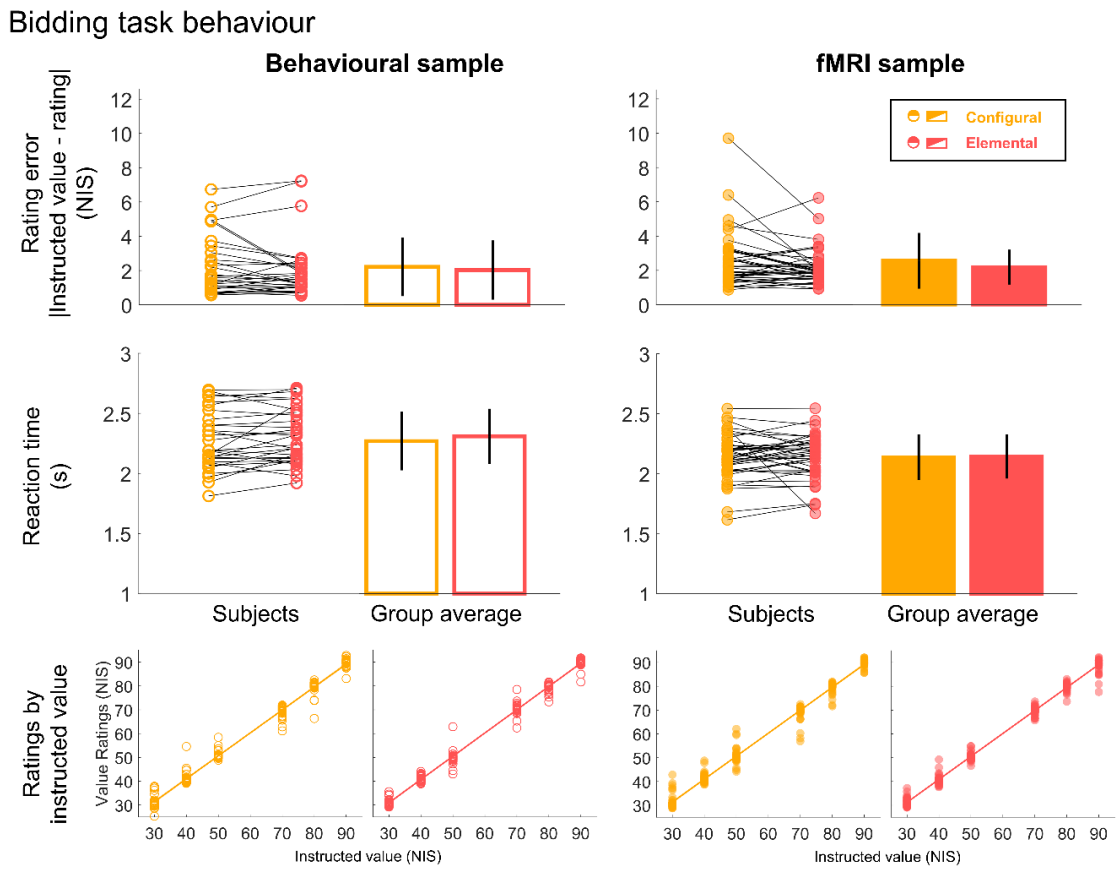

Figure 3.4. Accuracy and reaction time during the fMRI bidding phase. Individual and group average value rating error (top) and reaction time (middle) collapsed across all trials for each condition. The instructed value corresponds to the sum of the two attribute-values in the elemental condition. In the configural condition, instructed value corresponds to the value associated with the unique combination (configuration) of two attributes. Error bars represent one standard deviation from the group mean. Bottom panels show mean ratings for individual participants over the six presentations of each object with group-level linear regression fit.

Eye-tracking

We investigated whether eye movements during the 3-s object presentation epoch of the bidding task trials were different for objects learned in the elemental and configural condition (**Fig. 3.5**). The average number of fixations made on the whole object was similar between conditions (behavioural sample $t_{(32)} = 1.741$, $p = 0.091$, Cohen's $d = 0.303$; fMRI sample $t_{(32)} = 0.479$, $p = 0.635$, Cohen's $d = 0.083$). However, we found consistent condition differences across samples in eye movements with respect to fixations to the value-predictive attributes. Participants made significantly more transitions between these attributes in the configural compared to the elemental condition (behavioural sample $t_{(32)} = 3.364$, $p = 0.002$, Cohen's $d = 0.586$; fMRI sample $t_{(32)} = 2.659$, $p = 0.012$, Cohen's $d = 0.463$), and the average duration of individual fixations was longer in the elemental condition (behavioural sample $t_{(32)} = 3.611$, $p = 0.001$, Cohen's $d = 0.559$; fMRI sample $t_{(32)} = 2.211$, $p = 0.034$, Cohen's $d = 0.385$).

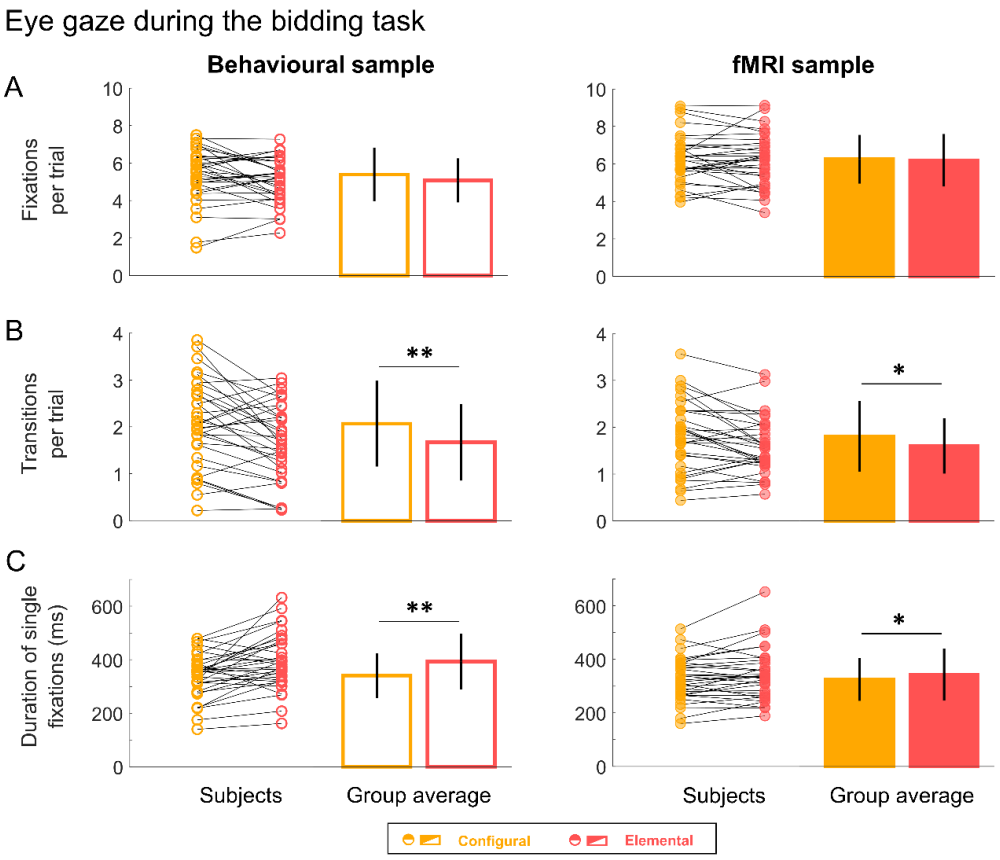

Figure 3.5. Eye-tracking results. Average number of fixations per trial (top), average number of transitions between attribute-AOIs per trial (middle) and average duration of individual fixations on attribute-AOIs (bottom). Error bars represent one standard deviation from the group mean. * indicate significant differences between conditions at $p < 0.05$, ** $p < 0.01$.

Brain imaging

vmPFC

We hypothesized that the fMRI signal in vmPFC would correlate with configural object value, and that the correlation of signal in vmPFC and value would be stronger for configural compared to elemental trials. To test this hypothesis, we preregistered analysis of value modulation effects at the time of object presentation in the *a priori* defined vmPFC region of interest using small volume correction. We did not find the hypothesized value signal in the vmPFC during the object presentation epoch. Signal in this region did not significantly correlate with value in any condition and there was no significant condition by value interaction.

However, we found evidence in support of our hypothesis at the time of value rating. Two clusters in the vmPFC were significantly correlated with value for configural, but not elemental trials in the rating phase (**Fig. 3.6A**). The direct condition contrast did not reveal a significant condition by value interaction, although this effect did emerge at a more liberal cluster-forming threshold of $Z = 2.3$, revealing a cluster in the vmPFC in which signal was correlated more strongly with value in configural compared to elemental trials, and in which signal correlated with value in configural trials (**Fig. 3.6B**).

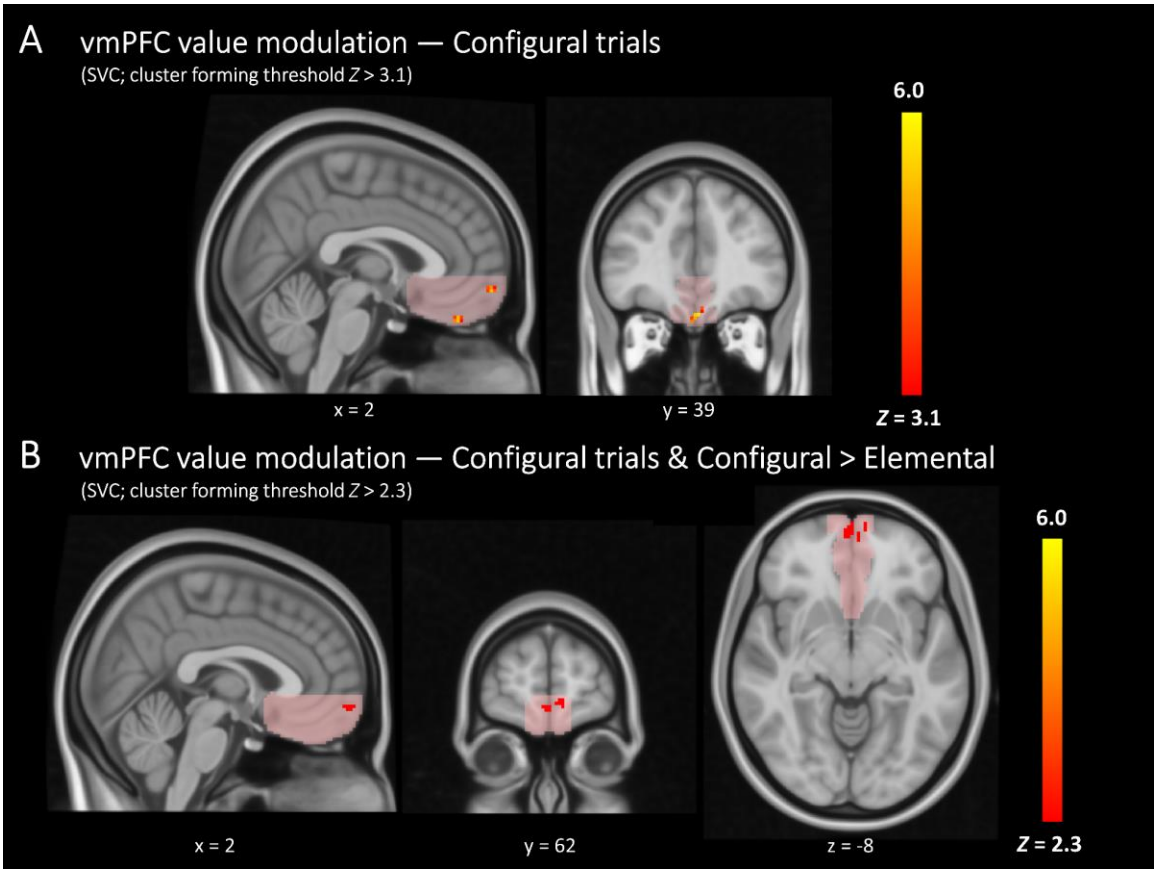

Figure 3.6. Value-modulated activation clusters during value rating in the vmPFC. **A)** Clusters where the fMRI signal was significantly modulated by value in configural trials using the preregistered cluster forming threshold ($Z > 3.1$). **B)** Conjunction analysis using a more liberal cluster forming threshold of $Z > 2.3$ revealed a vmPFC cluster where signal was significantly modulated by value in configural trials but not in elemental trials, and where value modulation was stronger for configural compared to elemental trials. Results were small volume corrected (SVC) for the pre-registered vmPFC region of interest (shaded area), $p < 0.05$. The color bar indicates Z-statistics. Numbers below slices indicate MNI coordinates. L = left, R = right.

Ventral visual stream

We next tested whether the ventral visual stream regions of interest were sensitive to valuation condition. Our preregistered hypothesis was that at the time of object presentation, signal in the PRC, and not in anterior VVS regions, would be greater when recognizing objects learned in the configural condition. We found no significant main effect of condition on BOLD in the PRC (p = 0.460) or any other VVS region (LOC p = 0.286; FFA p = 0.731; PPA p = 0.136) (**Fig. 3.7B***,* left) at the time of object presentation, indicating that during this time VVS ROIs were similarly activated in response to objects learned in the configural and elemental condition.

We performed exploratory analyses to examine whether VVS regions were sensitive to value. We found a significant condition by value interaction in the PRC: in this region, the BOLD signal for subjective value was stronger for configural compared to elemental trials (p = 0.016, Bonferroni corrected for four ROIs) (**Fig. 3.7B**, right). This effect was specific to the PRC and was not found in more posterior regions of the VVS (LOC, FFA and PPA uncorrected *ps* > 0.727). This effect was also specific to the object presentation epoch as there was no significant effect of condition (uncorrected *ps* > 0.216) and no condition by value interaction (uncorrected *ps* > 0.394) in any VVS regions during value ratings (**Fig. 3.7C**). We note that signal in the PRC and other VVS regions did not demonstrate significant value modulation for the configural or elemental trials examined separately (Supplementary Material, **Fig. S3.2**).

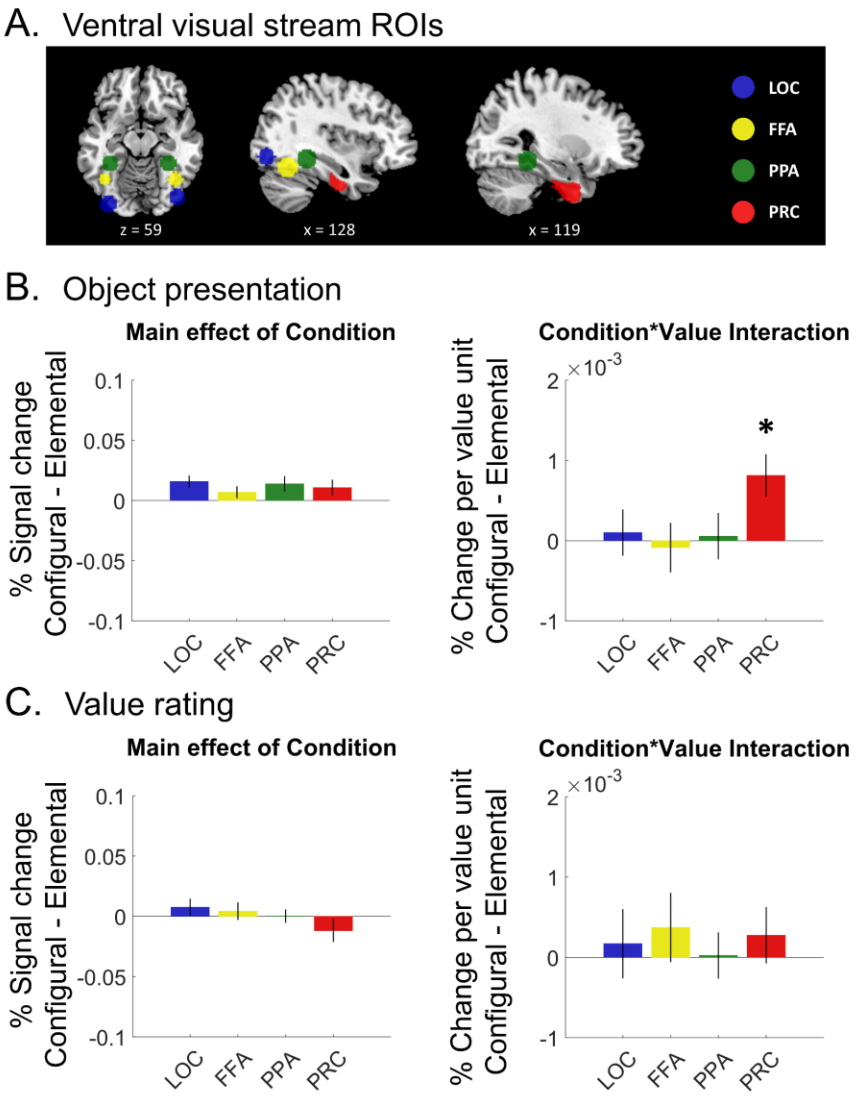

Figure 3.7. Ventral visual stream regions of interest analysis. **A)** Ventral visual stream regions of interest. The lateral occipital complex (LOC), fusiform face area (FFA) and parahippocampal place area (PPA) ROIs shown for a representative participant. The perirhinal cortex (PRC) ROI was the same for all participants. Numbers indicate coordinates in MNI space. **B)** Group average percent signal change during the object presentation epoch. **C)** Group average percent signal change at the value rating epoch. The left panels show the main effects of condition, assessed with the configural minus elemental trials contrast. The right panels show the condition by value interaction, assessed by contrasting the effect of value modulation in configural trials, minus value the effect of value modulation in elemental trials. Error bars represent SEM. Asterisk indicates significance at $p < 0.05$ for one sample t-test against 0, after Bonferroni correction for four comparisons.

Functional connectivity

We carried out exploratory functional connectivity analysis using gPPI, defining the seed as the significant vmPFC clusters found for configural trials value modulation (**Fig. 3.6A**). The gPPI analysis did not reveal any clusters across the whole-brain, and no VVS region displaying evidence for greater functional connectivity with the vmPFC seed in the configural compared to the elemental trials or vice versa.

Whole brain analyses

For completeness, we report exploratory whole brain analyses for the effects of condition as well as the value modulation effects, during object presentation and value rating epochs. We accompany each figure with a table reporting the Pearson correlation between the group-level unthresholded statistical map and the 10 terms most strongly associated with this activation pattern across fMRI studies using the reverse inference tool of Neurosynth (Yarkoni et al., 2011). We first report the main effects of condition on brain activity at the time of object presentation.During the object presentation epoch, the condition contrast revealed several brain regions that were significantly more active during the configural trials, including the right caudate, left lateral orbitofrontal cortex, the right inferior frontal gyrus, bilateral precuneus, bilateral lateral occipital complex and the cerebellum (**Fig. 3.8A**). The opposite contrast revealed that primary sensory-motor cortex, supplementary motor cortex and the superior frontal gyrus were more active during elemental trials (**Fig. 3.8B**). Complete information on all significant clusters is presented in Supplementary Material (**Table S3.1**). A cluster encompassing the left pre- and post-central gyrus correlated with value in the two conditions (**Fig. 8*C-D***). This

activation likely reflects motor preparation to report the value rating, as a longer index finger press was systematically associated with moving the slider to higher values on the scale.

During the value rating epoch, we did not find any clusters where activity was significantly greater in one condition compared to the other. Clusters common to both conditions contained signal which was significantly modulated by value, including a cluster encompassing the pre- and post-central gyrus, in addition to occipital and fusiform clusters (**Fig. 3.9**). The fMRI signal did not correlate with value more in one condition compared to the other in any brain region.

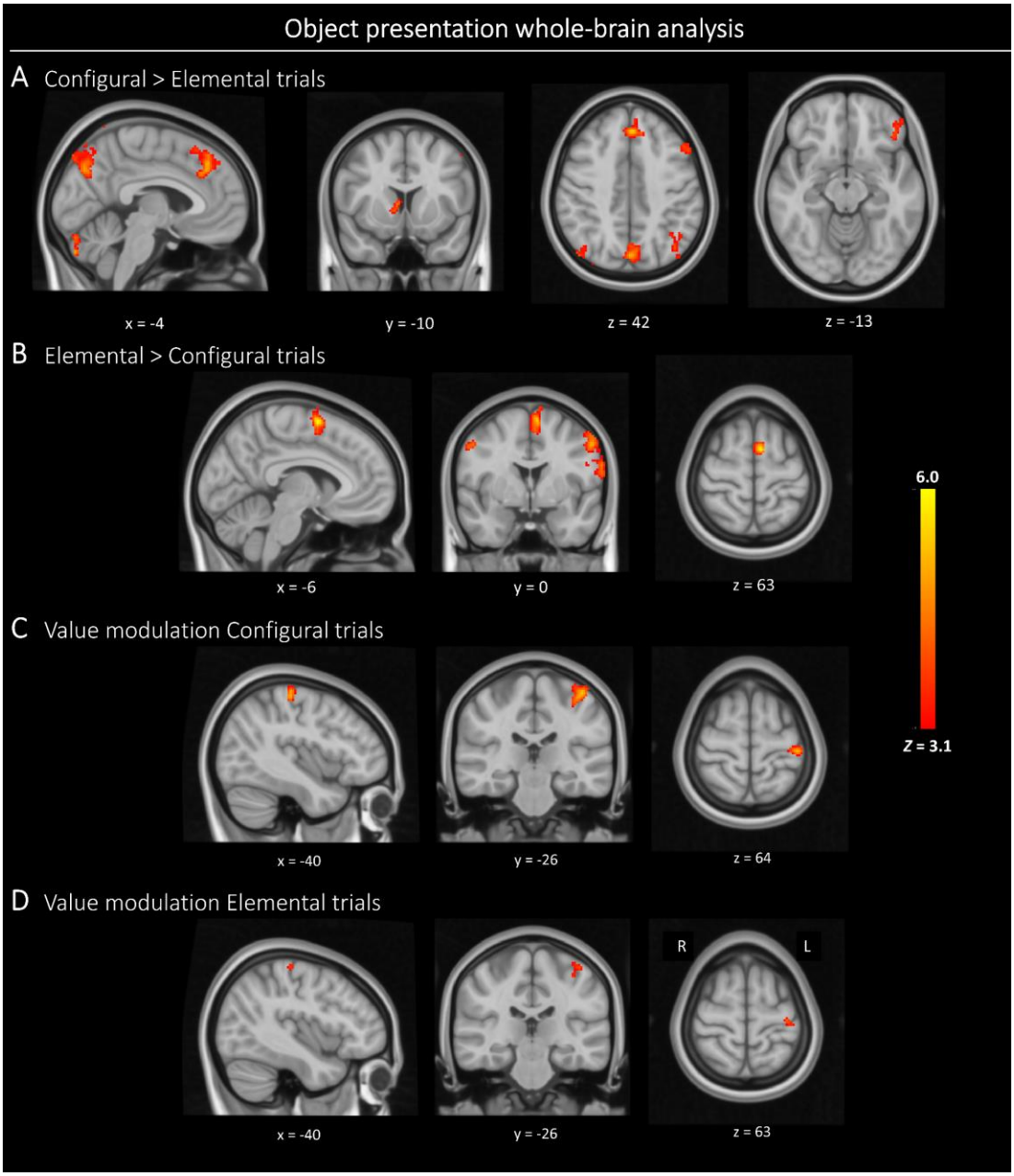

Figure 3.8. Whole-brain analysis of object presentation epoch. **A)** Clusters exhibiting greater activity in configural compared to elemental trials. **B)** Clusters exhibiting greater activity in elemental compared to configural trials. **C)** Clusters exhibiting value modulation in configural trials. **D)** Clusters exhibiting value modulation in elemental trials. Results were whole-brain cluster-corrected, $p < 0.05$. Color bar indicates Z-statistics. Numbers below slices indicate MNI coordinates. L = left, R = right.

Table 3.1. Pearson correlations between term-based reverse inference maps from Neurosynth and the unthresholded statistical maps of the contrasts shown in Fig. 8.

Object presentation epoch	Term	Correlation (r)
A) Configural > Elemental	Retrieval	0.187
	precuneus	0.176
	Episodic	0.145
	memory retrieval	0.137
	Memory	0.122
	recognition memory	0.122
	episodic memory	0.114
	Semantic	0.111
	navigation	0.101
	retrosplenial	0.098
B) Elemental > Configural	Motor	0.303
	Premotor	0.279
	premotor cortex	0.262
	movements	0.245
	sensorimotor	0.238
	motor imagery	0.237
	supplementary	0.232
	supplementary motor	0.225
	primary motor	0.219
	movement	0.218
C) Value modulation Configural	medial prefrontal	0.215
	Medial	0.19
	Social	0.155
	Resting	0.152
	ventromedial	0.15
	Amygdala	0.147
	resting state	0.146
	orbitofrontal	0.143
	emotional	0.142
	Mpfc	0.137
D) Value modulation Elemental	Fa	0.082
	orbitofrontal	0.064
	orbitofrontal cortex	0.063
	prefrontal	0.061
	Corpus	0.061

	Retrieval	0.061
	corpus callosum	0.059
	medial prefrontal	0.059
	Callosum	0.059
	prefrontal cortex	0.058

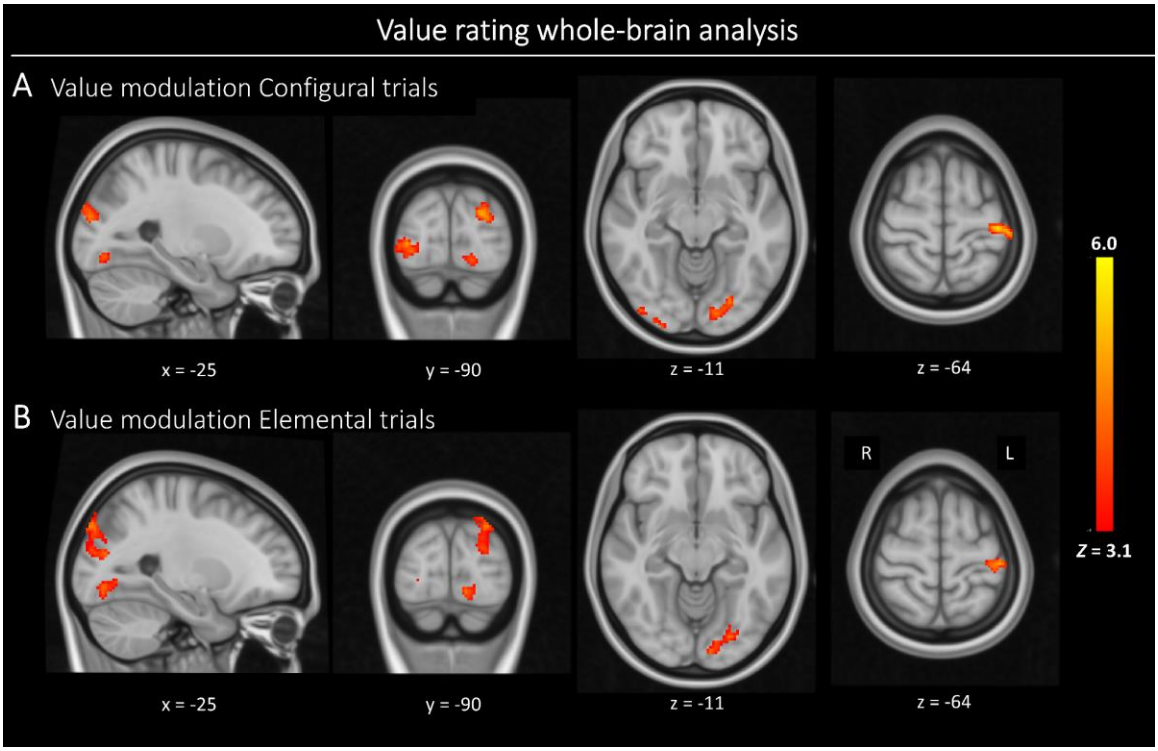

Figure 3.9. Whole brain analysis of the value rating epoch. **A)** Clusters exhibiting value modulation in configural trials. **B)** Clusters exhibiting value modulation in elemental trials. Results were whole-brain cluster-corrected, $p < 0.05$. Color bar indicates Z-statistics. Numbers below slices indicate MNI coordinates. L = left, R = right.

Table 3.2. Pearson correlations between term-based reverse inference maps from Neurosynth and the unthresholded statistical maps of the contrasts shown in Fig. 9.

Value rating epoch	Term	Correlation (r)
A) Value Modulation Configural	medial prefrontal	0.187
	Medial	0.165
	ventromedial	0.145
	orbitofrontal	0.143
	Default	0.14
	ventromedial prefrontal	0.136
	autobiographical	0.136
	orbitofrontal cortex	0.135
	default mode	0.134
	posterior cingulate	0.131
B) value modulation elemental	hand movements	0.065
	visual cortex	0.062
	Occipital	0.061
	Pitch	0.060
	Musical	0.059
	planum temporale	0.059
	auditory cortex	0.059
	primary auditory	0.058
	auditory	0.056
	extrastriate	0.056

Discussion

This study provides behavioural, eye-tracking and fMRI evidence that there are two ways to "see" the value of multi-attribute decision options. We found that evaluation of complex objects relied on different patterns of information acquisition, indexed by eye movements, and engaged different brain regions when value is predicted by configural relationships between attributes compared to when value could be summed up from the values of individual attributes. Activity in the perirhinal cortex was related to value in configural more

than elemental trials during object presentation, whereas at the time of value rating, the vmPFC showed value-modulated signal for configural trials only. Participants made more gaze transitions from one attribute to another when observing objects in the configural condition and made longer fixations on individual attributes in the elemental condition.

Strengths of this study design include replication of the behavioural effect in two samples and inclusion of a pilot imaging sample to inform the design of the full fMRI experiment, which was pre-registered. Further, these experiments directly build on a recent study in patients with vmPFC damage using the same stimuli, providing converging evidence in keeping with the goal of triangulation (Munafò and Smith, 2018). The lesion study found that vmPFC damage impaired binary decisions between fribbles in the configural condition, but not in the elemental condition (Pelletier and Fellows, 2019). The current work provides converging support for the hypothesis that vmPFC has a unique role in inferring the value of objects based on configural information: BOLD signal in that region was only detectably modulated by object value in the configural and not the elemental condition. It further argues that evaluation under this condition relies on the perirhinal cortex, a region known to be critical for multi-attribute object recognition, but here for the first time also implicated in the evaluation of such objects.

We did not find that object-value obtained by combining two separately learned attribute-values was reflected in the fMRI vmPFC signal. This null result alone cannot be used to conclude that this region is not involved in value integration from multiple elements, but taken together with the finding that such evaluation was also spared in those with vmPFC damage, it suggests alternate routes to value construction under such summative conditions which do not require involvement of the vmPFC. Across a large body of existing fMRI work, vmPFC is reliably

associated with subjective value (Bartra et al., 2013; Rushworth and Behrens, 2008). Activity in the vmPFC has previously been shown to reflect the value of items composed of multiple attributes, each modelled as independently predictive of value (Basten et al., 2010; Lim et al., 2013; Suzuki et al., 2017). One study using a very similar approach to the elemental condition here and found that integrated value could be decoded from vmPFC signal using multivariate pattern analysis (MVPA) (Kahnt et al., 2011). MVPA has greater sensitivity to detect value-related signals exhibiting larger variability across participants and voxels than univariate analysis (Davis et al., 2014; Kahnt, 2018). It is possible that we did not detect value related fMRI signals in the elemental condition in vmPFC using univariate analysis simply because it is represented more heterogeneously than in the configural condition. However, if that were the case, given the previous lesion finding, it would suggest that vmPFC univariate value representations, or lack thereof, might better predict whether this region is required in a decision task than multivariate representations.

Other neuroimaging studies of multi-attribute decisions found correlates of value summed across attributes in other brain regions, not vmPFC (Berker et al., 2019; Fujiwara et al., 2009). The current findings add to the view that the vmPFC is not critical for value integration in general, but rather engaged under a more narrow set of conditions. We propose a more specific account whereby the vmPFC is required for inferring value from the configural relationships among lower-level attributes. This view might explain prior observations that patients with vmPFC damage are able to evaluate complex social or aesthetic stimuli, but seem to draw on different information to assess the value of such stimuli, compared to healthy participants (Vaidya et al., 2018; Xia et al., 2015).

This current work also studied whether regions known to be involved in complex object recognition are likewise involved in assessing the value of such options. Given previous findings of PRC activation in tasks requiring holistic object representations, but not in tasks accomplished on the basis of individual attributes (Devlin and Price, 2007), and lesion studies demonstrating a causal role for PRC in configural object discrimination (Barense et al., 2007; Buckley and Gaffan, 1998; Bussey et al., 2002, 2003), we predicted greater activity in the PRC for evaluating objects in the configural condition. This hypothesis was not supported by our data, with no main effect of condition in the PRC or other VVS regions. It is possible that objects were processed similarly through the VVS in both conditions to support holistic recognition, as their general appearance (the body and position of appendages) was informative of whether a given stimulus was from the elemental or configural set. In any case, such holistic processing may be obligatory even if not task-relevant.

We found that fMRI VVS signals were differently sensitive to value between conditions. Specifically, BOLD activity in the PRC was modulated by value more for configural compared to elemental trials. There are previous reports of value-correlated signal across the VVS, including in the primary visual cortex (Nelissen et al., 2012; Serences, 2008), lateral occipital complex (Persichetti et al., 2015), the PRC (Mogami and Tanaka, 2006) and several of these regions combined (Arsenault et al., 2013; Kaskan et al., 2017). Across studies, reward was paired with stimuli ranging in complexity from simple colored gratings to complex real-world objects, but no work previously contrasted conditions in which valuation tap on different stages of the VVS hierarchy. Our findings suggest a selective involvement of the PRC in encoding value when it is associated with the high-level (i.e. configural) object representation that this region supports.

The condition by value interaction observed for PRC activity was only observed at the time of object presentation, on average six seconds before the rating phase where the value signal was detected in the vmPFC, arguing against the possibility that value-related PRC activation is driven by the vmPFC. The findings rather suggest that configural value emerges at least in part from activity in the VVS regions involved in holistic object recognition, with vmPFC activation following later. Electrophysiological recordings in macaques revealed that PRC neurons are sensitive to objects value slightly later than neurons of the immediately preceding VVS stage (area IT) (Mogami and Tanaka, 2006), suggesting that value emerges along VVS object processing. In this work, PRC neurons demonstrated value sensitivity at ~200 ms after stimulus onset, whereas other work reported value selectivity only after ~400-500ms in the OFC (Kennerley et al., 2008; Wallis and Miller, 2003). Accordingly, electroencephalography recordings in humans found that upon presentation of a reward-paired object, a value-correlated signal was detected rapidly in occipital cortex and traveled anteriorly to the prefrontal cortex as time passes (Larsen and O'Doherty, 2014). The current work adds to these data in supporting the emerging view that value arises gradually in the course of a distributed and hierarchical processing from visual inputs to action generation (Yoo and Hayden, 2018).

We did not find evidence for increased functional connectivity between the vmPFC and PRC (or any other brain regions) during configural object valuation. This null result must be taken with caution, as the study was not powered to find such an effect. There are anatomical connections (Heide et al., 2013) and there is evidence of functional connectivity (Andrews-Hanna et al., 2014) between the vmPFC and the medial temporal lobe in humans, and the PRC and medial OFC are reciprocally connected in macaques (Kondo et al., 2005). Together with the

current findings of value-related activations at different stages of the trial in the PRC and the vmPFC, this suggests that interactions between these two regions might be important for value estimation in configural conditions. Further work using methods with better temporal resolution will be needed to test this hypothesis.

We found systematic differences in eye gaze patterns between conditions, replicated in two samples, one behavioural and one inside the fMRI. Fixations were shorter and more transitions were made between attributes of objects in the configural condition. Sequential sampling models have shown that value and gaze interact in driving the decision process (Krajbich et al., 2010), and that gaze duration has a causal influence on value (Shimojo et al., 2003). However, little is known about fixation patterns within multi-attribute objects during choice (Krajbich, 2019), and how they relate to the value construction process, regardless of expected value. Consumer research extensively studied value construction strategies employed during multi-attribute decisions using process tracing measures including eye-tracking (Bettman et al., 1998; Russo and Dosher, 1983). However, this work artificially decomposes options by laying out attributes as text and numbers in decision grids, thus disrupting normal object recognition processes occurring in real-life choices. Elucidating the interplay between gaze patterns and value construction for multi-attribute decisions where value predictions are based on visual information will be an important avenue of future research (Schonberg and Katz, 2020).

Although we attempted to match the two conditions for difficulty, and further addressed this potential confound by controlling for trial-by-trial rating reaction time and accuracy in all fMRI analyses, we could not account for potential condition differences in speed

of evaluation during the fixed object presentation time and the subsequent ITI. If evaluation was faster in the elemental condition, value-correlated signal might have been passed on to motor regions earlier than in the configural condition (Hare et al., 2011b; Yoo and Hayden, 2018). The slider response requirement also meant that motor responses were confounded with rated values, potentially explaining why only motor regions showed value-correlated activation at the time of object presentation in the elemental condition.

In conclusion, this neuroimaging study and our previous work in lesion patients together provide evidence for two ways of building the value of complex objects, supported by distinct neural mechanisms. By leveraging object-recognition research to inform studies of multi-attribute value-based decisions, this work suggests that value might drive how an object is recognized through VVS processing, blurring the lines between object recognition and value construction research.

Footnotes

The authors declare no competing financial interests. This work was supported by the Canadian Institutes of Health Research (Grant MOP 249071), the H2020 European Research Council, (Grant number: 715016); a Sandwich Fellowship to GP from the Israeli Ministry for Higher Education and the Zavalkoff Family foundation. We also thank volunteers for their participation. Correspondence should be addressed to Gabriel Pelletier at gabriel.pelletier@mail.mcgill.ca.

Supplementary material

Table S3.1. Regions showing significant activations clusters for whole brain imaging contrasts. For each cluster, the list shows all regions from the Harvard-Oxford atlas that contained more than 5 voxels within that cluster, along with the peak X/Y/Z location for the cluster in MNI space

Contrast	Cluster #	Cluster size	X	Y	Z	Peak Z-value	p	Region	# of voxels in region
Configural > Elemental Object Presentation	1	65	8	8	6	4.980	0.0168		
								R._Caudate	34
	2	77	40	-68	-46	4.900	0.00635		
								Cerebellum	77
	3	176	56	28	22	4.580	7.69e-06		
								R._Inferior_Frontal_Gyrus_pars_triangularis	44
								R._Middle_Frontal_Gyrus	35
								R._Inferior_Frontal_Gyrus_pars_opercularis	13
								R._Frontal_Pole	8
	4	184	-44	-60	46	4.110	4.77e-06		
								L._Lateral_Occipital_Cortex_superior_division	118
								L._Angular_Gyrus	32
	5	193	14	-68	28	4.340	2.8e-06		
								R._Precuneous_Cortex	183
	6	307	42	-74	48	4.760	6.25e-09		
								R._Lateral_Occipital_Cortex_superior_division	262
	7	354	-14	-82	-36	5.200	6.34e-10		
								Cerebellum	290
	8	374	-2	36	42	5.320	2.47e-10		
								L._Superior_Frontal_Gyrus	189
								L._Paracingulate_Gyrus	106
								R._Superior_Frontal_Gyrus	29
								R._Paracingulate_Gyrus	16
	9	478	14	-72	-30	5.720	2.35e-12		
								Cerebellum	370
	10	1060	-38	22	-4	4.940	9.6e-22		
								L._Frontal_Pole	358
								L._Middle_Frontal_Gyrus	148
								L._Frontal_Orbital_Cortex	116
								L._Inferior_Frontal_Gyrus_pars_triangularis	115
								L._Insular_Cortex	21

								L._Inferior_Frontal_Gyrus_pars_opercularis	12
	11	1097	2	-68	60	5.060	2.85e-22		
								L._Precuneous_Cortex	650
								R._Precuneous_Cortex	150
								L._Cuneal_Cortex	45
								R._Cuneal_Cortex	12

Contrast	Cluster #	Cluster size	X	Y	Z	Peak Z-value	p	Region	# of voxels in region
Elemental > Configural Object Presentation	1	67	54	-2	40	5.200	0.0142		
								R._Precentral_Gyrus	67
	2	219	-6	2	64	6.160	6.56e-07		
								L._Juxtapositional_Lobule_Cortex_(formerly _Supplementary_Motor_Cortex)	174
								L._Superior_Frontal_Gyrus	19
	3	288	-64	8	22	5.290	1.63e-08		
								L._Precentral_Gyrus	185
								L._Inferior_Frontal_Gyrus_pars_opercularis	19
	4	505	-56	-4	38	5.520	7.42e-13		
								L._Precentral_Gyrus	372
								L._Postcentral_Gyrus	16

Contrast	Cluster #	Cluster size	X	Y	Z	Peak Z-value	p	Region	# of voxels in region
Configural Object Presentation modulated by Value	1	172	-42	-26	62	5.340	3.34e-06		
								L._Postcentral_Gyrus	138
								L._Precentral_Gyrus	19

Contrast	Cluster #	Cluster size	X	Y	Z	Peak Z-value	p	Region	# of voxels in region
Elemental Object Presentation modulated by Value	1	56	-36	-22	64	4.150	0.0231		
								L._Postcentral_Gyrus	40
								L._Precentral_Gyrus	16

Contrast	Cluster #	Cluster size	X	Y	Z	Peak Z-value	p	Region	# of voxels in region
Elemental trials Rating Scale modulated by Value	1	110	-46	-78	6	4.930	0.000254		
								L._Lateral_Occipital_Cortex_inferior_division	66
								L._Lateral_Occipital_Cortex_superior_division	37
	2	147	-22	-88	22	5.090	1.78e-05		

								L._Lateral_Occipital_Cortex_superior_division	75
								L._Occipital_Pole	70
	3	165	-14	-86	-16	5.050	5.3e-06		
								L._Occipital_Fusiform_Gyrus	117
								L._Occipital_Pole	21
								L._Lingual_Gyrus	15
	4	273	-42	-26	62	6.060	7.83e-09		
								L._Postcentral_Gyrus	158
								L._Precentral_Gyrus	50
	5	367	26	-98	0	5.110	5.36e-11		
								R._Occipital_Pole	270
								R._Lateral_Occipital_Cortex_inferior_division	92

Contrast	Cluster #	Cluster size	X	Y	Z	Peak Z-value	p	Region	# of voxels in region
Elemental trials Rating Scale modulated by Value	1	117	28	-94	2	4.550	0.000178		
								R._Occipital_Pole	116
	2	205	-44	-26	62	5.120	5.36e-07	L._Postcentral_Gyrus	157
								L._Postcentral_Gyrus	157
								L._Precentral_Gyrus	32
	3	237	-48	-78	18	4.750	5.96e-08		
								L._Lateral_Occipital_Cortex_inferior_division	171
								L._Lateral_Occipital_Cortex_superior_division	38
	4	242	-16	-84	-10	4.620	5.96e-08		
								L._Occipital_Fusiform_Gyrus	166
								L._Occipital_Pole	23
								L._Lingual_Gyrus	16
	5	411	-24	-86	34	4.690	9.17e-12		
								L._Lateral_Occipital_Cortex_superior_division	281
								L._Occipital_Pole	59

Contrast	Cluster #	Cluster size	X	Y	Z	Peak Z-value	p	Region	# of voxels in region
Configural Rating Scale modulated by Value, SVC for vmPFC ROI	1	15	-4	30	-26	3.780	0.0376		
								L._Subcallosal_Cortex	8
								L._Frontal_Medial_Cortex	6
	2	17	2	60	-10	3.720	0.0283		
								R._Frontal_Pole	13
	3	18	0	40	-26	3.940	0.0247		

	L._Frontal_Medial_Cortex	12
	R._Frontal_Medial_Cortex	6

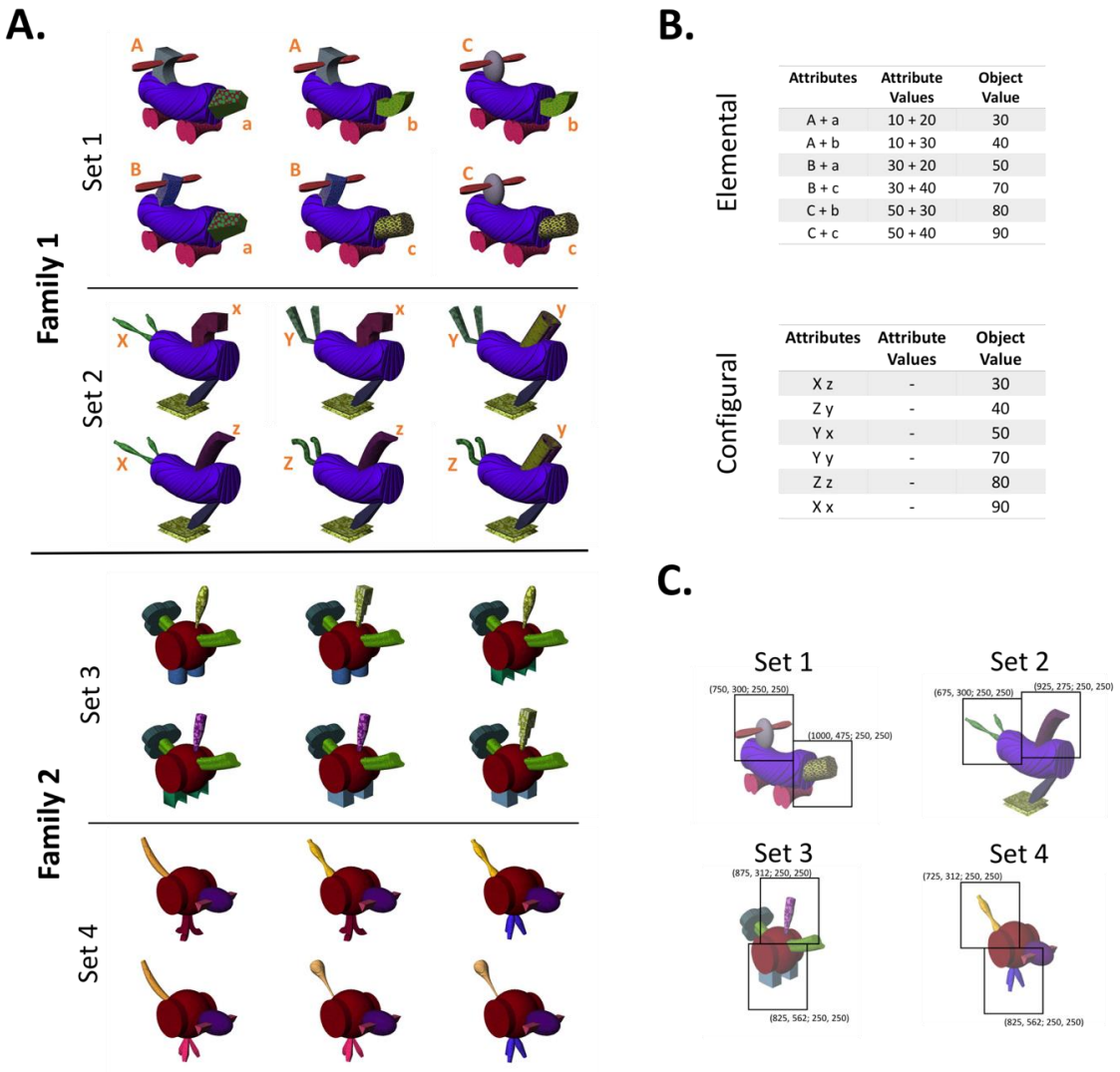

Figure S3.1. Object sets, object-value associations and areas of interest used for eye-tracking analysis. **A)** Object sets. Each participant is assigned one of the two fribbles families. Each condition is then assigned one object set from the selected family. The condition-object set pairing is counterbalanced across participants. **B)** Example of object value-association for one participant. **C)** Pre-registered areas of interest (AOI) for eye-tracking analysis, overlaid on an example object for each of the 4 object sets. AOIs are identical for all six objects within each object set. Numbers indicate (x origin, y origin; height; width) in screen pixels.

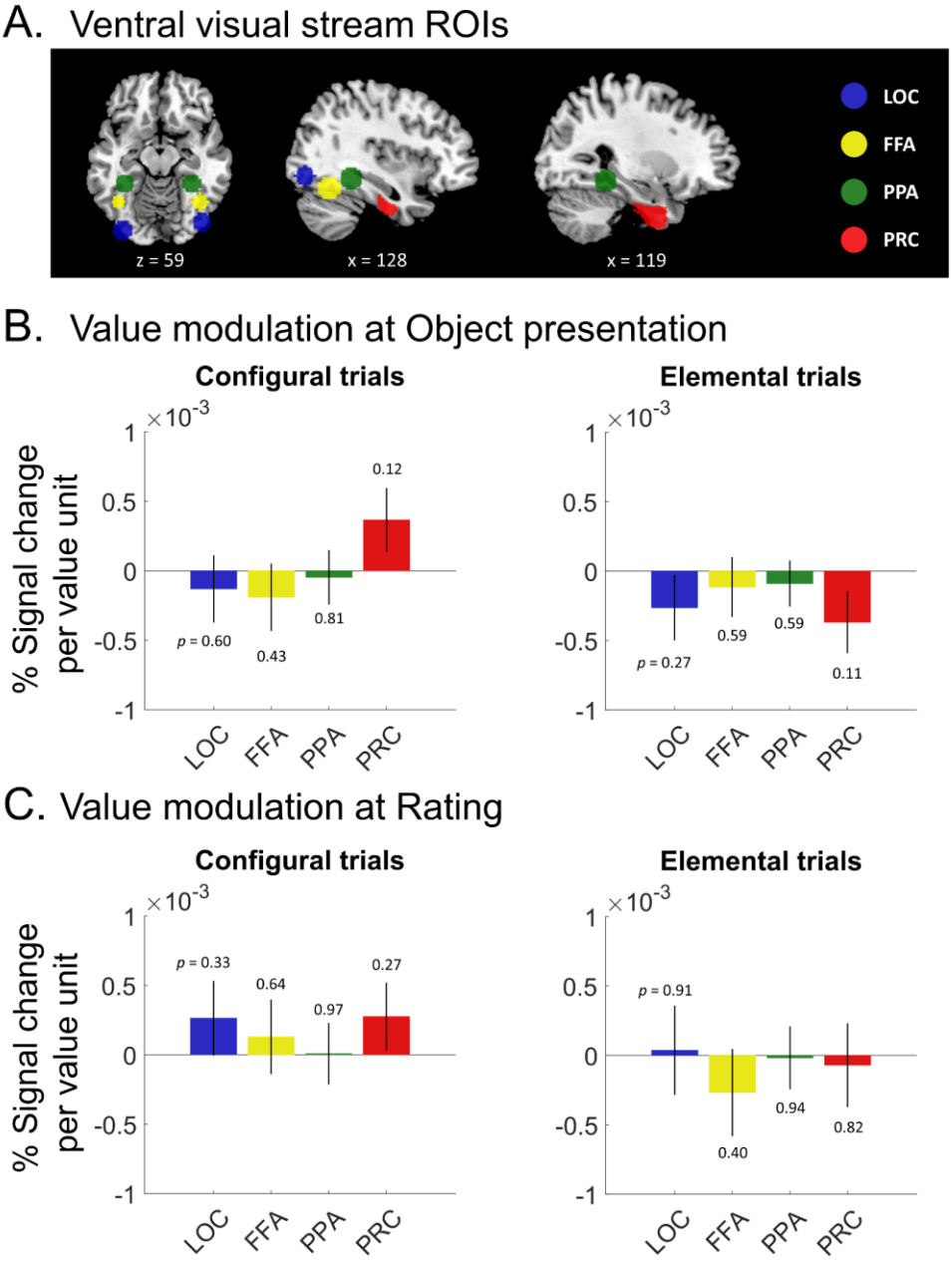

Figure S3.2. Value modulation in ventral visual stream regions of interest. **A)** Ventral visual stream regions of interest. The lateral occipital complex (LOC), fusiform face area (FFA) and parahippocampal place area (PPA) ROIs shown for a representative participant. The perirhinal cortex (PRC) ROI was the same for all participants. Numbers indicate coordinates in MNI space. **B)** Average contrasts of parameter estimate for value modulation at the object presentation epoch. **C)** Average contrasts of parameter estimate for value modulation at the rating epoch. Error bars represent SEM. Numbers above or bellow bars indicate uncorrected *p*-values for one-sample t-tests against 0 (baseline).

Chapter 4. Value neglect: a critical role for ventromedial frontal lobe in learning the value of spatial locations

Preface

The two previous chapters examined value-based decisions between complex objects and provided evidence to suggest that VMF contributions depend on the visual processing mechanisms involved in the recognition of *what* is being evaluated. So far, nearly all studies of value-based decision-making examined choices based on "what" the options are (often, complex objects), leaving unclear the contributions of the VMF to decisions based on the value of other types of visual information processed through distinct pathways, notably spatial locations.

In this last study, published in Cerebral Cortex, we tested whether VMF damage impairs decision-making when value was exclusively predicted by the spatial location of the options. Leveraging the dataset reported in Chapter 2, we further tested whether decisions based on the spatial relationship between objects and the environment, and decisions based on the configural associations between attributes of objects, are dissociable among VMF patients.

Value neglect: A critical role for ventromedial frontal lobe in learning the value of spatial locations[*]

Gabriel Pelletier and Lesley K. Fellows

Department of Neurology & Neurosurgery, Montreal Neurological Institute, Faculty of Medicine, McGill University

[*] Original source: Pelletier, G., & Fellows, L. K. (2020). Value Neglect: A Critical Role for Ventromedial Frontal Lobe in Learning the Value of Spatial Locations. Cerebral Cortex, 30(6), 3632–3643. https://doi.org/10.1093/cercor/bhz331

Abstract

Whether you are a gazelle bounding to the richest tract of grassland or a return customer heading to the freshest farm stand at a crowded market, the ability to learn the value of spatial locations is important in adaptive behavior. The ventromedial frontal lobe (VMF) is implicated in value-based decisions between objects and in flexibly learning to choose between objects based on feedback. However, it is unclear if this region plays a material-general role in reward learning. Here, we tested whether VMF is necessary for learning the value of spatial locations. People with VMF damage were compared with healthy participants and a control group with frontal damage sparing VMF in an incentivized spatial search task. Participants chose among spatial targets distributed among distractors, rewarded with an expected value that varied along the right-left axis of the screen. People with VMF damage showed a weaker tendency to reap reward in contralesional hemispace. In some individuals, this impairment could be dissociated from the ability to make value-based decisions between objects, assessed separately. This is the first evidence that the VMF is critically involved in reward-guided spatial search and offers a novel perspective on the relationships between value, spatial attention, and decision-making.

Introduction

Learning the reward value of locations in the environment is important for survival. For example, animals learn from experience where the best feeding sites are located, whether in laboratory settings or in natural habitats (Trapanese et al., 2018). In humans, it has been shown that reward feedback influences spatial attention and decision-making: targets appearing in previously rewarded locations are detected more quickly (Chelazzi et al., 2014) and selected more often (Lucas et al., 2013). However, the brain basis for learning the reward value of spatial locations has not been established.

Functional neuroimaging (fMRI) has shown that activity in the ventromedial prefrontal cortex (vmPFC) and orbitofrontal cortex (OFC), here referred to together as ventromedial frontal lobe (VMF), correlates with subjective value in a wide variety of tasks (Bartra et al., 2013) and that this area integrates value-relevant visual and semantic features into an overall option value (Basten et al., 2010; Kahnt et al., 2011; Lim et al., 2013). Damage to VMF reduces sensitivity to varying magnitude of prospective reward (Manohar and Husain, 2016) and impairs value-based choices for a variety of stimulus types, ranging from foods to faces to artwork, providing causal support for a general role for this region in comparing the value of options (Bowren et al., 2018; Henri-Bhargava et al., 2012; Vaidya et al., 2018; Xia et al., 2015). Such damage also impairs learning the value of objects or features of objects (e.g., colors) based on reward feedback, particularly in dynamic conditions, as with probabilistic feedback or in reversal learning (Tsuchida et al., 2010; Vaidya and Fellows, 2015a). These findings have been taken as evidence that VMF is generally important in learning about value and in representing

that information in a “common currency”, independent of the value-associated material (Delgado et al., 2016; Levy and Glimcher, 2012).

However, humans and macaques with VMF lesions are able to learn the value of actions from probabilistic feedback, despite impairments in learning the value of visual stimuli (Camille et al., 2011b; Rudebeck et al., 2008), arguing against an entirely domain-general account (Cisek, 2012). If VMF is not required for all forms of flexible value-based learning, what are the limits for this region’s engagement? VMF has strong anatomical connections with the ventral visual stream involved in complex object processing (the so-called “what” pathway) (Kondo et al., 2005), whereas parietal regions involved in the processing of visuospatial (“where”) information are preferentially interconnected with dorsolateral prefrontal cortex (Cavada et al., 2000; Price, 2007). This raises the possibility that VMF may be narrowly involved only in object-based value processing.

Research on spatial attention has suggested that posterior parietal and dorsal prefrontal regions encode attentional priority, mapping the behavioral salience of spatial locations in the visual field by integrating low-level sensory salience of stimuli composing a scene with top-down signals relating to goals and reward expectation to guide attentional orienting and action selection (Fecteau and Munoz, 2006; Gottlieb, 2007; Ptak, 2012). Modulation of these priority maps in this frontoparietal network has been proposed to explain findings that targets appearing in previously more rewarded locations are prioritized and thus more likely to be selected (Chelazzi et al., 2014). Lesions to these regions, especially in the right hemisphere, lead to hemi-spatial neglect in humans. Provocatively, however, such lesions do not diminish the influence of reward on choices between targets where value is solely predicted by spatial

position (Lucas et al., 2013), suggesting that other brain regions encode spatial location-value associations.

The hippocampus is a second candidate region that might be involved in spatial location-value associations, perhaps via interactions with VMF. The hippocampus represents the current position of an organism and the spatial organization of the environment (O'Keefe and Nadel, 1978). The activity of spatially selective cells in the human hippocampus is modulated by the location of a rewarded goal (Ekstrom et al., 2003). Imaging work in humans has found that activity in both vmPFC and hippocampus is parametrically modulated by the proximity of a goal (Viard et al., 2011), and that these regions interact during value-based decisions (Barron et al., 2013; Gluth et al., 2015). VMF damage in humans disrupted memory for visited (rewarded) locations in a virtual maze navigation task (Dahmani et al., 2018). There is also some, albeit mixed, electrophysiological evidence that OFC neurons in nonhuman primates carry information about the spatial location of decision options (reviewed in (Yoo and Hayden, 2018)). Thus, the role of VMF in value-based decisions between objects might extend to decisions based on the value of spatial locations.

Here, we tested whether VMF damage disrupts learning in an incentivized spatial search task where reward value was predicted by the spatial location of otherwise identical options. We also took advantage of pre-existing data on value-based choices between objects collected in the same sample to explore whether deficits in associating reward to spatial locations were dissociable from deficits in object evaluation.

Materials and methods

Participants

Twenty-six people with focal frontal lobe damage and 24 healthy control participants matched for age and education were recruited through the cognitive neuroscience research database at McGill University. The study was approved by the local Institutional Review Board. Participants provided written informed consent in accordance with the declaration of Helsinki. Lesions were characterized with MRI or CT imaging, and registered manually to the Montreal Neurological Institute standard brain by a neurologist blind to task performance, using MRIcro (Rorden and Brett, 2000). Patients were assigned a priori to a group with damage involving vmPFC and/or OFC (here referred to together as VMF), the region of interest in this study (N = 13) or a frontal comparison group with damage sparing VMF (FC, N = 13). Lesion overlap images of the two groups are depicted in **Figure 4.1**.

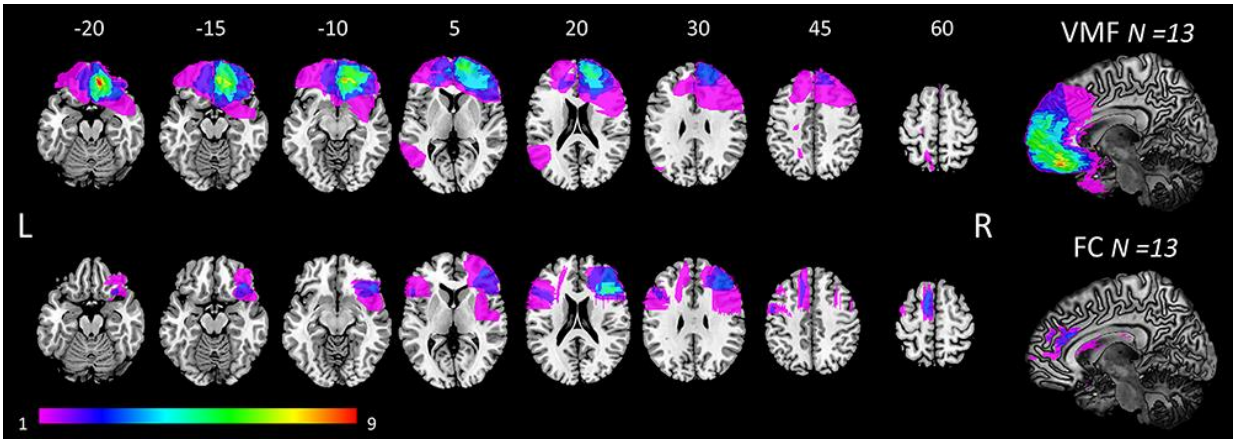

Figure 4.1. Lesion overlap images. (Top row) Ventromedial frontal group (VMF) and (bottom row) frontal comparison group (FC). Colors indicate the extent of lesion overlap, as shown in the legend. Numbers indicate axial slices by z-coordinate in MNI space.

Damage to the VMF was caused by aneurysm rupture in two cases, hemorrhagic stroke in three cases, and tumor resection in eight cases. Damage in the FC group was caused by ischemic stroke in five cases, hemorrhagic stroke in two cases, and tumor resection in six cases. Nine patients (seven VMF and two FC) were taking one or more psychoactive drugs, most commonly an antidepressant or anticonvulsant. All patients had fixed, circumscribed lesions of at least 6-months duration (mean = 8.1 years, SD = 4.8 years).

Neuropsychological characterization

Participants with frontal lobe damage completed tests of working memory (backwards digit span) (Lezak et al., 2012), verbal fluency (Animal, Fluency-F) (Benton et al., 1989), language comprehension (similar to the Token test [(De Renzi and Vignolo, 1962)]), and incidental

memory for faces (Bower and Karlin, 1974). Participants completed a self-report questionnaire of anxiety and depression symptoms (Hospital Anxiety and Depression Scale (HADS) [(Zigmond and Snaith, 1983)]), as well as the American National Reading Test (AMNART [(Grober and Sliwinski, 1991)]). Motor symptoms were assessed with a structured interview and basic neurological exam.

Apparatus

Stimuli were presented on a 17-inch touchscreen (1280 × 800 pixels). All healthy controls and 21 patients were tested in-lab. Five participants with frontal damage (four VMF, one FC) were tested at home. Subjects responded by touching the screen or with a keyboard, depending on the task. Experiments were programmed in Matlab (version 2014b, The Mathworks, Inc.), using the Psychtoolbox extension (Brainard, 1997).

Experimental tasks

Hemi-spatial neglect assessment

All participants completed the Posner Cueing task (Posner, 1980) on the same day as the rewarded search task. The task comprised 100 trials in which participants were instructed to press a key as soon as a target (black asterisk) appeared on the screen. A trial started with a central fixation cross for 1000 ms, after which a cue (black square) appeared on either the left or right side for 300 ms. The cue disappeared, and after a variable delay (50–200 ms), the target was displayed at the same location as the cue (valid cue) on 80% of the trials, or on the opposite side (invalid cue) on 20% of the trials. The target was displayed for a maximum 5000 ms or until the response was registered.

Patients also completed a circle cancelation task assessing both body-centered and stimulus-centered hemi-spatial neglect, adapted from (Ota et al., 2001), at the time of registry enrollment. On each trial, 20 complete circles were displayed among 40 incomplete circles on the screen in a random manner with 10 complete and 20 incomplete circles on each side of the vertical midline. Half of the incomplete circles had a missing portion on their right side, and the other half had a missing portion of their left side. The task comprised four trials. On the first two trials, participants were asked to select (cancel) all the complete circles by pointing on the touch screen. On the last two trials, participants had to select the incomplete circles.

Rewarded spatial search task

We assessed the ability to learn spatial location-value associations with a rewarded search task adapted from Lucas et al. (2013). On each trial, eight identical targets (purple circles) were presented among 12 identical distractors (purple crosses) on a black background (**Fig. 4.2**). Participants chose one target per trial, seeking the one that would yield the highest reward. They were told that targets could yield 0, 5, 10, or 50 points and that their goal was to gather as many points as possible over the session. On each trial, targets and distractors were displayed until a choice was made by touching the screen with the index finger of the dominant hand. Immediately after a response was registered, reward feedback (a yellow circle showing the number of points earned) was displayed for 2 s at the location of the chosen target, accompanied by a melodic sound that was distinct for each reward magnitude. Feedback indicating 0 points (no reward) was a grey dot accompanied by a "tick" sound. The selection of a distractor was followed by a short burst of white noise. The total number of accumulated points was then displayed on a black screen for 1 s.

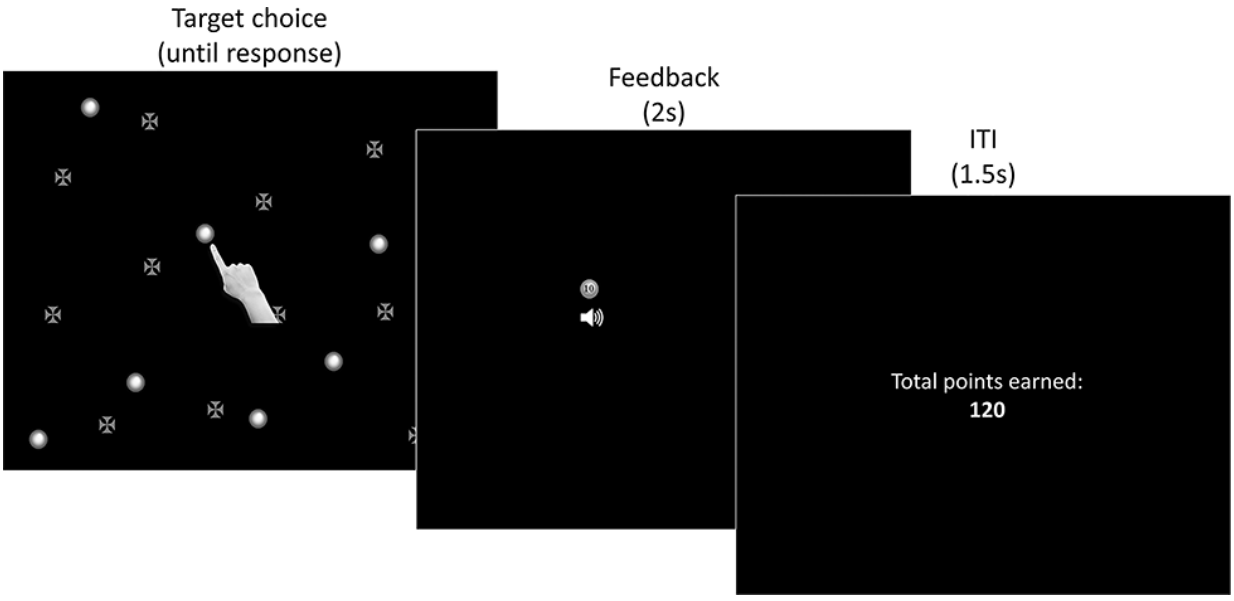

Figure 4.2. Trial structure of the reward search task. The search display containing targets and distractors remained until a target was selected by a touch of the finger. Reward feedback was then presented along with a melodic sound, followed by a screen showing the total number of points earned so far. Targets (circles) and distractors (crosses) are displayed in purple color. Feedback is displayed in bright yellow.

Participants were not told that reward contingencies varied systematically with spatial location across the horizontal axis of the screen (**Fig. 4.4**, Supplementary Fig. 4.1). During the first 56 trials (baseline phase), reward was distributed across the horizontal axis such that targets appearing at the extreme left and right sides of the screen were more rewarded, with a decreasing reward gradient towards the center of the display. In the next 84 trials, reward was asymmetrically distributed, biased either to the right or the left side of the display. This spatial reward gradient was then reversed to the opposite side of the screen for the final 84 trials.

After the baseline phase, the order of left or right asymmetric reward bias was counterbalanced across healthy comparison participants and the two VMF participants with bilateral damage. For patients with unilateral damage, the reward asymmetry was greater in the contralesional side of the display initially and then reversed to the ipsilesional side.

Targets were evenly distributed across the horizontal and vertical axis of the screen, and reward was probabilistic: the target appearing in the sector that was the most rewarded over an experiment phase did not yield the highest reward on every trial. The probability and magnitude of reward by spatial location and experiment phase are shown in Supplementary **Figure 4.1**.

Object decision task

A total of 47 of the 50 participants (23 HC, 12 VMF, and 12 FC) also completed a value-based decision task between objects, as part of a second experiment that has been published elsewhere (Pelletier and Fellows 2019). Participants learned the monetary value of six novel multiattribute objects (fribbles [(Williams and Simons, 2000)]) and then made value-based choices. On each trial, two objects were presented, and participants were instructed to choose the highest-value object by pressing the left or right arrow key. As in the reward search task, decisions were self-paced. All 15 possible pairs were presented six times in random order for a total of 90 trials. Correct responses were defined as choices of the higher-value object in each pair. The percentage of accurate responses was calculated for each subject.

Statistical analysis

Statistical analyses were run using IBM SPSS Statistics for Windows (version 22). Demographic and neuropsychological tests variables were compared between patients and healthy comparison groups using uncorrected t-test or Mann–Whitney U test when assumptions for parametric analysis were not met. The distribution of lesion etiology between patient groups was compared using a chi-squared test of independence.

The Posner cueing task results were analyzed by comparing the difference in detection reaction times between the left and right targets using mixed-measures ANOVAs, with group status as between-subjects factor and target side as within-subjects factor (contralesional/ipsilesional and left/right). Performance in the circle cancelation task was analyzed separately for body-centered and stimulus-centered errors. A Wilcoxon's signed rank test was used to compare errors on the contralesional or ipsilesional side within each patient group. A Wilcoxon's signed rank test was used to compare errors for circles missing their contralateral or ipsilesional portion. For completeness, the same tests were repeated comparing errors on the left and right side of the screen or stimulus, regardless of lesion laterality.

Choice behavior in the rewarded search task was analyzed in terms of the horizontal coordinates of the chosen targets, expressed as percent of screen width. For the purposes of display, horizontal coordinates are expressed as though all participants completed the task with the reward-asymmetry first biased to the left and then reversed to the right side of the screen, by inverting the coordinates in those participants who completed the task following the

opposite pattern. To quantify the evolution of preferred target locations and the spatial dispersion of choices, we divided the session in 16 bins of 14 trials, calculating the average and standard deviation of chosen targets' horizontal coordinate for each participant and each trial-bin. The mean and standard deviation of chosen target locations were then compared using mixed-effect ANOVAs with trial bin as within-subjects factor (four or six levels) and group status as between-subjects factor (three levels). Pairwise comparisons with Bonferroni correction were used to decompose significant main effects. Choice reaction times across trial bins of each experimental phase were analyzed using the same model.

We explored whether spatial location- and object-value comparisons rely on different substrates within VMF by testing whether performance in the two tasks could be dissociated in individual lesion patients, using the methods described in (Crawford et al., 2010) implemented with the freely available Dissocs_ES software (https://homepages.abdn.ac.uk/j.crawford/pages/ dept/Single_Case_Effect_Sizes.htm). This statistical method was devised to test for a dissociation between two tasks in a single case, comparing performance with a normative sample of modest size while minimizing false positives. To meet criteria for a classical dissociation, a case must be significantly impaired in task A but not in task B and, additionally, the difference between the case's performance in task A and task B must be significantly abnormal compared with the difference observed in the normative sample. Although multiple participants were separately compared with the healthy control sample, we did not correct for multiple comparisons given that several concordant tests are needed to conclude that a classical dissociation is present, and because this method is partly based on Bayesian inference which is not subject to the same limitations as frequentist

statistics. For this analysis, performance in the reward search task was summarized as the average coordinates of chosen targets across all 84 trials in the initial reward asymmetry phase, expressed as a percent of screen width, 100 being the most rewarded edge of the screen.

Data availability

Data supporting these findings are available upon request.

Results

Participant characteristics

Demographic and clinical characteristics are reported in **Table 4.1**. There was no significant difference in age or years of education between groups. Patient groups did not differ in lesion volume. There was no significant group difference in estimated premorbid intelligence quotient (IQ) or in anxiety or depression symptoms, although complete data were not available for the IQ measure. No participant had an active, clinically diagnosed mood disorder, based on self-report and chart review. Neuropsychological test results are shown in **Table 4.2**. There were no significant differences between patient groups in tests of incidental memory for faces, verbal fluency or language comprehension. No participant reported or was observed to have hemiparesis. Patient groups did not differ significantly in lesion etiology distribution (Chi-Squared test; $\chi^2_{(3)} = 6.63$, $p = 0.09$).

Table 4.1. Demographic characteristics

Group	HC	VMF	FC
N	24	13	13
Age (y)	61 (11.6)	57 (10.7)	60 (10.7)
Sex (M/F)	7/17	6/7	6/7
Handedness (R/L/Ambidextrous)	20/3/1	10/1/2	11/2/0
Education (y)	15.8 (3.1)	13.8 (2.7)	16.1 (3.1)
HADS-A	3.8 (3.1)	5.6 (1.7)	5.6 (3.7)
HADS-D	2.1 (3.1)	3.9 (1.7)	4.3 (3.7)
Estimated IQ[a]	126 (5)	122 (9)	120 (10)
Lesion laterality (R/L/Bilateral)	–	8/3/2	6/7/0
Lesion volume (cc)	–	45 (8–192)	23 (5–37)

Note: All values mean (SD), except sex (count) and lesion volume (median (range)). HC, healthy comparison; VMF, ventromedial frontal damage; FC, frontal comparison. HADS, Hospital Anxiety and Depression Scale; A, anxiety; D, depression. [a] Not all subjects completed the estimated IQ test (HC N = 11, VMF N = 7, FC N = 6). This test was not available in French; those who did not complete it are more likely to speak French as their first language.

Table 4.2. Neuropsychological screening test performance for patient groups.

Group	VMF	FC
Fluency (animals, 60 s)	17.4 (2.7)	18.5 (6.9)
Fluency (F, 60 s)	9.0 (3.4)	12.2 (6.3)
Backward digit span	2.5 (0.6)	3.1 (1.3)
Incidental memory (accuracy)	0.82 (0.1)	0.84 (0.1)
Sentence comprehension (accuracy)	0.99 (0.02)	0.97 (0.07)

Note: Mean (SD). One VMF and one FC participant did not complete the screening tests.

Hemispatial neglect assessment

Performance of frontal groups in control tasks assessing hemispatial neglect is presented in **Figure 4.3**. We compared reaction times with detect targets appearing on the contralesional and ipsilesional side of the screen in the Posner cueing task in the 24 patients with unilateral damage (13 FC and 11 VMF patients). There was no significant effect of target side ($F_{(1,22)} = 0.56$, $p = 0.46$, $\eta_p^2 = 0.03$), group ($F_{(1,22)} = 1.81$, $p = 0.19$, $\eta_p^2 = 0.08$), and no group by target side interaction ($F_{(1,22)} = 0.82$, $p = 0.38$, $\eta_p^2 = 0.04$). We also examined whether there were differences in reaction times for the right and left targets in the whole sample (N = 26). Again, we found no main effect of target side ($F_{(1,24)} = 1.36$, $p = 0.26$, $\eta_p^2 = 0.06$), nor group ($F_{(1,24)} = 2.61$, $p = 0.12$, $\eta_p^2 = 0.11$), nor target side by group interaction ($F_{(1,24)} = 0.28$, $p = 0.60$, $\eta_p^2 = 0.01$). At the individual participant level, no VMF participant was significantly slower to detect ipsi- compared with contralesional targets. Two FC participants were significantly slower in detecting ipsilesional targets.

We also tested whether there were differences in the number of body-centered errors on the contralesional or ipsilesional side in a circle cancelation task (**Fig. 4.3B**). We found no significant difference in missed targets for the VMF group (Wilcoxon's signed-rank tests; Z = 0.0, $p = 1.0$) or the FC group (Z = 0.58, $p = 0.56$). Further, we found no significant difference in the number of missed targets on the left or right side of the screen, regardless of lesion side for the VMF (Z = 0.38, $p = 0.71$) or FC groups (Z = 0.58, $p = 0.56$). The same task allowed us to probe stimulus-centered neglect, by testing whether there were differences in the number of errors for stimuli missing contralesional or ipsilesional portions (**Fig. 4.3C**). We found no difference in the number of errors in the VMF (Z = 1.41, $p = 0.16$) or FC groups (Z = 1.41, $p = 0.16$). Again,

there were no differences in the number of errors for stimuli missing their left or right portion regardless of lesion side (VMF and FC; Zs = 1.41, *p*'s = 0.16).

At the individual level, we found that only three VMF participants made any body-centered errors: two participants made two contralesional errors (out of 40 targets), and one participant made one ipsilesional error. In the FC group, one participant made one contralesional error and two ipsilesional errors, one participant made one ipsilesional error, and a third participant made one contralesional error. Participants similarly made very few stimulus-centered errors: one VMF participant and one FC participant made two contralesional errors each. Thus, no patient showed strong evidence of hemispatial neglect.

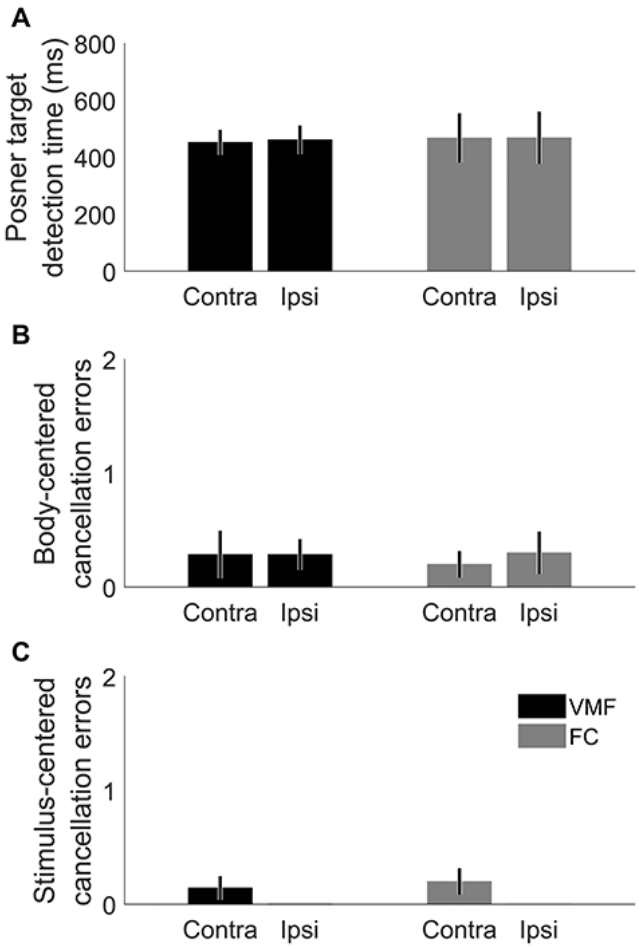

Figure 4.3. Hemispatial neglect assessment. Performance of the lesion groups in the Posner Cueing task (A) and the circle cancelation task separately for body-centered (B) and stimulus-centered errors (C). Error bars indicate standard error from the mean (SEM).

Spatial location-reward learning

Having established that participants with frontal damage did not have deficits in hemispatial attention based on conventional screening tests for neglect, we next assessed the effect of such damage on learning to choose targets appearing in more rewarded spatial locations. Groups were broadly comparable on the task, overall, arguing that they understood and were engaged by the task: There was no significant effect of group on total reward accrued ($F_{(2,47)} = 1.15$, $p = 0.33$, $\eta_p^2 = 0.05$).

We next focused on learning, reflected in target selection as the spatial location-reward contingencies shifted across phases of this dynamic task. In the baseline phase of the experiment (trial bins 1–4), reward was symmetrically biased towards the horizontal edges of the screen, such that the left and right peripheral sectors were more rewarded than the central sectors. As expected, in this phase, there was no effect of trial bin on the average horizontal coordinate of chosen targets ($F_{(3,141)} = 0.98$, $p = 0.41$, $\eta_p^2 = 0.02$) (**Fig. 4.4**). We found no effect of group ($F_{(2,47)} = 0.79$, $p = 0.46$, $\eta_p^2 = 0.03$) and no significant group by trial-bin interaction ($F_{(6,141)} = 1.29$, $p = 0.27$, $\eta_p^2 = 0.05$) during the baseline phase. At the end of the baseline phase (bin 4), the average horizontal coordinate of chosen targets did not differ significantly from the midline in any group (one-sample t-tests; HC $p = 0.92$, VMF $p = 0.93$, FC $p = 0.60$). Thus, no group showed an a priori horizontal spatial bias.

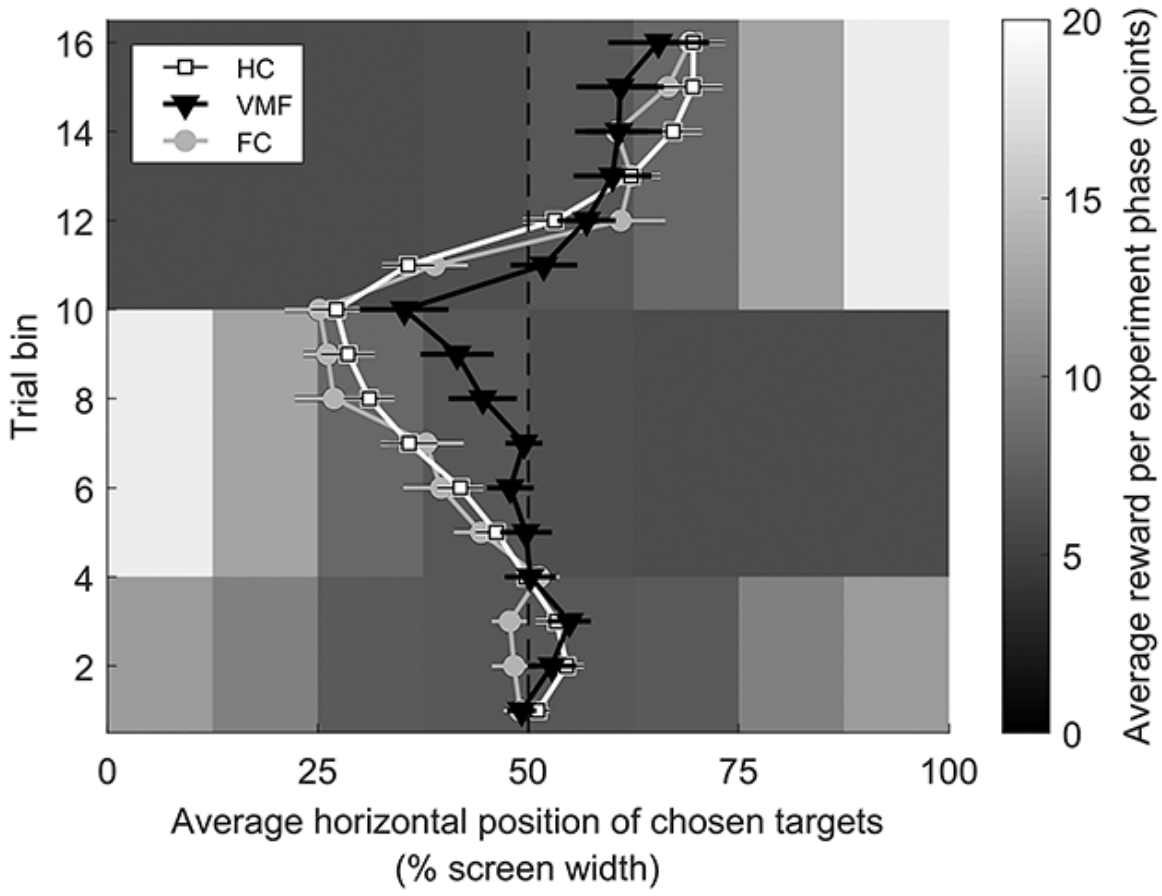

Figure 4.4. Group performance in the incentivized spatial search task overlaid on the reward distributions. The spatial distribution of reward was manipulated across three phases; baseline (symmetric-peripheral bias) (bins 1–4), initial hemispatial reward asymmetry (bins 5–10), and reversal of the hemispatial reward asymmetry phases (bins 11–16). Each of the eight sectors of the screen contained one target per trial. The background greyscale represents the average reward associated with targets located in each sector across a given phase (see Legend). Reward was probabilistic: the target appearing in the sector with the highest average value was not always the most rewarded (see Supplementary Fig. 4.1 for details). Trial bins each contained 14 trials. Error bars represent SEM.

We next asked whether participants tended to choose more targets on the periphery compared with the central sectors of the screen in the baseline phase. We divided the horizontal axis of the screen in eight sectors of equal size, each containing one target per trial, and compared the number of targets chosen in the peripheral sectors (the two rightmost and two leftmost sectors) and in the central region of the screen (the four remaining sectors). Across all trials of the baseline phase, participants chose more targets in the peripheral compared with the central region of the screen (ANOVA, $F_{(1,47)} = 5.99$, $p = 0.018$, $\eta_p^2 = 0.11$) (**Fig. 4.5A**). There was no significant group by region (peripheral vs. central) interaction ($F_{(2,47)} = 0.23$, $p = 0.79$, $\eta_p^2 = 0.01$). As the baseline phase unfolded, participants chose increasingly more targets located in the peripheral sectors (rmANOVA, main effect of trial bin; $F_{(3,141)} = 13.16$, $p < 0.001$, $\eta_p^2 = 0.22$) (**Fig. 4.5B**), providing evidence that they were learning spatial location-reward contingencies. There was no significant effect of group ($F_{(2,47)} = 0.23$, $p = 0.80$, $\eta_p^2 = 0.01$) or group by bin interaction ($F_{(6,141)} = 1.29$, $p = 0.27$, $\eta_p^2 = 0.05$).

Because most patients in the sample (13 FC and 11 VMF) had unilateral damage, we next tested whether the number of chosen targets differed for the contralesional and ipsilesional peripheral sectors during this phase in those patients. VMF and FC groups did not differ significantly in the number of peripheral targets chosen (rmANOVA main effect of group; $F_{(1,22)} = 0.46$, $p = 0.50$, $\eta_p^2 = 0.21$), but there was a significant interaction between group and side (contra−/ipsilesional) ($F_{(1,22)} = 5.90$, $p = 0.024$, $\eta_p^2 = 0.12$). Whereas the FC group made about as many choices in the contralesional and ipsilesional peripheral sectors ($t_{(12)} = 0.51$, $p = 0.62$, $d = 0.14$), VMF participants chose significantly fewer targets in the contralesional peripheral sector ($t_{(10)} = 2.96$, $p = 0.014$, $d = 0.89$). As shown in **Figure 4.5B**, all groups chose increasingly

more targets in the peripheral sectors as the baseline phase unfolded. However, patient groups differed in the number of contralesional and ipsilesional choices contributing to the total number of peripheral choices across trial bins: the number of contralesional choices did not increase as much in the VMF group compared with the FC group as the baseline phase wore on. A repeated measures ANOVA revealed a significant main effect of bin on the number of contralesional choices ($F_{(3,66)} = 5.45$, $p = 0.002$, $\eta_p^2 = 0.20$), a main effect of group ($F_{(1,22)} = 6.04$, $p = 0.023$, $\eta_p^2 = 0.21$), and a group by bin interaction ($F_{(3,66)} = 2.74$, $p = 0.050$, $\eta_p^2 = 0.11$). Thus, during the baseline phase when reward was symmetrically distributed, VMF participants learned that the peripheral sectors were more rewarded than the central sectors and those with unilateral damage exhibited a small but significant bias towards the ipsilesional peripheral sector.

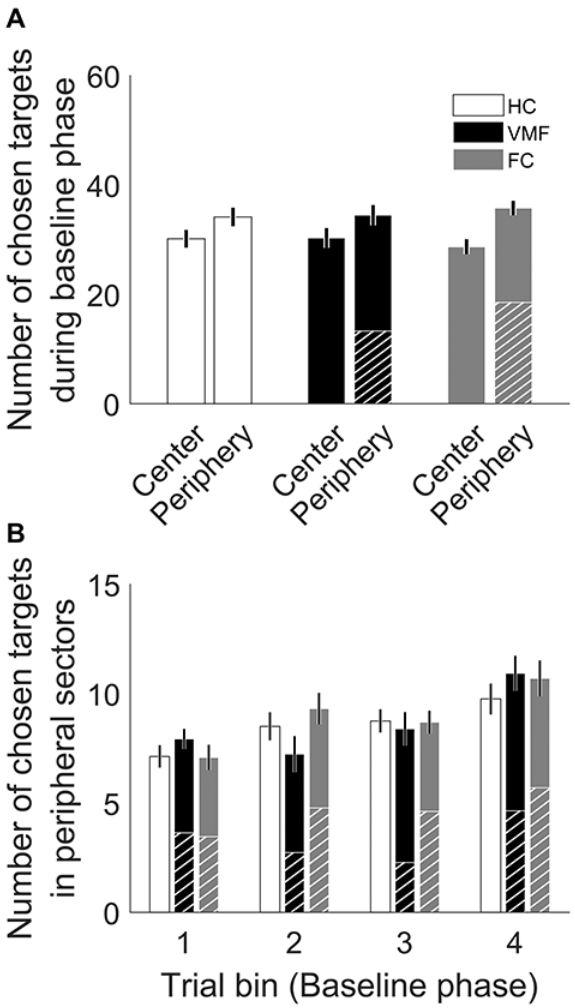

Figure 4.5. Choices in the central and peripheral sectors of the screen in the baseline (symmetric reward) phase. (A) Number of choices in the four peripheral and four central screen sectors across the 65 trials of the baseline phase. (B) Choices in the peripheral sectors across the four trial bins of the baseline phase. The peripheral choices for each lesion group are shown for contralesional (hatched) and ipsilesional (filled) sectors. Error bars represent SEM.

After the baseline phase, an asymmetric reward bias was introduced such that targets appearing on one side were more likely to yield higher reward (**Fig. 4.4**, bins 5–10). There was a significant effect of trial bin ($F_{(5,235)} = 21.44$, $p < 0.001$, $\eta_p^2 = 0.31$) on the horizontal position of chosen targets. As shown in **Figure 4.4**, participants gradually shifted their responses to the rewarded side of the display as trials wore on, consistent with learning the association between reward and location in space. There was a significant effect of group ($F_{(2,47)} = 4.32$, $p = 0.019$, $\eta_p^2 = 0.15$), but no significant group by bin interaction ($F_{(10,235)} = 1.05$, $p = 0.40$, $\eta_p^2 = 0.04$). We decomposed the main effect of group using pairwise comparisons with Bonferroni correction, revealing that the VMF group's choices were on average less biased towards the rewarded side of the screen compared with both the HC ($p = 0.04$, d = 0.64) and FC groups ($p = 0.03$, d = 0.76). The comparison groups did not differ significantly from each other ($p = 0.98$, d = 0.11).

Given that participants chose more targets in peripheral sectors in the baseline phase, the observed difference in the average spatial bias in the initial reward-asymmetric phase could be driven by a deficit in learning that one side is now more rewarded, a deficit in stopping to choose targets in the peripheral, nonrewarded sectors (i.e., perseveration) or both. We carried out an exploratory follow-up analysis examining the evolution in the number of chosen targets in the two peripheral sectors on the more rewarded (contralesional) side and in the two peripheral sectors on the less-rewarded side of the display. We found that participants chose fewer targets in the two less-rewarded peripheral sectors as the initial asymmetric phase wore on (rmANOVA, main effect of trial bin; $F_{(5,235)} = 14.35$, $p < 0.001$, $\eta_p^2 = 0.23$) (Supplementary Fig. 4.2A). There was no group by bin interaction; $F_{(10,235)} = 1.29$, $p = 0.24$, $\eta_p^2 = 0.05$. There was a trend towards an effect of group on the number of chosen targets in these sectors during the

initial asymmetric reward phase ($F_{(2,47)} = 2.95$, $p = 0.06$, $\eta_p^2 = 0.11$). Analysis of the number of choices in the two rewarded peripheral sectors also revealed a main effect of trial bin, such that participants chose increasingly more targets in these rewarded sectors ($F_{(5,235)} = 19.87$, $p < 0.001$, $\eta_p^2 = 0.30$). There was no significant group by bin interaction ($F_{(10,235)} = 1.24$, $p = 0.27$, $\eta_p^2 = 0.05$). However, there was a significant main effect of group ($F_{(2,47)} = 3.89$, $p = 0.027$, $\eta_p^2 = 0.14$). Bonferroni-corrected pairwise comparisons indicated that the VMF group chose fewer targets in these sectors compared with the FC group ($p = 0.022$, d = 1.04). The VMF and HC groups did not differ at conventional significance thresholds ($p = 0.064$, d = 0.76). There was no difference between the two comparison groups ($p = 0.83$, d = 0.28). These results are consistent with a deficit in learning to choose targets on the more rewarded (contralesional) side of the screen in the VMF group. We did not find evidence to support a deficit in refraining from choosing targets in the previously rewarded (ipsilesional) sectors.

The final phase involved a reversal of the asymmetric spatial reward gradient, now favoring the opposite side of the display (bins 11–16). We again found a significant main effect of bin on the position of chosen targets ($F_{(5,235)} = 26.55$, $p < 0.001$, $\eta_p^2 = 0.60$). There was no significant effect of group ($F_{(2,47)} = 0.004$, $p = 0.996$, $\eta_p^2 < 0.001$), but a significant group by bin interaction ($F_{(10,235)} = 2.75$, $p = 0.003$, $\eta_p^2 = 0.11$). We decomposed this interaction by testing for a group effect on each bin, finding a significant effect of group on the first bin of the reversal phase (bin 11, $F_{(2,47)} = 5.18$, $p = 0.009$, $\eta_p^2 = 0.18$). Pairwise comparisons revealed that VMF differed significantly from HC ($p = 0.003$, d = 1.12) and FC ($p = 0.03$, d = 0.91) on this bin, with no significant difference between the comparison groups ($p = 0.53$, d = 0.22). As can be seen in **Figure 4.4**, the VMF group shifts its responses to the opposite hemi-field faster than the other

two groups, perhaps reflecting a weaker initial bias towards the previously rewarded hemi-field. There was no significant effect of group in any other bin of this phase (ps > 0.37).

We next explored whether the variance in the spatial location of chosen targets differed across trial bins (**Fig. 4.6A**). We hypothesized that as participants learned that locations along the horizontal axis yield higher rewards, choices should get closer to one another (i.e., participants would "exploit" the location), such that the subject-level standard deviation in horizontal coordinates of chosen targets should decrease. On the other hand, after a change in reward distribution, participants should explore the choice environment, resulting in greater standard deviation in chosen target location.

In the baseline phase of the experiment, we found a significant effect of trial bin on the standard deviation of the horizontal positions of the chosen targets ($F_{(3,141)} = 4.46$, $p = 0.01$, $\eta_p^2 = 0.09$) (**Fig. 4.6A**). Post hoc t-tests revealed that across groups, the standard deviation was greater in the last bin of the baseline phase compared with the other bins in that phase (all ps < 0.048). We found no significant effect of group ($F_{(2,47)} = 2.41$, $p = 0.10$, $\eta_p^2 = 0.09$) and no group by bin interaction ($F_{(6,141)} = 1.43$, $p = 0.21$ $\eta_p^2 = 0.06$). In the initial reward asymmetry phase (bins 5–10), there was a significant effect of bin ($F_{(5,235)} = 10.26$, $p < 0.001$, $\eta_p^2 = 0.18$). We found no significant effect of group ($F_{(2,47)} = 2.60$, $p = 0.09$, $\eta_p^2 = 0.10$) and no group by bin interactions ($F_{(10,235)} = 1.30$, $p = 0.23$, $\eta_p^2 = 0.05$). Across groups, the position of chosen targets was less variable as the initial asymmetric phase went on, indicative of learning the reward-spatial position contingency. Similarly, in the reversal phase (bins 11–16), there was a significant effect of trial bin ($F_{(5,235)} = 6.36$, $p < 0.001$, $\eta_p^2 = 0.12$), with no significant effect of group ($F_{(2,47)} = 0.51$, $p = 0.60$, $\eta_p^2 = 0.02$) or group by trial bin interaction ($F_{(10,235)} = 0.80$, $p = 0.63$,

$\eta_p^2 = 0.03$). We further asked whether the standard deviation of chosen targets was greater in the first bin of the reversal phase (bin 11) compared with the last bin of the initial reward asymmetry (bin 10). We found a significant effect of bin, ($F_{(1,47)} = 17.76$, $p < 0.001$, $\eta_p^2 = 0.27$), but no significant effect of group ($F_{(2,47)} = 1.10$, $p = 0.34$, $\eta_p^2 = 0.05$) and no group by bin interaction ($F_{(2,47)} = 1.11$, $p = 0.33$, $\eta_p^2 = 0.05$).

Overall, these results indicate that participants explored less and increasingly exploited the more rewarded spatial locations as each asymmetric reward phase unfolded, then explored more when the spatial location-reward contingencies changed. Group status did not have a significant impact on this behavior. This change in exploration behavior only occurred along the horizontal, value-relevant dimension, with the standard deviation in the chosen target's vertical position stable across the three experiment phases (**Fig. 4.6B**). We found no significant effect of bin on the standard deviation of the chosen targets' vertical location during the baseline ($F_{(6,141)} = 0.20$, $p = 0.91$, $\eta_p^2 = 0.04$), initial reward asymmetry ($F_{(10,235)} = 0.83$, $p = 0.53$, $\eta_p^2 = 0.17$), or reversal ($F_{(10,235)} = 0.96$, $p = 0.45$, $\eta_p^2 = 0.20$) phases. We found no significant effect of group and no group by bin interaction in any phase.

Finally, we tested whether reaction times varied across trial bins or between groups (**Fig. 4.6C**). In the initial reward asymmetry phase, there was a significant effect of bin on reaction times ($F_{(5,235)} = 4.42$, $p = 0.001$, $\eta_p^2 = 0.09$); participants were faster as the phase went on. We found no significant effect of bin on reaction time in the baseline nor the reversal phase. We found no significant effect of group or group by bin interaction in any experiment phase.

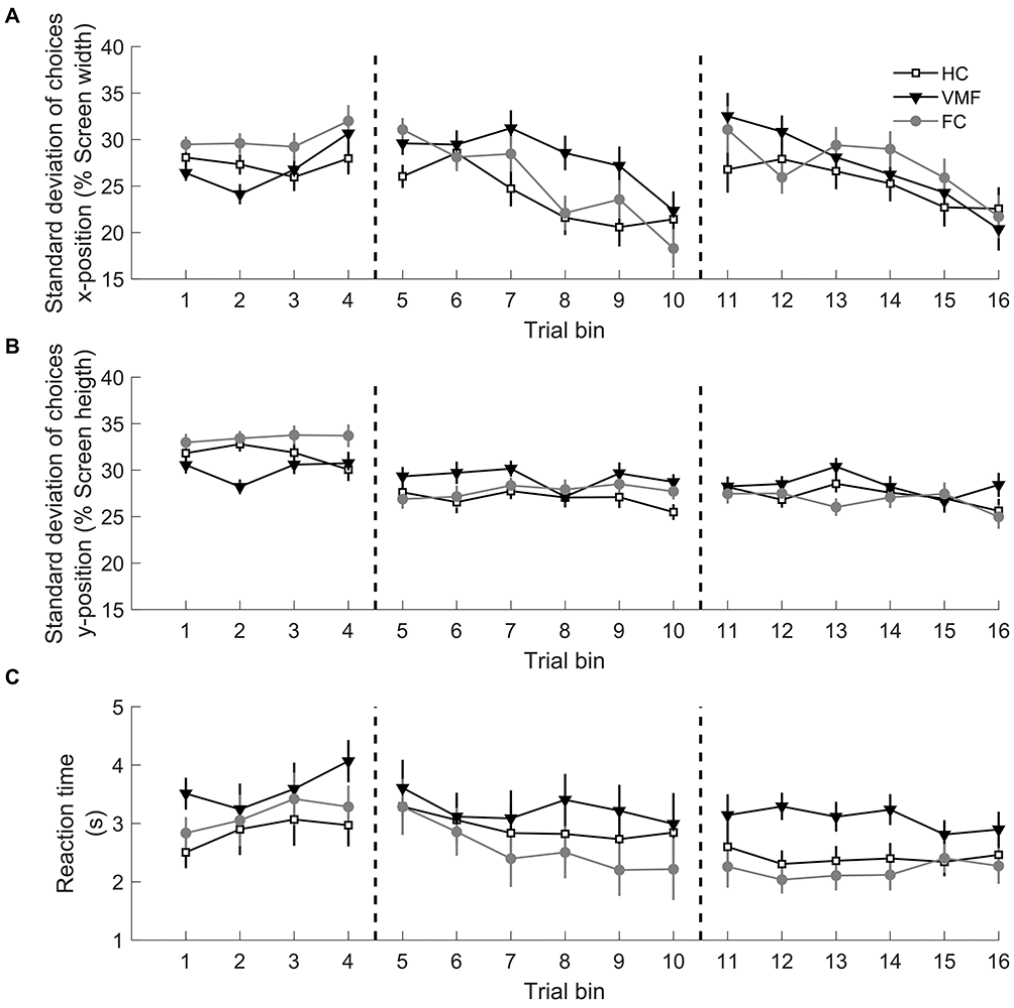

Figure 4.6. Standard deviation in choice locations and reaction times across bins of the search task. (A) Standard deviation in chosen targets horizontal (x-axis) position, (B) standard deviation in chosen targets vertical (y-axis) position and (C) reaction times. Vertical lines demarcate the three phases of the experiment (baseline: trial bins 1–4, initial reward asymmetry: bins 5–10, reversed reward asymmetry: bins 11–16). Error bars indicate SEM.

Spatial versus object value-based choice

We took advantage of data from an object-value decision task collected in parallel in the same participants to ask whether the effects of VMF damage on spatial location-value and object-value decisions could be dissociated (Pelletier and Fellows, 2019). We first asked whether performance in the two tasks was correlated in participants with VMF damage, as would be expected if both processes rely on a common neural substrate. As shown in **Figure 4.7**, among participants with VMF damage, accuracy in choosing the highest value option in the object task (x-axis) was not correlated with the choice bias towards targets located in the most rewarded location in the spatial task (y-axis) (Pearson r = 0.004, $p = 0.989$). We then applied a more stringent approach to test for dissociation, comparing the performance of each participant with VMF damage to the HC group on both tasks using statistical methods devised to test for deficits in single cases compared with a normative sample of modest size (Crawford and Garthwaite, 2002; Crawford et al., 2010). According to this very stringent test, only two participants with damage affecting VMF were significantly impaired on both the spatial and the object tasks. These two participants had the largest lesions among the VMF group (lesion volumes: 77 and 192 cc) and in both cases had right unilateral damage extending to the lateral and dorsal prefrontal cortex. Two VMF patients showed significant deficits in the object task but not in the spatial task. These participants further met the criteria to be considered "spared" in spatial task performance (both $t > 2.70$, $p < 0.02$, with less than 0.66% of the healthy population expected to exhibit a more extreme discrepancy between tasks), that is, a formal single dissociation. These participants both had left unilateral damage, although there were no commonly damaged voxels: one participant had damage extending anteriorly to the frontal

pole (volume = 7 cc), whereas the other had damage extending laterally (volume = 14 cc). One VMF patient with right unilateral damage (volume = 20 cc) was impaired in the spatial but not the object task, but this did not meet the criteria for a dissociation. No FC participant met the criteria for dissociation.

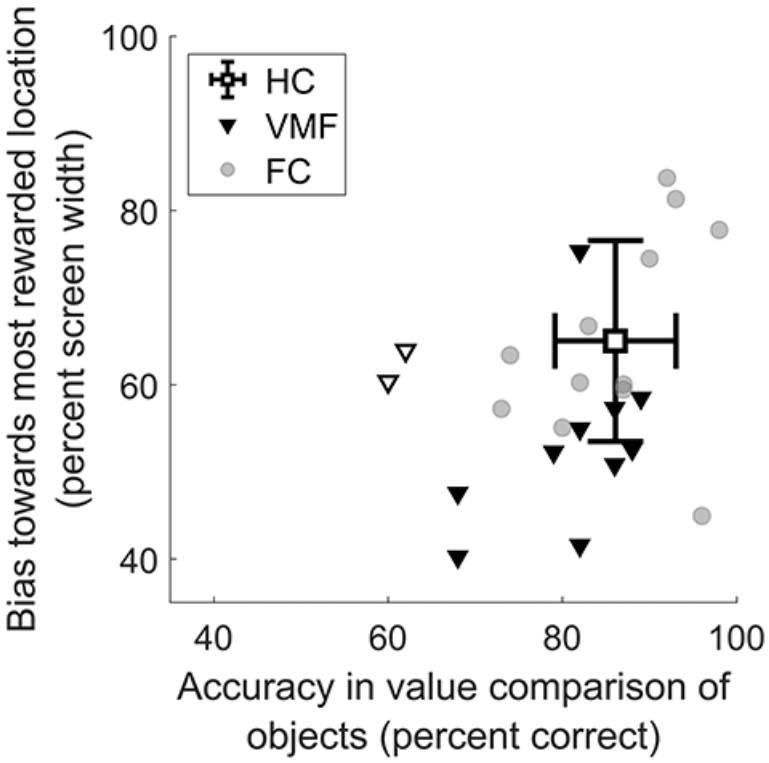

Figure 4.7. Performance in the spatial task as a function of performance in the object task. Average performance of the healthy comparison group is shown with error bars representing +/− one standard deviation. Participants with frontal damage are presented as individual cases. Empty triangles identify the two VMF cases showing a formal dissociation, with impaired object-value but intact spatial-value choices.

Discussion

The present study found that damage to VMF, but not prefrontal damage sparing this region, slowed learning the value of spatial locations based on probabilistic reward. In patients with unilateral damage, learning was most impaired when reward was higher in the contralesional hemifield. This adds to the growing body of work implicating VMF in value-guided behavior, providing the first causal evidence in humans for a role for this region in flexibly learning spatial location-reward associations in a spatial search paradigm. Work to date implicating VMF in value-related processes has largely focused on economic choices between "goods", typically complex real-world objects or monetary options with trade-offs of risk, delay, or effort (Delgado et al., 2016). Given that distinct networks are involved in object and spatial perception (Goodale and Milner, 1992), and that this organization extends to the prefrontal cortex (O'Reilly, 2010; Wilson et al., 1993), VMF might be specifically involved in object-based valuation and thus not required when value was instead linked to spatial locations. Our findings do not support this account, instead supporting a more domain-general valuation account for VMF. However, we provide preliminary evidence that the effects of VMF damage on spatial-value learning are dissociable from performance on a task requiring value-based decisions about complex objects, suggesting these may have distinct anatomical substrates within this broad region.

This work complements previous findings using a very similar task in patients with left hemi-spatial neglect due to right hemisphere frontoparietal damage. Larger rewards for targets on the neglected side led these patients to shift their choices into neglected hemi-space (Lucas et al., 2013). Strikingly, Lucas and colleagues found that the extent of that reward-driven shift

was comparable with that observed in healthy participants, suggesting that the spatial biasing effect of reward on choice was distinct from hemispatial attention. Here, we show the opposite dissociation in patients with VMF damage: such damage did not impair spatial orienting of attention, as assessed with two different tests of spatial neglect, but led to deficits in optimally selecting targets rewarded based on spatial location. Together, this suggests that spatial location-value associations do not critically rely on lateral frontoparietal spatial attention mechanisms, but rather are supported by a distinct network that includes VMF. This aligns with recent findings in nonhuman primates that OFC neurons encode the spatial location of options, even when this information is orthogonal to the stimulus value and irrelevant to task goals (Yoo and Hayden, 2018). Our findings suggest that spatial representations in VMF are critical to updating the value of rewarded locations based on feedback but are not required for spatial attention more generally.

A parallel stream of research has identified a network involving the hippocampus and the prefrontal cortex in goal-directed spatial navigation. Work in humans performing a spatial navigation task found that cells in the hippocampus changed their preferred firing location depending on the location of the currently rewarded goal (Ekstrom et al., 2003) and damage to VMF disrupted memory for previously visited locations in a virtual maze (Dahmani et al., 2018). A role for VMF-hippocampal interaction for spatial navigation is also supported by work in rodents showing that hippocampal spatial representations during foraging for food rewards were less stable after prefrontal cortex lesions (Kyd and Bilkey, 2003, 2005) and that hippocampus and prefrontal cortex are both necessary for learning the location of a safe area in the environment (Sutherland et al., 1982), although it is unclear to what extent the rodent

prefrontal cortex literature translates to humans. It is clear that there is strong anatomical and functional connectivity between the VMF and the hippocampus in humans (Andrews-Hanna et al., 2014; Eichenbaum, 2017; Heide et al., 2013), and there is evidence that these regions interact during value-based decisions (Barron et al., 2013; Gluth et al., 2015). Given the reviewed work and our current findings, VMF may contribute to spatial location-value learning through engagement with hippocampal place representations, rather than via lateral prefrontal spatial attentional mechanisms. Additional work is needed to test this possibility directly.

Finally, we took advantage of a second dataset collected for other purposes in the same participants to provide a preliminary test of the dissociability of location-value and object-value processes. The two VMF participants showed the worst performance in a task testing the ability to choose between novel objects based on reward performed within the normal range on the spatial task, and there was one VMF patient who performed poorly on the spatial-value task but was not impaired in the object-value task. This suggests that while both tasks require VMF, the observed impairment may reflect disruption of distinct processes relying on different subregions or connections within this region. The sample sizes were too small to define the subregions that may be critical for the performance of either task. This finding also must be treated with caution, as the two tasks were not designed to be compared and vary in several respects.

Given prior work implicating VMF in reversal learning (Fellows and Farah, 2003; Swainson et al., 2000), we included a spatial location-reward reversal manipulation. Consistent with previous reversal learning studies using probabilistic reward feedback, we found that VMF patients were impaired in initial learning (i.e., in the first reward-asymmetry phase) (Tsuchida et

al., 2010). However, we observed no significant group effect on chosen target location in the reversal phase. There are several explanations for this observation: The simplest is that the VMF group developed less of a spatial bias in the initial hemi-spatial reward condition and therefore had less of a bias to overcome when the reward-spatial association was reversed. Alternatively, this may reflect a lateralized effect of VMF damage on contralesional spatial location-reward representations. A priori, we expected that the VMF sample with unilateral damage would be too small to allow meaningful interpretation of lateralized effects if we randomized the reward-hemispace contingencies across subjects. We therefore elected to set the initial spatial location-reward advantage in contralesional space for such patients, to maximize detecting lesion effects, if present. Thus, if VMF has lateralized effects, in the reversal phase, such patients were shifting to their presumptively intact hemi-field. Furthermore, by chance, most patients with unilateral damage had right hemisphere lesions. Additional experiments will be needed to definitively establish whether the observed effects are lateralized to contralesional hemispace, or preferentially related to right VMF damage, or both. We note that in previous work in a larger sample of prefrontal patients studying reward priming effects in a rewarded visual target detection task, VMF deficits were similar in the contra- and ipsilesional hemifield (Vaidya and Fellows, 2015a).

Of note, the performance of those with VMF damage is not consistent with simple perseveration: those with VMF damage stopped choosing targets in previously rewarded locations as promptly as controls when contingencies changed. Participants with VMF damage also did not assign reward feedback to a plausible but irrelevant task dimension (vertical position of targets) as might be predicted by a generic “credit assignment” deficit (Rushworth

et al., 2011). Instead, our results are most compatible with a role for VMF in updating the value of spatial locations, perhaps particularly in contralesional hemispace.

It has been proposed that OFC represents a flexible cognitive map for goal-directed tasks, encoding the latent variables that together determine the current goals and rules (Schuck et al., 2016). In the current task, participants had to learn that the value-relevant variable was the horizontal location. Damage encompassing OFC may have slowed the acquisition of this task rule, but these patients did eventually show a bias toward the rewarded location in the initial phase, indicating that they learned that reward was related to spatial position. The absence of a group effect in the reversal phase could indicate that new reward associations were more readily acquired once the relevant "latent variable" (i.e., horizontal location) was inferred. Future work probing explicit knowledge of task rules during learning might be informative in this regard.

The task used here has commonalities with foraging paradigms, in which organisms must explore the environment to find reward. A key component of foraging behavior is the decision to stay and exploit a current "patch" or leave to explore, that is, when the rate of reward drops below the average expected value of the environment (Hayden et al., 2011; Stephens and Krebs, 1986). Studies in humans and nonhuman primates have suggested that the dorsal anterior cingulate cortex, rather than vmPFC, is involved in the decision to stay or leave a currently rewarded option in response to dropping value (Hayden et al., 2011; Kolling et al., 2012). Although the paradigm we used here was not specifically designed to assess explore/exploit behavior, we examined the spatial variance in choices across task phases as an indicator of this tradeoff. Those with VMF damage showed similar exploration behavior

compared with other groups in the initial phase of the task and following reversal, suggesting that this region is not required for increasing exploration when reward contingencies change. Too few patients with dorsal medial PFC damage were included in this sample to test whether anterior cingulate cortex damage influenced the exploration/exploitation tradeoff. In other work, we have found evidence that dorsomedial prefrontal damage impairs deliberation in object-based choices, consistent with weaker representation of the value of alternatives to the currently attended option (Vaidya and Fellows, 2015b).

This study has limitations, including those inherent to human lesion research. While all patients included in this study had well characterized focal lesions, disruption of underlying white matter tracts (fibers of passage) can affect regions distant from the lesion site (Rudebeck et al., 2013b). The inclusion of a frontal control group rules out nonspecific effects of chronic illness or generic frontal injury as explanations for our findings. Converging evidence, especially from nonhuman primates where more selective lesions are possible, would be helpful in establishing whether the observed effects of VMF damage are caused by white matter disruption, cortical damage, or both.

In conclusion, these findings provide the first evidence that human VMF plays a critical role in learning spatial location-value associations under dynamic reward conditions. Such patients showed no impairment of hemispatial attention, adding to emerging data that the effects of reward on attention to locations in space calls on mechanisms distinct from those supporting hemispatial attention typically disrupted in patients with neglect due to parietal damage. Finally, we provide preliminary evidence that learning the value of spatial locations

and making value-based choices between objects may not rely on the same brain mechanisms, although both are disrupted following VMF damage.

Funding

This work was supported by the Canadian Institutes of Health Research (Grant MOP 249071) and the Natural Sciences and Engineering Research Council of Canada (RGPIN 2016–06066).

Notes

We would like to thank Patrick Vuilleumier and Alexia Bourgeois for sharing the experiment codes and stimuli and for helpful discussions regarding the experimental design. We also thank Christine Déry for her help with participant recruitment, the patients and healthy volunteers for their participation, and the McGill clinicians who referred patients for this study.

Supplementary material

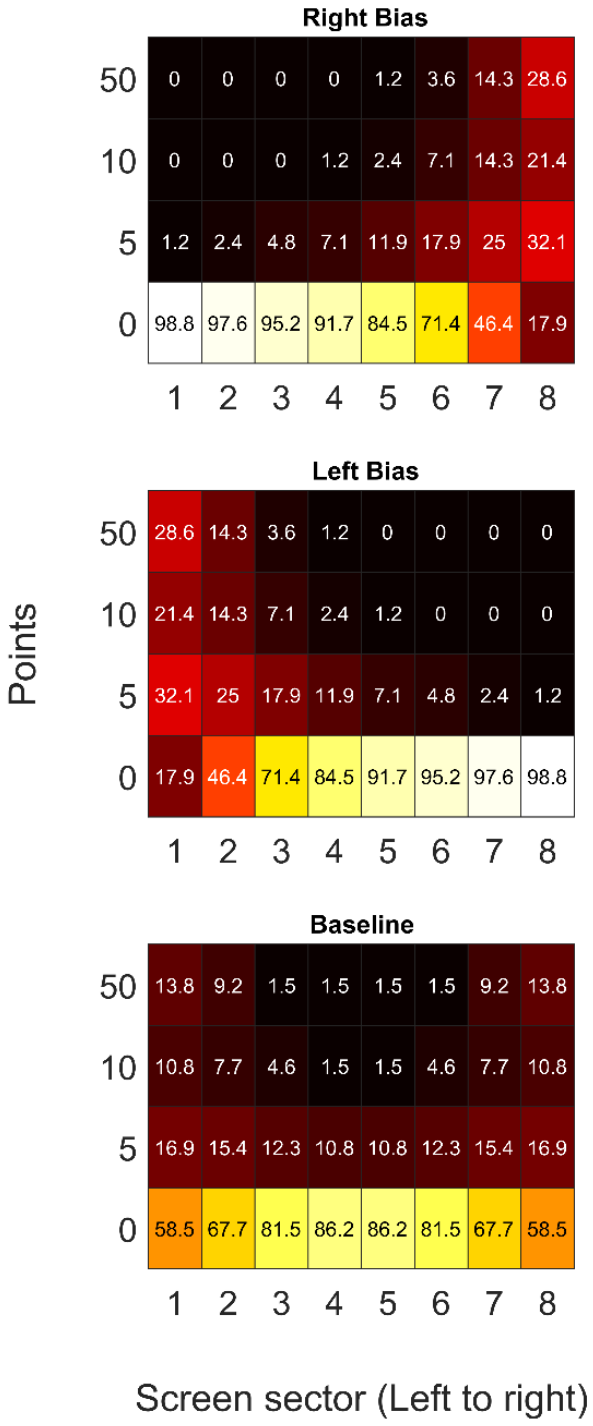

Supplementary Figure 4.1. Reward probability and magnitude for each spatial location and experiment phase. The number in each cell and the background heatmap color indicate the probability (in %) that choosing the target appearing in this screen sector (in this phase) yields the points indicated.

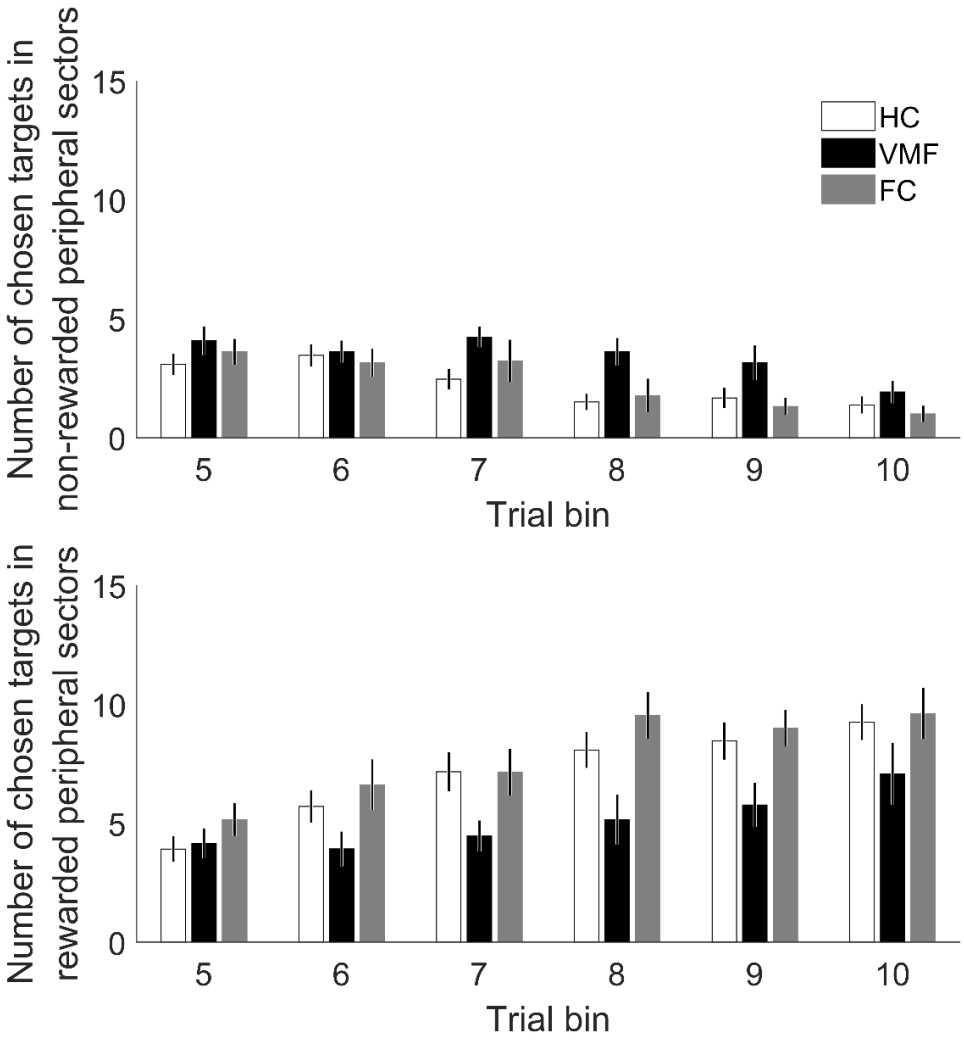

Supplementary Figure 4.2. Number of chosen targets in the rewarded and non-rewarded peripheral sectors of the screen across trial bins of the first asymmetric reward phase. Top panel; Number of chosen targets in the two peripheral sectors on the least rewarded side of the screen across trial bins of the first asymmetric phase. Bottom panel; Number of chosen targets in the two peripheral sectors on the most rewarded side of the screen. Error bars represent SEM.

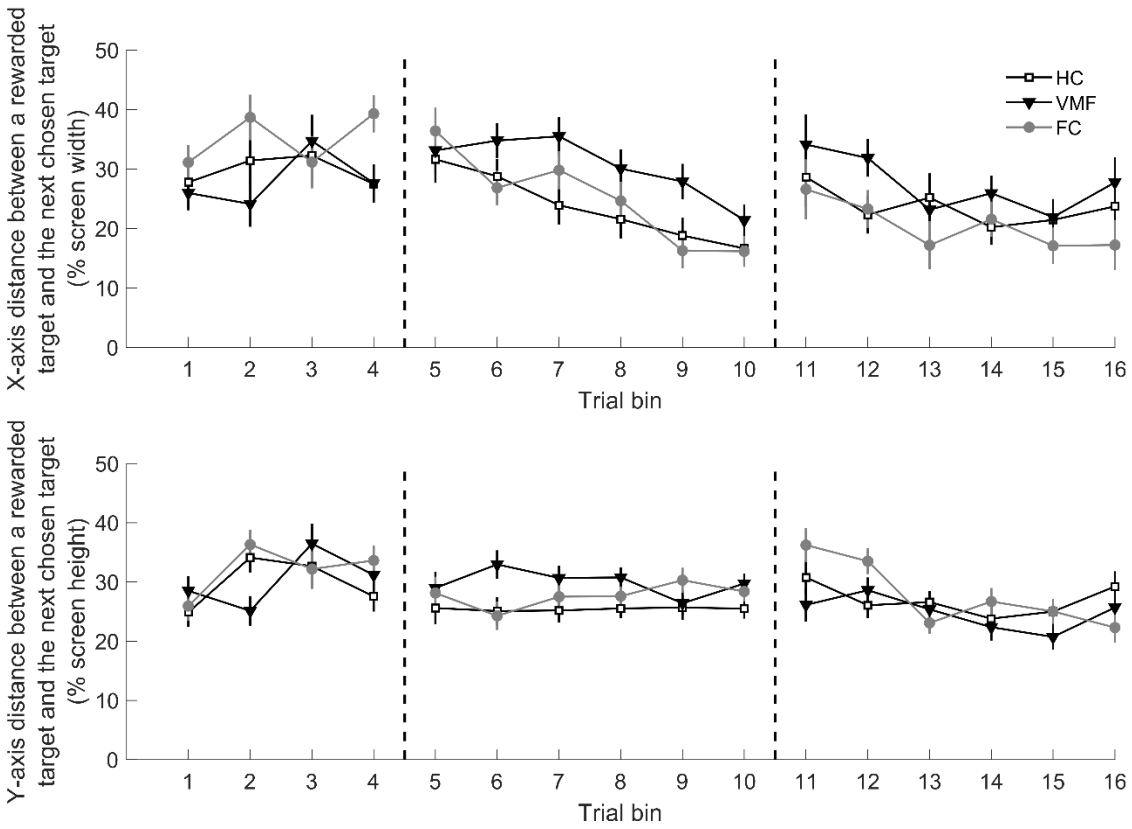

Supplementary Figure 4.3. Mean horizontal and vertical distance between a rewarded target and the subsequently chosen target in each trial bin. Top panel; Vertical (y-axis) distance. Bottom panel; Horizontal (x-axis) distance. Dotted lines demarcate experiment conditions (baseline: trial bins 1-4, initial reward asymmetry: bins 5-10, reversed reward asymmetry: bins 11-16). Error bars represent SEM.

Chapter 5. Discussion

Summary of the main findings

A major focus of the still-new field of decision neuroscience has been to establish the neural correlates of an abstract instantiation of subjective value as described by economic theories. While this work has identified a set of brain regions, notably including VMF, that seem to track value information, we still have a very incomplete understanding of how the brain supports value-based decisions. One challenge is that VMF lesion findings are not fully compatible with influential models of the role of VMF in evaluation and choice that are based largely on neuroimaging data. In this thesis, I studied the neural underpinnings of value-based decisions through a somewhat different lens, investigating the role of the VMF in value-based choice in relation to the options (objects or spatial locations) with which value is associated, rather than considering value as an abstract "quantity", separable in the brain from the option representations themselves. Using complementary methods including VMF lesions, fMRI, and eye tracking paired with experimental paradigms inspired by visual cognition research, I provided novel insights into the roles of VMF in value-guided choice.

The first two studies examined the neural basis of binary decisions and subjective value estimation for multi-attribute objects. I contrasted a condition where individual attributes of each object independently contributed to the whole value ('elemental') with a condition in which the combination of two attributes predicted value ('configural'). Making decisions about objects by integrating elemental attribute values was spared after VMF damage, and hemodynamic signal in VMF invoked by multi-attribute option evaluation was not consistent with a role for this region in elemental value integration. In contrast, VMF damage impaired

decisions when value was associated with attribute configurations, and BOLD signal in the VMF tracked the value of whole objects in this condition. These studies support the claim that the neural substrates of multi-attribute object evaluation are at least partially distinct under these two conditions, with VMF required only for the configural condition. Further pursuing the question of the specificity of the role of VMF in evaluation, the third study tested the causal role of VMF in assigning value to spatial locations. Subjects with VMF damage were impaired in optimally selecting targets when reward was predicted by their spatial location. While VMF patients were, as a group, impaired both in deciding based on spatial information and on configural multi-attribute objects, these deficits were dissociable at the individual patient level, arguing for distinct mechanisms underlying decisions in the object and spatial domains.

In this chapter, I will discuss the main contributions of this work, address some of the key limitations, and suggest future directions to address some of the outstanding questions raised by the findings presented in this thesis.

A novel perspective on multi-attribute decision-making

The first two studies provide converging evidence that the brain processes underlying multi-attribute decision-making are not fully described by accounts assuming that the value of an option is constructed by integrating the individual values associated with component attributes. While attributes might be separately evaluated under some conditions, real-world decisions often involve the consideration of attribute configurations, i.e. when attributes are not individually predictive of rewards, but rather predict reward only in conjunction with other attributes. While the neuroeconomic literature has suggested such conjunctions are likely to be

relevant (e.g. (Suzuki et al., 2017; Xia et al., 2015)), and there is an extensive literature showing that this distinction is important in the brain processes underlying object recognition, this framework was directly tested for the first time in the work described in this thesis. The findings argue for neural and behavioural differences in configural and elemental value construction.

The finding that eye-movement patterns differ when evaluating complex objects in elemental vs configural conditions (Chapter 3) adds to a body of work using process-tracing measures including eye-tracking to understand how information is gathered as decisions unfold. This work has involved decisions expressed in an explicitly multi-attribute format, with attributes usually printed out as discrete 'chunks' of information, in a table or grid. This research argues that during choice between multi-attribute options, the number of attributes sampled and the order in which they are sampled can be used to infer the underlying valuation process (Payne et al., 1992, 1993). For instance, a decision in which all attributes of one option are sampled before transitioning to another option is thought to reflect an alternative-based strategy, in which individual attribute-values (for example, cost, colour, mileage, and safety for a given car option) are combined to produce whole option-values (a.k.a. alternative-values), which are then compared. On the other hand, a pattern of information acquisition in which an attribute is sampled across options (for example, the prices of different cars) would reflect an attribute-based strategy, in which a decision is made without estimating the value of each option as a whole. Within this body of work, gaze patterns are used as indicators of differences in top-down processes relating to the decision-maker's goals, or to the use of heuristics to

reduce information load in the face of high decision complexity or time pressure (Bettman et al., 1998; Payne, 1976; Payne et al., 1988; Russo and Dosher, 1983).

The process-tracing decision research is grounded in psychology, not neuroscience. As such, there has been no effort to link it with our understanding of how information about complex objects is acquired, despite the potential relevance of object recognition mechanisms to value construction. When we consider an apple or an orange in the store, our perception of these options is unified; we see a ripe apple, not a round shape, red color and smooth surface separately. Arguably we do not construct an abstract "table" of characteristics, but rather holistically process the attributes that together contribute to the rewardingness of each option. Process tracing paradigms using abstract grids likely disrupt holistic object processing, instead emphasizing evaluation of isolated attributes. Thus, findings from process-oriented work so far might not translate well to many real-world decisions. It may be that more naturalistic experimental paradigms using real-world-type objects paired with process tracing studies would shed light on more ecologically relevant value-based decision making.

In keeping with this idea, Chapter 3 reports eye-tracking analysis inspired from the process-tracing literature during evaluation of object stimuli. In this experiment, objects were evaluated individually, such that eye-movements could only be made between attributes of a single object and could not reflect the use of alternative- or attribute-based strategies. Nevertheless, we found that participants made more transitions between attributes in the configural compared to the elemental condition. Interestingly, we found that the perirhinal cortex (PRC), a region in the ventral visual stream (VVS) specialized for configural object recognition, was differentially involved in configural and elemental evaluation. This suggests

that eye movements during multi-attribute choice might reflect differences in object recognition mechanisms deployed to process visual information at the value-relevant level (attribute or whole object). Teasing apart the contributions of top-down decision strategies and of object recognition mechanisms to information sampling patterns during decision-making will be crucial to understand value construction processes for complex objects that are the most common real-world decision options.

Considering decision options as complex objects may help to bridge the gap between process-oriented decision psychology and computational modelling research on the dynamics of value-based decisions, in a way that can connect with an extensive body of visual neuroscience knowledge. help to bridge the gap between process-oriented decision psychology and computational modelling research on the dynamics of value-based decisions, in a way that can connect with an extensive body of visual neuroscience knowledge. Sequential sampling models (e.g. drift diffusion model) were first applied to study perceptual decisions, modelling binary choice as an accumulation of noisy sensory evidence in favor of one option or the other until a threshold is reached, at which point a decision is made (Ratcliff, 2002; Usher and McClelland, 2001). This approach has later been adapted to the study of value-based choice. Such models can predict the outcome of decisions, and estimate the moment (i.e., reaction time) at which a decision will be made based on the value difference between the options under deliberation (Milosavljevic et al., 2010; Rangel et al., 2008). Within this framework, it was found that evidence accumulation can be indexed by eye gaze; at any time point during deliberation, evidence accumulation is biased in favor of the option being fixated at that time (Krajbich et al., 2010). Experimentally increasing time spent fixating on an option also increases

the likelihood of choosing it (Shimojo et al., 2003), suggesting a causal link between gaze, value construction and choice. However, the nature of the evidence being accumulated and how the value of an option is built from multiple attributes is still unclear. In fact, typical instantiations of drift diffusion models give the model access to the value of whole options from the onset of a decision process, regardless of the number or type of value-relevant attributes. This simplifying assumption overlooks decades of process tracing research reviewed earlier, which argues that value is constructed by sampling attributes following a variety of strategies across conditions and individuals. A recent extension to the drift-diffusion model introduced attribute-level influences in evidence accumulation and found that attributes (i.e. healthiness and tastiness of food options) begin to weigh in a decision at different latencies (Maier et al., 2020). The model devised by Maier and colleagues (2020) states that when an attribute starts to be considered, it contributes to evidence accumulation continuously until a decision is made (i.e. once a second attribute begins to be considered, the first and second attributes together contribute to evidence accumulation). This work is an important first step in leveraging attribute-level resolution to model how decisions unfold, but it does not fully capture the dynamics of information sampling described in process tracing studies. Process tracing work demonstrates that eye-movements transition back and forth between attributes during choice (Russo and Dosher, 1983). This suggests that attributes contribute to evidence accumulation as they are sampled, rather than cumulatively.

So far, sequential sampling models incorporating eye-tracking were limited in using fixations directed at whole options, as attributes of the naturalistic stimuli used in these studies (food items, trinkets) are typically spatially overlapping (Busemeyer et al., 2019). The

experimental paradigms described in Chapters 2 and 3 provide new opportunities to refine our understanding of the dynamics of decision-making by allowing eye movements to reveal how attributes are considered within a complex object, as Fribble attributes are spatially separated.

The value of 'where'

While the first two experiments studied decisions based on the value of objects, the third study (Chapter 4) examined value in relation to spatial locations, a type of information which has been given much less attention in decision-making research. Given evidence that the VMF is more strongly connected with the ventral visual ('what') stream than the dorsal visual ('where') pathway (Cavada et al., 2000; Kravitz et al., 2013), and previous findings that action-value associations rely on the dorsomedial prefrontal cortex and not the VMF (Camille et al., 2011b; Rudebeck et al., 2008), the VMF might be specifically involved in assigning value to objects, and not to spatial information. The novel finding reported in Chapter 4 that VMF damage impairs decisions when value is exclusively predicted by spatial location suggests that this region is both involved in assigning value to 'what' and 'where', under specific conditions.

This work is only a first step in understanding the role of the VMF in decisions based on the value of spatial locations. Indeed, the nature of spatial location-value associations that require intact VMF remains unclear. As reviewed in Chapter 1, the brain processes spatial information in at least two major reference frames supported by distinct neural mechanisms: an egocentric reference frame represented in the dorsal visual pathway and frontoparietal attentional network, and an allocentric reference frame supported by the hippocampal spatial navigation system.

One possibility is that VMF has a role in integrating the value of spatial locations in egocentric spatial reference frames (e.g. higher rewards on my left-hand side), echoing deficits of spatial attention after damage to the frontoparietal network causing hemilateral neglect (Corbetta and Shulman, 2011). If VMF damage had caused lateralized deficits in associating value to spatial locations in the contralesional hemifield, a strong case could have been made in support of this egocentric hypothesis. However, it is unclear from our data whether the effects were lateralized. First, by chance, most participants with VMF damage in that study had unilateral damage restricted to the right hemisphere. Second, the experimental paradigm confounded the initial learning phase with contralesional rewards, and reversal phase with ipsilesional rewards. This was done by design, for practical reasons, but now needs to be studied further to resolve these ambiguities. Further work including more patients with left-hemisphere and bilateral damage will be needed to conclusively answer whether the role of VMF in spatial location-value association is lateralized. The experimental paradigm should also be improved for future work. The inclusion of additional reversal cycles would remove the confound of reward side (ipsi- or contra-lesional) and task phase (initial learning or reversal) which would allow stronger conclusions regarding reward learning (as discussed in Chapter 4) and functional lateralization.

Alternatively, VMF damage might disrupt the association of value with spatial locations in hippocampal allocentric spatial maps (e.g. higher rewards on the top left corner of the screen) via disruption of VMF-hippocampal connections. Previous work found that frontoparietal damage causing deficits of egocentric spatial attention (i.e., neglect) spare spatial-location value associations (Lucas et al., 2013), suggesting that in those patients, the

spared hippocampal allocentric reference system might support location-value associations in a very similar task. Moreover, in our study, VMF damage did not impair egocentric spatial attention orienting, and VMF damage has been shown to impair performance in a spatial navigation task (virtual maze) (Dahmani et al., 2018). Together, these studies suggest a causal role for the VMF in tasks involving the allocentric navigation system, but not the egocentric spatial reference frame. This proposal aligns with studies in rodents which found that forming preferences for rewarding spatial locations (i.e. conditioned place preference) critically relies on the hippocampus (Tzschentke, 2007), and that lesions to the OFC disrupt the stability of behaviourally relevant spatial representations in hippocampal place cells (Kyd and Bilkey, 2003, 2005). These lines of evidence suggest that the VMF and the hippocampus together support spatial location-value associations, and decision-making based on the value of 'where'.

More work will be needed to test the hypothesis that VMF has a critical role in decisions leveraging location-value associations mapped in the hippocampal navigation system in humans. Experimental paradigms will need to be developed in which participants decide which one of several locations to navigate to based on their expected value, as opposed to typical spatial navigation tasks where participants are instructed to navigate to a goal location to obtain a generic reward (e.g. (Dahmani et al., 2018)).

A VMF-medial temporal lobe decision-making system

The idea that the VMF has a role in biasing decisions by interacting with the hippocampal spatial navigation system, along with the finding suggesting that the VMF and the PRC are together involved in using configural associations between attributes to guide decisions

(Chapter 3) echoes the emerging view that the VMF and the medial-temporal lobe interact to support high-level cognitive functions (McCormick et al., 2018), and emerging evidence suggesting that the well-studied roles of the MTL in associative memory are important in supporting motivated behaviour. FMRI studies found that the hippocampus is involved in generalizing value from a rewarded stimulus to another which was never directly rewarded, but associated with the former through repeated exposure (Wimmer and Shohamy, 2012; Wimmer et al., 2012). The hippocampus was also found to be more active when using configurations of visual cues to learn about potential outcomes compared to when using elemental cues (Duncan et al., 2018). Lesion work found that hippocampal damage affects patterns of behaviour and physiological responses during moral decision-making (McCormick et al., 2016). Additional neuroimaging work found that the hippocampus and the VMF are together involved in multi-attribute decision-making between novel configurations of food ingredients (Barron et al., 2013), and that these two regions are functionally connected during decisions mediated by hippocampal memory encoding (Gluth et al., 2015), and during decisions involving the retrieval of stimulus-stimulus associations (Wang et al., 2020). To sum up, the results presented in this thesis add to growing evidence suggesting that the VMF and the MTL (including the hippocampus and PRC) together support value-based decisions in conditions where information is carried in the associations between stimuli, whether between elements that make up complex objects, or between objects and the environment.

This proposed role of a VMF-MTL system for decisions-making is not monolithic; deficits in decisions between objects were dissociable from deficits in decisions involving spatial information in some patients with VMF damage (Chapter 4), suggesting that different networks

or sub-regions within the VMF might support different interactions with MTL sub-regions involved in the processing of complex objects and spatial locations. However, it must be noted that the two types of decisions were studied in different tasks not designed to be directly compared. Additional studies manipulating the value of object features and spatial locations within the same experimental task would allow for a more rigorous test for dissociations in lesion patients. Complementary evidence from neuroimaging will be needed to test whether sub-regions of the VMF and the MTL are activated and interact differently in decisions based on the value of spatial locations and those based on objects.

Revisiting subjective value

Findings from the three studies included in this thesis suggest that value is processed through parallel and partially dissociable mechanisms for decisions involving different kinds of information. This argues that VMF value representations detected by correlational methods in multiple conditions (Bartra et al., 2013; Levy and Glimcher, 2012; Montague and Berns, 2002; Rangel and Hare, 2010; Rangel et al., 2008) are not required for all types of value-based decisions. Other brain regions have been consistently associated with subjective value across human fMRI studies, most commonly the ventral striatum and the posterior cingulate cortex (Bartra et al., 2013; Levy and Glimcher, 2012; Peters and Büchel, 2010). Much less is known about the causal contributions of these regions to value estimation and decision-making in humans. More work will be needed using methods allowing for causal inference to address which brain regions are required for value-based choice in the conditions where VMF does not seem to be critical.

Emerging neurobiological frameworks propose that decision-making unfolds through a distributed and gradual integration of information from perception to actions, without explicit pure value representations supported by the VMF or any other region (Balasubramani et al., 2018; Cisek, 2012; Cisek and Kalaska, 2010; Gardner et al., 2018, 2019; Yoo and Hayden, 2018). Yoo and Hayden (2018) argued that subjective value should be conceived as the behavioural output (e.g. likelihood of choosing the option) of a series of neural computations from inputs to the retina to the selection of a chosen item, rather than a quantity explicitly stored in the brain. Any process that increases the representation of an option at any step of processing, such as saliency, memory or attention, can contribute to the likelihood of choosing it (i.e. value) (Yoo and Hayden, 2018). This model implies that different brain regions or networks contribute to the decision process depending on the type of information relevant for a decision. The distributed view of decision-making further suggests that signal correlating with value should be found across the brain, although the strength of value correlation should be generally weaker for regions at earlier (sensory) stages and stronger at later stages as increasingly more decision-relevant inputs are integrated. The studies presented in this thesis could be consistent with such views, providing some evidence that different neural mechanisms are involved in estimating the value associated with information processed by distinct visual pathways. The fMRI investigation presented in Chapter 3 also provides tentative support for this view, with findings that signal relating to value of configural objects can be detected in regions of the VVS specifically involved in configural recognition at which value was associated through reward learning, and not at lower VVS stages where no value-relevant information could have been integrated. In addition, we found that signal in the VMF, which is higher in the processing

hierarchy than the VVS, only correlated with value later in the trial, closer to the motor implementation of the decision.

However, this distributed value framework is not entirely consistent with the work of this thesis and previous lesion studies. In addition to making the broad claim that value emerges from a gradual integration and transformation of perception to actions, the model proposed by Yoo and Hayden (2018) rejects the principle of modular, specialized contributions of any discrete brain region to value-based choice. This is inconsistent with evidence presented here that the VMF has specific roles in inferring value only for certain types of information, which adds to existing evidence that sub-regions of the frontal lobes have specialized and dissociable roles in motivated behaviour (Dias et al., 1996; Vaidya and Fellows, 2017). A compromise between these views could reconcile these streams of research: subjective value may not be explicitly represented in the brain, yet some brain regions and networks may nonetheless support discrete component processes of decision-making.

Whereas this thesis work is consistent with distributed views of how the brain supports decision-making, the new evidence presented here does not require abandoning the idea that the brain carries explicit value representations. Whether the brain explicitly represents subjective value remains unclear, and much work remains to be done before we can fully grasp the neurobiological foundations of decision-making. Based on this thesis work, I surmise that as the brain basis of value-based decision-making begins to be examined from a more holistic perspective, incorporating the contributions of perception and object recognition mechanisms, we may find that decisions are supported by a number of distinct pathways rather than relying on explicit value representations in a narrow set of 'value regions'.

Future directions and conclusion

While we found evidence supporting the view that value is processed partly within the streams of visual perception and argued that object evaluation might be occurring within the object processing stream, it is unclear whether object processing is influenced by value. We are currently undertaking follow-up experiments using behavioural measures developed in object processing research to study the nature of mental object representations deployed during decision-making under different conditions. Evidence that learning the value of individual attributes or attribute configurations changes how objects are recognized when they are evaluated would argue that recognition and valuation are interacting and are not independent modules of the decision-making process. Brain imaging measures with high temporal resolution (e.g. magnetoencephalography) will further help in understanding whether visual processing is affected by valuation, and whether value emerges at different times and stages of the visual processing hierarchy when predicted by individual attributes or by attribute configurations, and along different processing streams for value associated with objects or spatial locations.

This work studied value in relation to stimuli processed by the visual system. Real-life decisions, however, often involve the integration of information from multiple senses for value assessment. Functional neuroimaging work in humans has provided evidence that signal in the VMF correlates with the value of auditory stimuli (Caria et al., 2011; Salimpoor et al., 2013, 2015), odours (Grabenhorst and Rolls, 2009; Howard and Kahnt, 2017; Howard et al., 2015), and tastes (Chambers et al., 2009; Grabenhorst et al., 2010; Haase et al., 2011; Kim et al., 2011). Future work should test whether the hypothesised role for the VMF in decisions based on value inferred from relational encoding in the MTL extends beyond object attributes in a single

modality. Based on the work reported here and previous findings that the PRC has a role in binding information across modalities (Goulet and Murray, 2001; Holdstock et al., 2009; Taylor et al., 2006), the PRC might be involved in assessing value from multimodal attributes through interactions with the VMF.

In addition, it will be important to test whether the distinction between configural and elemental valuation proposed in this thesis using pseudo-objects generalizes to choices between real-life options. Using food choice tasks holds great potential in that regard, as food items are composed of multiple attributes (i.e. ingredients) which might predict subjective value in an elemental or configural fashion depending on the foods. Questionnaires could be developed to quantify the 'configural-ness' of different food items, i.e. the extent to which ingredients are considered separately or in configurations in a given food. Neuroimaging or lesion studies could then test the neural underpinnings of this measure and ask whether the detection of value-correlated signal in the VMF depends on the degree of elemental/configural valuation, and whether decision-making deficits following VMF damage are more severe for configural food options. Importantly, this research might be carried out using existing datasets of food decision-making to reassess value representations in the light of this novel perspective.

The VMF has been associated with other functions that are consistent with the hypothesis that the region has a critical role in drawing on associative knowledge to guide decisions. One account proposes that the OFC represents a cognitive map of task-space, which can be described as a configuration of task-relevant variables (Bao et al., 2019; Niv, 2019; Schuck et al., 2016). For instance, if there is rain on the forecast and it is windy, I should close the windows before going to bed, but wind or rain alone are not separately informative of the

action to be taken. Another area of research proposes that the VMF and the hippocampus together support the instantiations of schemas to guide behaviour. Schemas are defined as knowledge structures linking the common elements of repeated experiences which provide context to facilitate encoding of new information, memory retrieval, and object recognition (Ghosh and Gilboa, 2014; Hebscher and Gilboa, 2016). Schemas are naturally composed of the configuration of elements; for instance, when entering an unknown room, the joint presence of a curtain, a sink and a mirror will activate the 'bathroom' schema and as a result, an ambiguous object located on the countertop is more likely to be identified as a blow-dryer than a drill (Bar et al., 2006). While the cognitive map and schemas accounts are conceptually compatible with a role of VMF in using configural associations to guide value-guided behaviour, further work will be needed to establish whether these different accounts reflect the same underlying processes.

The research presented in this thesis primarily advances fundamental knowledge on the brain basis of value-based decisions. It might also be of relevance to clinical populations. Understanding how the brain combines value-relevant sources of information to guide choice and how this process goes awry in lesion patients could help us to better understand the neurological impairments caused by VMF damage, which are still poorly understood and not well-assessed by standard neuropsychological tests, despite having, at times, severe real-life consequences (Eslinger and Damasio, 1985). Other neurological conditions, such as autism spectrum disorders (ASD), are associated with impairments in associative memory and configural processing (e.g. for faces), paired with an over-reliance on intact elemental processing (Gaigg et al., 2008; O'Reilly et al., 2017; Stevenson et al., 2019). Better understanding the dissociable pathways for information integration in configural and elemental

conditions as these apply in decision-making might help in designing behavioural interventions to reduce the configural/elemental processing imbalance in these populations, or could offer a way to support decision-making by presenting information in the manner that can be successfully processed by a patient, despite their deficits.

In summary, after examining how the brain supports value-based decisions involving different streams of visual cognition, using multiple research methods, this thesis suggests that rather than being involved in value integration and comparison generally, the VMF is specifically required in inferring value from associations between attributes, objects and locations. It is likely that this involves interactions with regions within the medial temporal lobe. The view of VMF function proposed in this work and the new experimental paradigms developed to test it open new avenues to further understand the brain basis of human decision-making.

Bibliography

Anderson, B.A. (2015). Value-Driven Attentional Capture is Modulated by Spatial Context. Vis Cogn *23*, 67–81.

Anderson, B.A., Laurent, P.A., and Yantis, S. (2011). Value-driven attentional capture. PNAS *108*, 10367–10371.

Andrews-Hanna, J.R., Smallwood, J., and Spreng, R.N. (2014). The default network and self-generated thought: component processes, dynamic control, and clinical relevance. Ann. N. Y. Acad. Sci. *1316*, 29–52.

Arsenault, J.T., Nelissen, K., Jarraya, B., and Vanduffel, W. (2013). Dopaminergic Reward Signals Selectively Decrease fMRI Activity in Primate Visual Cortex. Neuron *77*, 1174–1186.

Avants, B.B., Epstein, C.L., Grossman, M., and Gee, J.C. (2008). Symmetric Diffeomorphic Image Registration with Cross-Correlation: Evaluating Automated Labeling of Elderly and Neurodegenerative Brain. Med Image Anal *12*, 26–41.

Balasubramani, P.P., Moreno-Bote, R., and Hayden, B.Y. (2018). Using a Simple Neural Network to Delineate Some Principles of Distributed Economic Choice. Front Comput Neurosci *12*, 22.

Bao, X., Gjorgieva, E., Shanahan, L.K., Howard, J.D., Kahnt, T., and Gottfried, J.A. (2019). Grid-like Neural Representations Support Olfactory Navigation of a Two-Dimensional Odor Space. Neuron *102*, 1066-1075.e5.

Bar, M., Kassam, K.S., Ghuman, A.S., Boshyan, J., Schmid, A.M., Dale, A.M., Hämäläinen, M.S., Marinkovic, K., Schacter, D.L., Rosen, B.R., et al. (2006). Top-down facilitation of visual recognition. PNAS *103*, 449–454.

Barbas, H. (2000). Connections underlying the synthesis of cognition, memory, and emotion in primate prefrontal cortices. Brain Res. Bull. *52*, 319–330.

Barense, M.D., Gaffan, D., and Graham, K.S. (2007). The human medial temporal lobe processes online representations of complex objects. Neuropsychologia *45*, 2963–2974.

Barron, H.C., Dolan, R.J., and Behrens, T.E.J. (2013). Online evaluation of novel choices by simultaneous representation of multiple memories. Nature Neuroscience *16*, 1492–1498.

Barry, T.J., Griffith, J.W., De Rossi, S., and Hermans, D. (2014). Meet the Fribbles: novel stimuli for use within behavioural research. Front Psychol *5*.

Bartko, S.J., Winters, B.D., Cowell, R.A., Saksida, L.M., and Bussey, T.J. (2007). Perirhinal cortex resolves feature ambiguity in configural object recognition and perceptual oddity tasks. Learn. Mem. *14*, 821–832.

Bartra, O., McGuire, J.T., and Kable, J.W. (2013). The valuation system: A coordinate-based meta-analysis of BOLD fMRI experiments examining neural correlates of subjective value. Neuroimage *76*, 412–427.

Basten, U., Biele, G., Heekeren, H.R., and Fiebach, C.J. (2010). How the brain integrates costs and benefits during decision making. Proc Natl Acad Sci U S A *107*, 21767–21772.

Bechara, A., Damasio, H., Tranel, D., and Damasio, A.R. (1997). Deciding Advantageously Before Knowing the Advantageous Strategy. Science *275*, 1293–1295.

Behzadi, Y., Restom, K., Liau, J., and Liu, T.T. (2007). A Component Based Noise Correction Method (CompCor) for BOLD and Perfusion Based fMRI. Neuroimage *37*, 90–101.

Benton, A., Hamster, K., and Sivan, A. (1989). Multilingual Aphasia Examination (Iowa City, IA: AJA Associates).

Berker, A.O. de, Kurth-Nelson, Z., Rutledge, R.B., Bestmann, S., and Dolan, R.J. (2019). Computing Value from Quality and Quantity in Human Decision-Making. J. Neurosci. *39*, 163–176.

Bettman, J.R., Luce, M.F., and Payne, J.W. (1998). Constructive Consumer Choice Processes. J Consum Res *25*, 187–217.

Bombari, D., Mast, F.W., and Lobmaier, J.S. (2009). Featural, Configural, and Holistic Face-Processing Strategies Evoke Different Scan Patterns. Perception *38*, 1508–1521.

Botvinik-Nezer, R., Holzmeister, F., Camerer, C.F., Dreber, A., Huber, J., Johannesson, M., Kirchler, M., Iwanir, R., Mumford, J.A., Adcock, R.A., et al. (2020a). Variability in the analysis of a single neuroimaging dataset by many teams. Nature *582*, 84–88.

Botvinik-Nezer, R., Salomon, T., and Schonberg, T. (2020b). Enhanced Bottom-Up and Reduced Top-Down fMRI Activity Is Related to Long-Lasting Nonreinforced Behavioral Change. Cereb Cortex *30*, 858–874.

Bower, G.H., and Karlin, M.B. (1974). Depth of processing pictures of faces and recognition memory. Journal of Experimental Psychology *103*, 751–757.

Bowren, M.D., Croft, K.E., Reber, J., and Tranel, D. (2018). Choosing Spouses and Houses: Impaired Congruence Between Preference and Choice Following Damage to the Ventromedial Prefrontal Cortex. Neuropsychology *32*, 280–303.

Brainard, D.H. (1997). The Psychophysics Toolbox. Spat Vis *10*, 433–436.

Brodmann, K. (1909). Vergleichende Lokalisationslehre der Grosshirnrinde in ihren Prinzipien dargestellt auf Grund des Zellenbaues (Leipzig: JA Barth).

Brodmann, K. (2006). Brodmann's: Localisation in the Cerebral Cortex (Springer US).

Buckley, M.J., and Gaffan, D. (1998). Perirhinal cortex ablation impairs configural learning and paired-associate learning equally. Neuropsychologia *36*, 535–546.

Burgess, N. (2006). Spatial memory: how egocentric and allocentric combine. Trends Cogn. Sci. (Regul. Ed.) *10*, 551–557.

Busemeyer, J.R., Gluth, S., Rieskamp, J., and Turner, B.M. (2019). Cognitive and Neural Bases of Multi-Attribute, Multi-Alternative, Value-based Decisions. Trends in Cognitive Sciences *23*, 251–263.

Bussey, T.J., and Saksida, L.M. (2002). The organization of visual object representations: a connectionist model of effects of lesions in perirhinal cortex. Eur. J. Neurosci. *15*, 355–364.

Bussey, T.J., Saksida, L.M., and Murray, E.A. (2002). Perirhinal cortex resolves feature ambiguity in complex visual discriminations. Eur. J. Neurosci. *15*, 365–374.

Bussey, T.J., Saksida, L.M., and Murray, E.A. (2003). Impairments in visual discrimination after perirhinal cortex lesions: testing 'declarative' vs. 'perceptual-mnemonic' views of perirhinal cortex function. European Journal of Neuroscience *17*, 649–660.

Bussey, T.J., Saksida, L.M., and Murray, E.A. (2005). The perceptual-mnemonic/feature conjunction model of perirhinal cortex function. Q J Exp Psychol B *58*, 269–282.

Button, K.S., Ioannidis, J.P.A., Mokrysz, C., Nosek, B.A., Flint, J., Robinson, E.S.J., and Munafò, M.R. (2013). Power failure: why small sample size undermines the reliability of neuroscience. Nature Reviews Neuroscience *14*, 365–376.

Camille, N., Griffiths, C.A., Vo, K., Fellows, L.K., and Kable, J.W. (2011a). Ventromedial frontal lobe damage disrupts value maximization in humans. J Neurosci *31*, 7527–7532.

Camille, N., Tsuchida, A., and Fellows, L.K. (2011b). Double dissociation of stimulus-value and action-value learning in humans with orbitofrontal or anterior cingulate cortex damage. J. Neurosci. *31*, 15048–15052.

Caria, A., Venuti, P., and de Falco, S. (2011). Functional and dysfunctional brain circuits underlying emotional processing of music in autism spectrum disorders. Cereb. Cortex *21*, 2838–2849.

Carmichael, S.T., and Price, J.L. (1996). Connectional networks within the orbital and medial prefrontal cortex of macaque monkeys. Journal of Comparative Neurology *371*, 179–207.

Carp, J. (2012). On the Plurality of (Methodological) Worlds: Estimating the Analytic Flexibility of fMRI Experiments. Front. Neurosci. *6*.

Cavada, C., Compañy, T., Tejedor, J., Cruz-Rizzolo, R.J., and Reinoso-Suárez, F. (2000). The anatomical connections of the macaque monkey orbitofrontal cortex. A review. Cereb. Cortex *10*, 220–242.

Chambers, E.S., Bridge, M.W., and Jones, D.A. (2009). Carbohydrate sensing in the human mouth: effects on exercise performance and brain activity. J. Physiol. (Lond.) *587*, 1779–1794.

Chelazzi, L., Perlato, A., Santandrea, E., and Della Libera, C. (2013). Rewards teach visual selective attention. Vision Res. *85*, 58–72.

Chelazzi, L., Eštočinová, J., Calletti, R., Lo Gerfo, E., Sani, I., Della Libera, C., and Santandrea, E. (2014). Altering spatial priority maps via reward-based learning. J. Neurosci. *34*, 8594–8604.

Chib, V.S., Rangel, A., Shimojo, S., and O'Doherty, J.P. (2009). Evidence for a Common Representation of Decision Values for Dissimilar Goods in Human Ventromedial Prefrontal Cortex. J. Neurosci. *29*, 12315–12320.

Cisek, P. (2012). Making decisions through a distributed consensus. Current Opinion in Neurobiology *22*, 927–936.

Cisek, P., and Kalaska, J.F. (2010). Neural mechanisms for interacting with a world full of action choices. Annu. Rev. Neurosci. *33*, 269–298.

Comoli, E., Das Neves Favaro, P., Vautrelle, N., Leriche, M., Overton, P.G., and Redgrave, P. (2012). Segregated anatomical input to sub-regions of the rodent superior colliculus associated with approach and defense. Front Neuroanat *6*, 9.

Corbetta, M., and Shulman, G.L. (2011). Spatial Neglect and Attention Networks. Annu Rev Neurosci *34*, 569–599.

Cowell, R.A., Bussey, T.J., and Saksida, L.M. (2006). Why Does Brain Damage Impair Memory? A Connectionist Model of Object Recognition Memory in Perirhinal Cortex. J. Neurosci. *26*, 12186–12197.

Cox, R.W., and Hyde, J.S. (1997). Software tools for analysis and visualization of fMRI data. NMR in Biomedicine *10*, 171–178.

Crawford, J.R., and Garthwaite, P.H. (2002). Investigation of the single case in neuropsychology: confidence limits on the abnormality of test scores and test score differences. Neuropsychologia *40*, 1196–1208.

Crawford, J.R., and Garthwaite, P.H. (2006). Methods of testing for a deficit in single-case studies: Evaluation of statistical power by Monte Carlo simulation. Cogn Neuropsychol *23*, 877–904.

Crawford, J.R., Garthwaite, P.H., and Porter, S. (2010). Point and interval estimates of effect sizes for the case-controls design in neuropsychology: rationale, methods, implementations, and proposed reporting standards. Cogn Neuropsychol *27*, 245–260.

Dahmani, L., Patel, R.M., Yang, Y., Chakravarty, M.M., Fellows, L.K., and Bohbot, V.D. (2018). An intrinsic association between olfactory identification and spatial memory in humans. Nature Communications *9*, 4162.

Dale, A.M., Fischl, B., and Sereno, M.I. (1999). Cortical surface-based analysis. I. Segmentation and surface reconstruction. Neuroimage *9*, 179–194.

Damasio, H., Grabowski, T., Frank, R., Galaburda, A.M., and Damasio, A.R. (1994). The return of Phineas Gage: clues about the brain from the skull of a famous patient. Science *264*, 1102–1105.

Davis, T., LaRocque, K.F., Mumford, J., Norman, K.A., Wagner, A.D., and Poldrack, R.A. (2014). What Do Differences Between Multi-voxel and Univariate Analysis Mean? How Subject-, Voxel-, and Trial-level Variance Impact fMRI Analysis. Neuroimage *97*, 271–283.

De Renzi, E., and Vignolo, L.A. (1962). The token test: A sensitive test to detect receptive disturbances in aphasics. Brain *85*, 665–678.

Deichmann, R., Gottfried, J.A., Hutton, C., and Turner, R. (2003). Optimized EPI for fMRI studies of the orbitofrontal cortex. Neuroimage *19*, 430–441.

Delgado, M.R., Beer, J.S., Fellows, L.K., Huettel, S.A., Platt, M.L., Quirk, G.J., and Schiller, D. (2016). Viewpoints: Dialogues on the functional role of the ventromedial prefrontal cortex. Nature Neuroscience *19*, 1545–1552.

Devlin, J.T., and Price, C.J. (2007). Perirhinal contributions to human visual perception. Curr. Biol. *17*, 1484–1488.

Dias, R., Robbins, T.W., and Roberts, A.C. (1996). Dissociation in prefrontal cortex of affective and attentional shifts. Nature *380*, 69.

Duncan, K., Doll, B.B., Daw, N.D., and Shohamy, D. (2018). More Than the Sum of Its Parts: A Role for the Hippocampus in Configural Reinforcement Learning. Neuron *98*, 645-657.e6.

Eichenbaum, H. (2017). Prefrontal-hippocampal interactions in episodic memory. Nat. Rev. Neurosci. *18*, 547–558.

Ekstrom, A.D., Kahana, M.J., Caplan, J.B., Fields, T.A., Isham, E.A., Newman, E.L., and Fried, I. (2003). Cellular networks underlying human spatial navigation. Nature *425*, 184–188.

Erez, J., Cusack, R., Kendall, W., and Barense, M.D. (2016). Conjunctive Coding of Complex Object Features. Cereb Cortex *26*, 2271–2282.

Eslinger, P.J., and Damasio, A.R. (1985). Severe disturbance of higher cognition after bilateral frontal lobe ablation: patient EVR. Neurology *35*, 1731–1741.

Esteban, O., Markiewicz, C.J., Blair, R.W., Moodie, C.A., Isik, A.I., Erramuzpe, A., Kent, J.D., Goncalves, M., DuPre, E., Snyder, M., et al. (2019). fMRIPrep: a robust preprocessing pipeline for functional MRI. Nature Methods *16*, 111.

Farah, M.J. (1996). Is face recognition 'special'? Evidence from neuropsychology. Behavioural Brain Research *76*, 181–189.

Fecteau, J.H., and Munoz, D.P. (2006). Salience, relevance, and firing: a priority map for target selection. Trends Cogn. Sci. (Regul. Ed.) *10*, 382–390.

Fellows, L.K. (2006). Deciding how to decide: ventromedial frontal lobe damage affects information acquisition in multi-attribute decision making. Brain *129*, 944–952.

Fellows, L.K. (2011). The Neurology of Value. In Neurobiology of Sensation and Reward, J.A. Gottfried, ed. (Boca Raton (FL): CRC Press/Taylor & Francis), p.

Fellows, L.K., and Farah, M.J. (2003). Ventromedial frontal cortex mediates affective shifting in humans: evidence from a reversal learning paradigm. Brain *126*, 1830–1837.

Fellows, L.K., and Farah, M.J. (2007). The role of ventromedial prefrontal cortex in decision making: judgment under uncertainty or judgment per se? Cereb. Cortex *17*, 2669–2674.

Fellows, L.K., Stark, M., Berg, A., and Chatterjee, A. (2008). Patient registries in cognitive neuroscience research: advantages, challenges, and practical advice. J Cogn Neurosci *20*, 1107–1113.

Fonov, V., Evans, A., McKinstry, R., Almli, C., and Collins, D. (2009). Unbiased nonlinear average age-appropriate brain templates from birth to adulthood. NeuroImage *47*, S102.

Friston, K.J., Williams, S., Howard, R., Frackowiak, R.S., and Turner, R. (1996). Movement-related effects in fMRI time-series. Magn Reson Med *35*, 346–355.

Fujiwara, J., Tobler, P.N., Taira, M., Iijima, T., and Tsutsui, K.-I. (2009). Segregated and integrated coding of reward and punishment in the cingulate cortex. J. Neurophysiol. *101*, 3284–3293.

Gaigg, S.B., Gardiner, J.M., and Bowler, D.M. (2008). Free recall in autism spectrum disorder: The role of relational and item-specific encoding. Neuropsychologia *46*, 983–992.

Gallagher, M., McMahan, R.W., and Schoenbaum, G. (1999). Orbitofrontal Cortex and Representation of Incentive Value in Associative Learning. J. Neurosci. *19*, 6610–6614.

Gardner, Conroy, J.C., Styer, C.V., Huynh, T., Whitaker, L.R., and Schoenbaum, G. (2018). Medial orbitofrontal inactivation does not affect economic choice. ELife *7*, e38963.

Gardner, Sanchez, D.C., Zhou, J., and Schoenbaum, G. (2019). Real-Time Value Integration during Economic Choice Is Regulated by Orbitofrontal Cortex. Current Biology *29*, 4315-4322.e4.

Ghosh, V.E., and Gilboa, A. (2014). What is a memory schema? A historical perspective on current neuroscience literature. Neuropsychologia *53*, 104–114.

Gitelman, D.R., Penny, W.D., Ashburner, J., and Friston, K.J. (2003). Modeling regional and psychophysiologic interactions in fMRI: the importance of hemodynamic deconvolution. Neuroimage *19*, 200–207.

Glimcher, P.W., and Rustichini, A. (2004). Neuroeconomics: The Consilience of Brain and Decision. Science *306*, 447–452.

Gluth, S., Sommer, T., Rieskamp, J., and Büchel, C. (2015). Effective Connectivity between Hippocampus and Ventromedial Prefrontal Cortex Controls Preferential Choices from Memory. Neuron *86*, 1078–1090.

Goodale, M.A., and Milner, A.D. (1992). Separate visual pathways for perception and action. Trends Neurosci. *15*, 20–25.

Gorgolewski, K., Burns, C.D., Madison, C., Clark, D., Halchenko, Y.O., Waskom, M.L., and Ghosh, S.S. (2011). Nipype: a flexible, lightweight and extensible neuroimaging data processing framework in python. Front Neuroinform *5*, 13.

Gorgolewski, K.J., Auer, T., Calhoun, V.D., Craddock, R.C., Das, S., Duff, E.P., Flandin, G., Ghosh, S.S., Glatard, T., Halchenko, Y.O., et al. (2016). The brain imaging data structure, a format for organizing and describing outputs of neuroimaging experiments. Sci Data *3*, 160044.

Gottlieb, J. (2007). From Thought to Action: The Parietal Cortex as a Bridge between Perception, Action, and Cognition. Neuron *53*, 9–16.

Goulet, S., and Murray, E.A. (2001). Neural substrates of crossmodal association memory in monkeys: The amygdala versus the anterior rhinal cortex. Behavioral Neuroscience *115*, 271–284.

Grabenhorst, F., and Rolls, E.T. (2009). Different representations of relative and absolute subjective value in the human brain. Neuroimage *48*, 258–268.

Grabenhorst, F., Rolls, E.T., Parris, B.A., and d'Souza, A.A. (2010). How the brain represents the reward value of fat in the mouth. Cereb. Cortex *20*, 1082–1091.

Greve, D.N., and Fischl, B. (2009). Accurate and robust brain image alignment using boundary-based registration. Neuroimage *48*, 63–72.

Grill-Spector, K., Kourtzi, Z., and Kanwisher, N. (2001). The lateral occipital complex and its role in object recognition. Vision Research *41*, 1409–1422.

Grober, E., and Sliwinski, M. (1991). Development and validation of a model for estimating premorbid verbal intelligence in the elderly. J Clin Exp Neuropsychol *13*, 933–949.

Gutnikov, S.A., Ma, Y.-Y., and Gaffan, D. (1997). Temporo-frontal Disconnection Impairs Visual-visual Paired Association Learning but not Configural Learning in Macaca Monkeys. European Journal of Neuroscience *9*, 1524–1529.

Haase, L., Green, E., and Murphy, C. (2011). Males and females show differential brain activation to taste when hungry and sated in gustatory and reward areas. Appetite *57*, 421–434.

Haber, S.N. (2011). Neuroanatomy of Reward: A View from the Ventral Striatum. In Neurobiology of Sensation and Reward, J.A. Gottfried, ed. (Boca Raton (FL): CRC Press/Taylor & Francis), p.

Hare, T.A., Camerer, C.F., and Rangel, A. (2009). Self-Control in Decision-Making Involves Modulation of the vmPFC Valuation System. Science *324*, 646–648.

Hare, T.A., Malmaud, J., and Rangel, A. (2011a). Focusing Attention on the Health Aspects of Foods Changes Value Signals in vmPFC and Improves Dietary Choice. J. Neurosci. *31*, 11077–11087.

Hare, T.A., Schultz, W., Camerer, C.F., O'Doherty, J.P., and Rangel, A. (2011b). Transformation of stimulus value signals into motor commands during simple choice. PNAS *108*, 18120–18125.

Harlow, J.M. (1868). Recovery from the passage of an iron bar through the head. Publications of the Massachusetts Medical Society *2*, 327–346.

Hayden, B.Y., Pearson, J.M., and Platt, M.L. (2011). Neuronal basis of sequential foraging decisions in a patchy environment. Nat. Neurosci. *14*, 933–939.

Heath, T.B., and Chatterjee, S. (1995). Asymmetric Decoy Effects on Lower-Quality versus Higher-Quality Brands: Meta-analytic and Experimental Evidence. J Consum Res *22*, 268–284.

Hebscher, M., and Gilboa, A. (2016). A boost of confidence: The role of the ventromedial prefrontal cortex in memory, decision-making, and schemas. Neuropsychologia *90*, 46–58.

Heide, V.D., J, R., Skipper, L.M., Klobusicky, E., and Olson, I.R. (2013). Dissecting the uncinate fasciculus: disorders, controversies and a hypothesis. Brain *136*, 1692–1707.

Henri-Bhargava, A., Simioni, A., and Fellows, L.K. (2012). Ventromedial frontal lobe damage disrupts the accuracy, but not the speed, of value-based preference judgments. Neuropsychologia *50*, 1536–1542.

Holdstock, J.S., Hocking, J., Notley, P., Devlin, J.T., and Price, C.J. (2009). Integrating Visual and Tactile Information in the Perirhinal Cortex. Cereb Cortex *19*, 2993–3000.

Howard, J.D., and Kahnt, T. (2017). Identity-specific reward representations in orbitofrontal cortex are modulated by selective devaluation. J. Neurosci. 3473–16.

Howard, J.D., Gottfried, J.A., Tobler, P.N., and Kahnt, T. (2015). Identity-specific coding of future rewards in the human orbitofrontal cortex. PNAS *112*, 5195–5200.

Huber, J., Payne, J.W., and Puto, C. (1982). Adding Asymmetrically Dominated Alternatives: Violations of Regularity and the Similarity Hypothesis. Journal of Consumer Research *9*, 90–98.

Hunt, L.T., Dolan, R.J., and Behrens, T.E.J. (2014). Hierarchical competitions subserving multi-attribute choice. Nat Neurosci *17*, 1613–1622.

Hunt, L.T., Malalasekera, W.M.N., Berker, A.O. de, Miranda, B., Farmer, S.F., Behrens, T.E.J., and Kennerley, S.W. (2018). Triple dissociation of attention and decision computations across prefrontal cortex. Nat Neurosci *21*, 1471–1481.

Izquierdo, A., Suda, R.K., and Murray, E.A. (2004). Bilateral Orbital Prefrontal Cortex Lesions in Rhesus Monkeys Disrupt Choices Guided by Both Reward Value and Reward Contingency. J. Neurosci. *24*, 7540–7548.

Jenkinson, M., Bannister, P., Brady, M., and Smith, S. (2002). Improved Optimization for the Robust and Accurate Linear Registration and Motion Correction of Brain Images. NeuroImage *17*, 825–841.

Jones, J.L., Esber, G.R., McDannald, M.A., Gruber, A.J., Hernandez, A., Mirenzi, A., and Schoenbaum, G. (2012). Orbitofrontal cortex supports behavior and learning using inferred but not cached values. Science *338*, 953–956.

Kahnt, T. (2018). A decade of decoding reward-related fMRI signals and where we go from here. Neuroimage *180*, 324–333.

Kahnt, T., Heinzle, J., Park, S.Q., and Haynes, J.-D. (2011). Decoding different roles for vmPFC and dlPFC in multi-attribute decision making. Neuroimage *56*, 709–715.

Kaping, D., Vinck, M., Hutchison, R.M., Everling, S., and Womelsdorf, T. (2011). Specific Contributions of Ventromedial, Anterior Cingulate, and Lateral Prefrontal Cortex for Attentional Selection and Stimulus Valuation. PLOS Biology *9*, e1001224.

Karnath, H.-O., Rennig, J., Johannsen, L., and Rorden, C. (2011). The anatomy underlying acute versus chronic spatial neglect: a longitudinal study. Brain *134*, 903–912.

Kaskan, P.M., Costa, V.D., Eaton, H.P., Zemskova, J.A., Mitz, A.R., Leopold, D.A., Ungerleider, L.G., and Murray, E.A. (2017). Learned Value Shapes Responses to Objects in Frontal and Ventral Stream Networks in Macaque Monkeys. Cereb Cortex *27*, 2739–2757.

Kennerley, S.W., Dahmubed, A.F., Lara, A.H., and Wallis, J.D. (2008). Neurons in the Frontal Lobe Encode the Value of Multiple Decision Variables. Journal of Cognitive Neuroscience *21*, 1162–1178.

Kennerley, S.W., Behrens, T.E.J., and Wallis, J.D. (2011). Double dissociation of value computations in orbitofrontal and anterior cingulate neurons. Nature Neuroscience *14*, 1581–1589.

Kim, H., Shimojo, S., and O'Doherty, J.P. (2011). Overlapping responses for the expectation of juice and money rewards in human ventromedial prefrontal cortex. Cereb. Cortex *21*, 769–776.

Klein, A., Ghosh, S.S., Bao, F.S., Giard, J., Häme, Y., Stavsky, E., Lee, N., Rossa, B., Reuter, M., Neto, E.C., et al. (2017). Mindboggling morphometry of human brains. PLOS Computational Biology *13*, e1005350.

Klink, P.C., Jentgens, P., and Lorteije, J.A.M. (2014). Priority Maps Explain the Roles of Value, Attention, and Salience in Goal-Oriented Behavior. J. Neurosci. *34*, 13867–13869.

Kolling, N., Behrens, T.E.J., Mars, R.B., and Rushworth, M.F.S. (2012). Neural Mechanisms of Foraging. Science *336*, 95–98.

Kondo, H., Saleem, K.S., and Price, J.L. (2005). Differential connections of the perirhinal and parahippocampal cortex with the orbital and medial prefrontal networks in macaque monkeys. J. Comp. Neurol. *493*, 479–509.

Krajbich, I. (2019). Accounting for attention in sequential sampling models of decision making. Current Opinion in Psychology *29*, 6–11.

Krajbich, I., Armel, C., and Rangel, A. (2010). Visual fixations and the computation and comparison of value in simple choice. Nat Neurosci *13*, 1292–1298.

Kravitz, D.J., Saleem, K.S., Baker, C.I., and Mishkin, M. (2011). A new neural framework for visuospatial processing. Nature Reviews Neuroscience *12*, 217–230.

Kravitz, D.J., Saleem, K.S., Baker, C.I., Ungerleider, L.G., and Mishkin, M. (2013). The ventral visual pathway: An expanded neural framework for the processing of object quality. Trends Cogn Sci *17*, 26–49.

Kriegeskorte, N., Simmons, W.K., Bellgowan, P.S., and Baker, C.I. (2009). Circular analysis in systems neuroscience – the dangers of double dipping. Nat Neurosci *12*, 535–540.

Kurtz-David, V., Persitz, D., Webb, R., and Levy, D.J. (2019). The neural computation of inconsistent choice behavior. Nature Communications *10*, 1583.

Kyd, R.J., and Bilkey, D.K. (2003). Prefrontal cortex lesions modify the spatial properties of hippocampal place cells. Cereb. Cortex *13*, 444–451.

Kyd, R.J., and Bilkey, D.K. (2005). Hippocampal Place Cells Show Increased Sensitivity to Changes in the Local Environment Following Prefrontal Cortex Lesions. Cereb Cortex *15*, 720–731.

Lanczos, C. (1964). Evaluation of Noisy Data. Journal of the Society for Industrial and Applied Mathematics: Series B, Numerical Analysis *1*, 76–85.

Larsen, T., and O'Doherty, J.P. (2014). Uncovering the spatio-temporal dynamics of value-based decision-making in the human brain: a combined fMRI–EEG study. Philos Trans R Soc Lond B Biol Sci *369*.

Lawlor, D.A., Tilling, K., and Davey Smith, G. (2016). Triangulation in aetiological epidemiology. Int J Epidemiol *45*, 1866–1886.

Levy, D.J., and Glimcher, P.W. (2012). The root of all value: a neural common currency for choice. Curr. Opin. Neurobiol. *22*, 1027–1038.

Lezak, M.D., Howieson, D.B., Loring, D.W., and Fischer, J.S. (2012). Neuropsychological Assessment (New York, NY, US: Oxford University Press).

Lim, S.-L., O'Doherty, J.P., and Rangel, A. (2013). Stimulus Value Signals in Ventromedial PFC Reflect the Integration of Attribute Value Signals Computed in Fusiform Gyrus and Posterior Superior Temporal Gyrus. J Neurosci *33*, 8729–8741.

Logothetis, N.K. (2008). What we can do and what we cannot do with fMRI. Nature *453*, 869–878.

Lucas, N., Schwartz, S., Leroy, R., Pavin, S., Diserens, K., and Vuilleumier, P. (2013). Gambling against neglect: unconscious spatial biases induced by reward reinforcement in healthy people and brain-damaged patients. Cortex *49*, 2616–2627.

Mackey, S., and Petrides, M. (2010). Quantitative demonstration of comparable architectonic areas within the ventromedial and lateral orbital frontal cortex in the human and the macaque monkey brains. Eur. J. Neurosci. *32*, 1940–1950.

Macko, K.A., Jarvis, C.D., Kennedy, C., Miyaoka, M., Shinohara, M., Sololoff, L., and Mishkin, M. (1982). Mapping the primate visual system with [2-14C]deoxyglucose. Science *218*, 394–397.

Maier, S.U., Raja Beharelle, A., Polanía, R., Ruff, C.C., and Hare, T.A. (2020). Dissociable mechanisms govern when and how strongly reward attributes affect decisions. Nature Human Behaviour 1–15.

Manohar, S.G., and Husain, M. (2016). Human ventromedial prefrontal lesions alter incentivisation by reward. Cortex *76*, 104–120.

Maunsell, J.H.R. (2004). Neuronal representations of cognitive state: reward or attention? Trends Cogn. Sci. (Regul. Ed.) *8*, 261–265.

Maunsell, J.H.R., and Cook, E.P. (2002). The role of attention in visual processing. Philos. Trans. R. Soc. Lond., B, Biol. Sci. *357*, 1063–1072.

McCormick, C., Rosenthal, C.R., Miller, T.D., and Maguire, E.A. (2016). Hippocampal Damage Increases Deontological Responses during Moral Decision Making. J. Neurosci. *36*, 12157–12167.

McCormick, C., Ciaramelli, E., De Luca, F., and Maguire, E.A. (2018). Comparing and Contrasting the Cognitive Effects of Hippocampal and Ventromedial Prefrontal Cortex Damage: A Review of Human Lesion Studies. Neuroscience *374*, 295–318.

McLaren, D.G., Ries, M.L., Xu, G., and Johnson, S.C. (2012). A generalized form of context-dependent psychophysiological interactions (gPPI): a comparison to standard approaches. Neuroimage *61*, 1277–1286.

McNaughton, B.L., Battaglia, F.P., Jensen, O., Moser, E.I., and Moser, M.-B. (2006). Path integration and the neural basis of the "cognitive map." Nature Reviews Neuroscience *7*, 663–678.

Melchers, K.G., Shanks, D.R., and Lachnit, H. (2008). Stimulus coding in human associative learning: flexible representations of parts and wholes. Behav. Processes *77*, 413–427; discussion 451-453.

Mesulam, M.M. (1999). Spatial attention and neglect: parietal, frontal and cingulate contributions to the mental representation and attentional targeting of salient extrapersonal events. Philos Trans R Soc Lond B Biol Sci *354*, 1325–1346.

Milosavljevic, M., Malmaud, J., Huth, A., Koch, C., and Rangel, A. (2010). The drift diffusion model can account for the accuracy and reaction time of value-based choices under high and low time pressure. Judgment and Decision Making *5*, 437–449.

Mishkin, M., Ungerleider, L.G., and Macko, K.A. (1983). Object vision and spatial vision: two cortical pathways. Trends in Neurosciences *6*, 414–417.

Mogami, T., and Tanaka, K. (2006). Reward Association Affects Neuronal Responses to Visual Stimuli in Macaque TE and Perirhinal Cortices. J. Neurosci. *26*, 6761–6770.

Montague, P.R., and Berns, G.S. (2002). Neural Economics and the Biological Substrates of Valuation. Neuron *36*, 265–284.

Moran, J., and Desimone, R. (1985). Selective attention gates visual processing in the extrastriate cortex. Science *229*, 782–784.

Mumford, J.A. (2007). A Guide to Calculating Percent Change with Featquery.

Mumford, J.A., and Nichols, T. (2008). Power Calculation for Group fMRI Studies Accounting for Arbitrary Design and Temporal Autocorrelation. Neuroimage *39*, 261–268.

Munafò, M.R., and Smith, G.D. (2018). Robust research needs many lines of evidence. Nature *553*, 399–401.

Murray, E.A., O'Doherty, J.P., and Schoenbaum, G. (2007a). What we know and do not know about the functions of the orbitofrontal cortex after 20 years of cross-species studies. J. Neurosci. *27*, 8166–8169.

Murray, E.A., Bussey, T.J., and Saksida, L.M. (2007b). Visual Perception and Memory: A New View of Medial Temporal Lobe Function in Primates and Rodents. Annual Review of Neuroscience *30*, 99–122.

Nelissen, K., Jarraya, B., Arsenault, J.T., Rosen, B.R., Wald, L.L., Mandeville, J.B., Marota, J.J., and Vanduffel, W. (2012). Neural correlates of the formation and retention of cocaine-induced stimulus-reward associations. Biol. Psychiatry *72*, 422–428.

von Neumann, J., Morgenstern, O., and Rubinstein, A. (1944). Theory of Games and Economic Behavior (60th Anniversary Commemorative Edition) (Princeton University Press).

Niv, Y. (2019). Learning task-state representations. Nature Neuroscience *22*, 1544–1553.

Nosek, B.A., Ebersole, C.R., DeHaven, A.C., and Mellor, D.T. (2018). The preregistration revolution. Proc. Natl. Acad. Sci. U.S.A. *115*, 2600–2606.

O'Keefe, J., and Nadel, L. (1978). The hippocampus as a cognitive map (Oxford : New York: Clarendon Press ; Oxford University Press).

Olson, I.R., Page, K., Moore, K.S., Chatterjee, A., and Verfaellie, M. (2006). Working Memory for Conjunctions Relies on the Medial Temporal Lobe. J. Neurosci. *26*, 4596–4601.

O'Reilly, R.C. (2010). The What and How of Prefrontal Cortical Organization. Trends Neurosci *33*, 355–361.

O'Reilly, C., Lewis, J.D., and Elsabbagh, M. (2017). Is functional brain connectivity atypical in autism? A systematic review of EEG and MEG studies. PLOS ONE *12*, e0175870.

Ota, H., Fujii, T., Suzuki, K., Fukatsu, R., and Yamadori, A. (2001). Dissociation of body-centered and stimulus-centered representations in unilateral neglect. Neurology *57*, 2064–2069.

Padoa-Schioppa, C., and Assad, J.A. (2006). Neurons in the orbitofrontal cortex encode economic value. Nature *441*, 223–226.

Park, S.Q., Kahnt, T., Rieskamp, J., and Heekeren, H.R. (2011). Neurobiology of value integration: when value impacts valuation. J. Neurosci. *31*, 9307–9314.

Payne, J.W. (1976). Task complexity and contingent processing in decision making: An information search and protocol analysis. Organizational Behavior and Human Performance *16*, 366–387.

Payne, J.W., Bettman, J.R., and Johnson, E.J. (1988). Adaptive strategy selection in decision making. Journal of Experimental Psychology: Learning, Memory, and Cognition *14*, 534–552.

Payne, J.W., Bettman, J.R., Coupey, E., and Johnson, E.J. (1992). A constructive process view of decision making: Multiple strategies in judgment and choice. Acta Psychologica *80*, 107–141.

Payne, J.W., Bettman, J.R., and Johnson, E.J. (1993). The Adaptive Decision Maker (Cambridge: Cambridge University Press).

Pearson, J.M., Watson, K.K., and Platt, M.L. (2014). Decision making: the neuroethological turn. Neuron *82*, 950–965.

Pelletier, G., and Fellows, L.K. (2019). A Critical Role for Human Ventromedial Frontal Lobe in Value Comparison of Complex Objects Based on Attribute Configuration. J. Neurosci. *39*, 4124–4132.

Persichetti, A.S., Aguirre, G.K., and Thompson-Schill, S.L. (2015). Value is in the eye of the beholder: early visual cortex codes monetary value of objects during a diverted attention task. J Cogn Neurosci *27*, 893–901.

Peters, J., and Büchel, C. (2010). Neural representations of subjective reward value. Behav. Brain Res. *213*, 135–141.

Petrides, M., and Pandya, D.N. (1994). Comparative architectonic analysis of the human and the macaque frontal cortex. Handbook of Neuropsychology 17–58.

Petrides, M., and Pandya, D.N. (2007). Efferent Association Pathways from the Rostral Prefrontal Cortex in the Macaque Monkey. J. Neurosci. *27*, 11573–11586.

Petrides, M., Tomaiuolo, F., Yeterian, E.H., and Pandya, D.N. (2012). The prefrontal cortex: Comparative architectonic organization in the human and the macaque monkey brains. Cortex *48*, 46–57.

Philiastides, M.G., Biele, G., and Heekeren, H.R. (2010). A mechanistic account of value computation in the human brain. Proc Natl Acad Sci U S A *107*, 9430–9435.

Poldrack, R.A. (2007). Region of interest analysis for fMRI. Soc Cogn Affect Neurosci *2*, 67–70.

Poldrack, R.A., Baker, C.I., Durnez, J., Gorgolewski, K.J., Matthews, P.M., Munafò, M.R., Nichols, T.E., Poline, J.-B., Vul, E., and Yarkoni, T. (2017). Scanning the horizon: towards transparent and reproducible neuroimaging research. Nature Reviews Neuroscience *18*, 115–126.

Posner, M.I. (1980). Orienting of attention. Quarterly Journal of Experimental Psychology *32*, 3–25.

Power, J.D., Mitra, A., Laumann, T.O., Snyder, A.Z., Schlaggar, B.L., and Petersen, S.E. (2014). Methods to detect, characterize, and remove motion artifact in resting state fMRI. Neuroimage *84*, 320–341.

Price, J.L. (2007). Definition of the orbital cortex in relation to specific connections with limbic and visceral structures and other cortical regions. Ann. N. Y. Acad. Sci. *1121*, 54–71.

Ptak, R. (2012). The Frontoparietal Attention Network of the Human Brain: Action, Saliency, and a Priority Map of the Environment. Neuroscientist *18*, 502–515.

Rangel, A., and Hare, T. (2010). Neural computations associated with goal-directed choice. Curr. Opin. Neurobiol. *20*, 262–270.

Rangel, A., Camerer, C., and Montague, P.R. (2008). A framework for studying the neurobiology of value-based decision making. Nat. Rev. Neurosci. *9*, 545–556.

Ratcliff, R. (2002). A diffusion model account of response time and accuracy in a brightness discrimination task: fitting real data and failing to fit fake but plausible data. Psychon Bull Rev *9*, 278–291.

Ray, J.P., and Price, J.L. (1993). The organization of projections from the mediodorsal nucleus of the thalamus to orbital and medial prefrontal cortex in macaque monkeys. J. Comp. Neurol. *337*, 1–31.

Riesenhuber, M., and Poggio, T. (1999). Hierarchical models of object recognition in cortex. Nat. Neurosci. *2*, 1019–1025.

Rolls, E.T. (2006). The neurophysiology and functions of the orbitofrontal cortex. In The Orbitofrontal Cortex, (Oxford: Oxford University Press), pp. 92–124.

Rolls, E.T., and O'Mara, S.M. (1995). View-responsive neurons in the primate hippocampal complex. Hippocampus *5*, 409–424.

Rorden, C., and Brett, M. (2000). Stereotaxic display of brain lesions. Behav Neurol *12*, 191–200.

Rorden, C., Karnath, H.-O., and Bonilha, L. (2007). Improving lesion-symptom mapping. J Cogn Neurosci *19*, 1081–1088.

Rousselet, G.A., Thorpe, S.J., and Fabre-Thorpe, M. (2004). How parallel is visual processing in the ventral pathway? Trends Cogn. Sci. (Regul. Ed.) *8*, 363–370.

Rudebeck, P.H., and Murray, E.A. (2011). Dissociable effects of subtotal lesions within the macaque orbital prefrontal cortex on reward-guided behavior. J. Neurosci. *31*, 10569–10578.

Rudebeck, P.H., Behrens, T.E., Kennerley, S.W., Baxter, M.G., Buckley, M.J., Walton, M.E., and Rushworth, M.F.S. (2008). Frontal Cortex Subregions Play Distinct Roles in Choices between Actions and Stimuli. J. Neurosci. *28*, 13775–13785.

Rudebeck, P.H., Mitz, A.R., Chacko, R.V., and Murray, E.A. (2013a). Effects of amygdala lesions on reward-value coding in orbital and medial prefrontal cortex. Neuron *80*, 1519–1531.

Rudebeck, P.H., Saunders, R.C., Prescott, A.T., Chau, L.S., and Murray, E.A. (2013b). Prefrontal mechanisms of behavioral flexibility, emotion regulation and value updating. Nat. Neurosci. *16*, 1140–1145.

Rudorf, S., and Hare, T.A. (2014). Interactions between dorsolateral and ventromedial prefrontal cortex underlie context-dependent stimulus valuation in goal-directed choice. J. Neurosci. *34*, 15988–15996.

Rudy, J.W., and Sutherland, R.J. (1995). Configural association theory and the hippocampal formation: an appraisal and reconfiguration. Hippocampus *5*, 375–389.

Rushworth, M.F.S., and Behrens, T.E.J. (2008). Choice, uncertainty and value in prefrontal and cingulate cortex. Nat Neurosci *11*, 389–397.

Rushworth, M.F.S., Noonan, M.P., Boorman, E.D., Walton, M.E., and Behrens, T.E. (2011). Frontal cortex and reward-guided learning and decision-making. Neuron *70*, 1054–1069.

Russo, J.E., and Dosher, B.A. (1983). Strategies for multiattribute binary choice. J Exp Psychol Learn Mem Cogn *9*, 676–696.

Saksida, L.M., and Bussey, T.J. (2010). The representational–hierarchical view of amnesia: Translation from animal to human. Neuropsychologia *48*, 2370–2384.

Salimpoor, V.N., Bosch, I. van den, Kovacevic, N., McIntosh, A.R., Dagher, A., and Zatorre, R.J. (2013). Interactions Between the Nucleus Accumbens and Auditory Cortices Predict Music Reward Value. Science *340*, 216–219.

Salimpoor, V.N., Zald, D.H., Zatorre, R.J., Dagher, A., and McIntosh, A.R. (2015). Predictions and the brain: how musical sounds become rewarding. Trends in Cognitive Sciences *19*, 86–91.

Salomon, T., Botvinik-Nezer, R., Oren, S., and Schonberg, T. (2020). Enhanced striatal and prefrontal activity is associated with individual differences in nonreinforced preference change for faces. Human Brain Mapping *41*, 1043–1060.

Samuelson, P.A. (1937). A Note on Measurement of Utility. Rev Econ Stud *4*, 155–161.

Samuelson, P.A. (1947). Foundations of Economic Analysis (Cambridge, Massachusetts, United States: Harvard University Press).

Schonberg, T., and Katz, L.N. (2020). A Neural Pathway for Nonreinforced Preference Change. Trends in Cognitive Sciences *0*.

Schonberg, T., Bakkour, A., Hover, A.M., Mumford, J.A., Nagar, L., Perez, J., and Poldrack, R.A. (2014). Changing value through cued approach: an automatic mechanism of behavior change. Nature Neuroscience *17*, 625–630.

Schuck, N.W., Cai, M.B., Wilson, R.C., and Niv, Y. (2016). Human Orbitofrontal Cortex Represents a Cognitive Map of State Space. Neuron *91*, 1402–1412.

Schultz, W., Dayan, P., and Montague, P.R. (1997). A Neural Substrate of Prediction and Reward. Science *275*, 1593–1599.

Scoville, W.B., and Milner, B. (1957). Loss of recent memory after bilateral hippocampal lesions. J Neurol Neurosurg Psychiatry *20*, 11–21.

Serences, J.T. (2008). Value-Based Modulations in Human Visual Cortex. Neuron *60*, 1169–1181.

Shimojo, S., Simion, C., Shimojo, E., and Scheier, C. (2003). Gaze bias both reflects and influences preference. Nature Neuroscience *6*, 1317–1322.

Simonson, I., and Tversky, A. (1992). Choice in context: Tradeoff contrast and extremeness aversion. Journal of Marketing Research *29*, 281–295.

Sjulson, L., Peyrache, A., Cumpelik, A., Cassataro, D., and Buzsáki, G. (2018). Cocaine place conditioning strengthens location-specific hippocampal coupling to the nucleus accumbens. Neuron *98*, 926-934.e5.

Smith, S.M., Jenkinson, M., Woolrich, M.W., Beckmann, C.F., Behrens, T.E.J., Johansen-Berg, H., Bannister, P.R., De Luca, M., Drobnjak, I., Flitney, D.E., et al. (2004). Advances in functional and structural MR image analysis and implementation as FSL. Neuroimage *23 Suppl 1*, S208-219.

Stephens, D.W., and Krebs, J.R. (1986). Foraging Theory (Princeton, New Jersey, US: Princeton University Press).

Stevenson, R.A., Philipp-Muller, A., Hazlett, N., Wang, Z.Y., Luk, J., Lee, J., Black, K.R., Yeung, L.-K., Shafai, F., Segers, M., et al. (2019). Conjunctive Visual Processing Appears Abnormal in Autism. Front. Psychol. *9*.

Sutherland, R.J., Kolb, B., and Whishaw, I.Q. (1982). Spatial mapping: definitive disruption by hippocampal or medial frontal cortical damage in the rat. Neuroscience Letters *31*, 271–276.

Suzuki, S., Cross, L., and O'Doherty, J.P. (2017). Elucidating the underlying components of food valuation in the human orbitofrontal cortex. Nature Neuroscience *20*, 1780–1786.

Swainson, R., Rogers, R.D., Sahakian, B.J., Summers, B.A., Polkey, C.E., and Robbins, T.W. (2000). Probabilistic learning and reversal deficits in patients with Parkinson's disease or frontal or temporal lobe lesions: possible adverse effects of dopaminergic medication. Neuropsychologia *38*, 596–612.

Taylor, K.I., Moss, H.E., Stamatakis, E.A., and Tyler, L.K. (2006). Binding crossmodal object features in perirhinal cortex. PNAS *103*, 8239–8244.

Teffer, K., and Semendeferi, K. (2012). Human prefrontal cortex: evolution, development, and pathology. Prog. Brain Res. *195*, 191–218.

Thiebaut de Schotten, M., Dell'Acqua, F., Valabregue, R., and Catani, M. (2012). Monkey to human comparative anatomy of the frontal lobe association tracts. Cortex *48*, 82–96.

Trapanese, C., Meunier, H., and Masi, S. (2018). What, where and when: spatial foraging decisions in primates. Biological Reviews *94*, 483–502.

Trouche, S., Perestenko, P.V., van de Ven, G.M., Bratley, C.T., McNamara, C.G., Campo-Urriza, N., Black, S.L., Reijmers, L.G., and Dupret, D. (2016). Recoding a cocaine-place memory engram to a neutral engram in the hippocampus. Nature Neuroscience *19*, 564–567.

Tsuchida, A., Doll, B.B., and Fellows, L.K. (2010). Beyond Reversal: A Critical Role for Human Orbitofrontal Cortex in Flexible Learning from Probabilistic Feedback. J. Neurosci. *30*, 16868–16875.

Tustison, N.J., Avants, B.B., Cook, P.A., Zheng, Y., Egan, A., Yushkevich, P.A., and Gee, J.C. (2010). N4ITK: Improved N3 Bias Correction. IEEE Transactions on Medical Imaging *29*, 1310–1320.

Tzschentke, T.M. (2007). REVIEW ON CPP: Measuring reward with the conditioned place preference (CPP) paradigm: update of the last decade. Addiction Biology *12*, 227–462.

Ungerleider, L.G., and Mishkin, M. (1982). Two cortical visual systems. In Analysis of Visual Behavior, (MIT Press), pp. 549–586.

Usher, M., and McClelland, J.L. (2001). The time course of perceptual choice: The leaky, competing accumulator model. Psychological Review *108*, 550–592.

Vaidya, A.R., and Fellows, L.K. (2015a). Ventromedial Frontal Cortex Is Critical for Guiding Attention to Reward-Predictive Visual Features in Humans. J. Neurosci. *35*, 12813–12823.

Vaidya, A.R., and Fellows, L.K. (2015b). Testing necessary regional frontal contributions to value assessment and fixation-based updating. Nature Communications *6*, 10120.

Vaidya, A.R., and Fellows, L.K. (2016). Necessary Contributions of Human Frontal Lobe Subregions to Reward Learning in a Dynamic, Multidimensional Environment. J. Neurosci. *36*, 9843–9858.

Vaidya, A.R., and Fellows, L.K. (2017). The Neuropsychology of Decision-Making: A View From the Frontal Lobes. In Decision Neuroscience, J.-C. Dreher, and L. Tremblay, eds. (San Diego: Academic Press), pp. 277–289.

Vaidya, A.R., and Fellows, L.K. (2020). Under construction: ventral and lateral frontal lobe contributions to value-based decision-making and learning. F1000Res *9*, 158.

Vaidya, A.R., Sefranek, M., and Fellows, L.K. (2018). Ventromedial Frontal Lobe Damage Alters how Specific Attributes are Weighed in Subjective Valuation. Cereb. Cortex *28*, 3857–3867.

Vaidya, A.R., Pujara, M.S., Petrides, M., Murray, E.A., and Fellows, L.K. (2019). Lesion Studies in Contemporary Neuroscience. Trends in Cognitive Sciences *23*, 653–671.

Viard, A., Doeller, C.F., Hartley, T., Bird, C.M., and Burgess, N. (2011). Anterior Hippocampus and Goal-Directed Spatial Decision Making. Journal of Neuroscience *31*, 4613–4621.

Wallis, J.D., and Miller, E.K. (2003). Neuronal activity in primate dorsolateral and orbital prefrontal cortex during performance of a reward preference task. Eur. J. Neurosci. *18*, 2069–2081.

Wang, F., Schoenbaum, G., and Kahnt, T. (2020). Interactions between human orbitofrontal cortex and hippocampus support model-based inference. PLOS Biology *18*, e3000578.

Watson, H.C., Wilding, E.L., and Graham, K.S. (2012). A Role for Perirhinal Cortex in Memory for Novel Object–Context Associations. J. Neurosci. *32*, 4473–4481.

Wicherts, J.M., Veldkamp, C.L.S., Augusteijn, H.E.M., Bakker, M., van Aert, R.C.M., and van Assen, M.A.L.M. (2016). Degrees of Freedom in Planning, Running, Analyzing, and Reporting Psychological Studies: A Checklist to Avoid p-Hacking. Front Psychol *7*.

Williams, P. (1998). Representational Organization of Multiple Exemplars of Object Categories. University of Massachusetts at Boston.

Williams, P., and Simons, D.J. (2000). Detecting Changes in Novel, Complex Three-dimensional Objects. Visual Cognition *7*, 297–322.

Wilson, F.A., Scalaidhe, S.P., and Goldman-Rakic, P.S. (1993). Dissociation of object and spatial processing domains in primate prefrontal cortex. Science *260*, 1955–1958.

Wimmer, G.E., and Shohamy, D. (2012). Preference by association: how memory mechanisms in the hippocampus bias decisions. Science *338*, 270–273.

Wimmer, G.E., Daw, N.D., and Shohamy, D. (2012). Generalization of value in reinforcement learning by humans. Eur J Neurosci *35*, 1092–1104.

Xia, C., Stolle, D., Gidengil, E., and Fellows, L.K. (2015). Lateral Orbitofrontal Cortex Links Social Impressions to Political Choices. J. Neurosci. *35*, 8507–8514.

Yarkoni, T., Poldrack, R.A., Nichols, T.E., Van Essen, D.C., and Wager, T.D. (2011). Large-scale automated synthesis of human functional neuroimaging data. Nature Methods *8*, 665–670.

Yoo, S.B.M., and Hayden, B.Y. (2018). Economic Choice as an Untangling of Options into Actions. Neuron *99*, 434–447.

Zaehle, T., Jordan, K., Wüstenberg, T., Baudewig, J., Dechent, P., and Mast, F.W. (2007). The neural basis of the egocentric and allocentric spatial frame of reference. Brain Res. *1137*, 92–103.

Zhang, Y., Brady, M., and Smith, S. (2001). Segmentation of brain MR images through a hidden Markov random field model and the expectation-maximization algorithm. IEEE Transactions on Medical Imaging *20*, 45–57.

Zigmond, A.S., and Snaith, R.P. (1983). The Hospital Anxiety and Depression Scale. Acta Psychiatrica Scandinavica *67*, 361–370.